University of Stavanger

Faculty of Science and Technology

MASTER'S THESIS

Study program/ Specialization: **Offshore Technology/ Subsea Technology**	Spring semester, 2014 ~~Open~~ / Restricted access
Writer: **Dody Aldilana**	…………………………………………… (Writer's signature)

Faculty supervisor:
Professor Ove Tobias Gudmestad, University of Stavanger

External supervisor(s):
Robert Ganski, DNV GL
Ole Gabrielsen, DNV GL

Thesis title:

Effects of Impacts from Large Supply Vessels on Jacket Structures

Credits (ECTS):
30

Key words: Jacket Platform Ship Collision Strain Energy Plasticity Accidental Limit State (ALS) Fracture	Pages: 67 + enclosure: 15 pages Stavanger, July 7th 2014 Date/year

ABSTRACT

The current jacket structures installed on the Norwegian Continental Shelf (NCS) are designed to resist the impact energy from supply vessels with a 5000 tons displacement. This agrees with the requirement that is stated in NORSOK N-003. In addition to that, a minimum of 2 m/s ship velocity at collision accident is specified for the Accidental Limit State (ALS) in the early design phase.

However, during the last decade there has been a development of supply vessels sizes in terms of displacement. This means that collision with supply vessels with displacement more than 5000 tons may be expected nowadays and for the near future. This corresponds to higher impact energy which should be resisted by the jacket structures. In addition, the speed at impact may vary and there is a huge possibility that the speed is more than 2 m/s. For example, during the collision of Big Orange XVIII with Ekofisk 2/4 W platform, the reported speed at the time of impact was 9.3 knots, or equal to 4.8 m/s [Ref. /19]. This will result in higher impact energy than the anticipated in the early design phase.

In this thesis, four platforms are investigated in order to check their capacity against high impact energy. The analysis is based on a quasi-static nonlinear approach. A finite element computer program is used to simulate the impact scenarios. Various impact scenarios have been simulated in order to cover as much as possible the possibility of impact locations in a jacket platform.

For each impact scenario, the maximum energy absorption is limited either by fracture or denting of the hit member, or failure of the adjacent joints. As for the fracture limit criteria, the proposed values in NORSOK N-004 are used.

ACKNOWLEDGEMENT

All praise is due to Allah, the Lord of the universe. It is indeed due to His mercy and His will that this master thesis report is completed.

This thesis work is submitted as partial requirement of completing the master degree in Offshore Technology program, specialization in Subsea Technology, in Faculty of Sciences and Technology, University of Stavanger. The thesis work is carried out under the collaboration between DNV GL and University of Stavanger during the period January 2014 – June 2014. Most portion of the work was done in DNV GL office in Stavanger.

I have to admit that the past few months have not been so easy for me as my beloved wife passed away in April. However, I feel blessed and grateful for all people who always supported me in completing my study.

Firstly, I would like to express my gratitude to my faculty supervisor, Professor Ove Tobias Gudmestad, for his guidance, advices, and supports during the work of this thesis. I would like to also thank him for his patience in checking the report and giving constructive comments.

Next, I would like also to thank Mr. Ole Gabrielsen and Mr. Robert Ganski from DNV GL for their assistance and valuable countless discussions regarding solving of various problems during the work of the thesis. Thanks also to Mr. Ole Gabrielsen for initiating the master thesis program. In general, I am much honored to have had the opportunity to join the structural engineering team of DNV GL and feel the friendly working environment there. My gratitude also goes to all members of structural department, and to my thesis mate, Mr. Tuan Minh Tran.

A great portion of acknowledgement also goes to my family, especially my mother, for the love and supports that have been sincerely given to me during the hard times of doing the thesis work, mainly during the last few months.

Last but not least, thanks to all Indonesian friends in Stavanger, especially students of 2012 intake. Togetherness with them during the past two years would never be forgotten. May we all have success in life and may we meet again sometime.

Stavanger, July 2014

Dody Aldilana

Specially dedicated to my beloved wife,

Herlani Wijayanti

02.04.87 - 19.04.14

Table of Contents

List of Figures

List of Tables

List of Symbols and Abbreviations

Alphabets

A	Cross section of tubular member
b	Width of a rectangular cross section
c	Non-dimensional spring stiffness
c_f	Axial flexibility factor
c_{lp}	Plastic zone length factor
c_w	Displacement factor
D	Diamater of tubular
d_c, w_c	Characteristic deformation for tubular member
E, E_p	Elastic modulus, plastic modulus
E_{sd}, E_{rd}	Impact energy of ship, capacity to take impact energy
f	Yield function
f_y	Yield stress
H	Non-dimensional plastic stiffness
h	Height of a rectangular cross section
k	Elastic axial stiffness
L, l	Member length
M, M_{EP}	Moment, elasto-plastic moment
m_a	Added mass of the ship
m_s	Ship mass
N_{Rd}	Design axial resistance
N_{Sd}	Design axial force
R_0	Plastic collapse resistance
R_d	Design resistance
R_k	Characteristic resistance
S_d	Design load effect
S_k	Characteristic load effect
t	Wall thickness of tubular member
U_0, U_D, U_V	Strain energy density, distortional strain energy, volumetric strain energy
v_s	Impact speed
$\overline{w}$	Non-dimensional deformation
w	Lateral deformation
W, W_p	Elastic modulus section, plastic modulus section
w_d	Dent depth
Z	Plastic modulus section

Greek Letter

α	Shape factor
β	Local buckling criteria
γ_f, γ_m	Load factor, material factor
ε_{cr}, ε_y	Critical strain, yield strain
σ	Stress
Φ	Outer diameter of tubular member
υ	Poisson's ratio
τ	Shear stress

Abbreviation

ALS	Accidenal Limit State
DNV	Det Norske Veritas
DWT	Deadweight Tonnage
LC	Load Case
MJ	Mega Joule
NCS	Norwegian Continental Shelf

1 INTRODUCTION

Ship impact is one of accident cases that should be accounted for during the design phase of an offshore platform. The design is importance since there is a certain risk of the event to happen. In a very coarse way risk is associated with probability and consequences of an unwanted event [Ref. /03].

Although a collision is a relatively rare event it may cause a quite severe consequence. The Petroleum Safety Authority Norway reported that there have been a total of 115 collisions between installations and visiting vessels since 1982, and no less than 26 between 2001 and 2010. None of these incidents have caused loss of human life or personal injury, but the material damage has been extensive in some cases [Ref. /18]

On June 8th 2009 an accident happened when the Big Orange XVIII vessel was about to perform well stimulation at Ekofisk 2/4-X platform. The crew on the deck lost control of the vessel when entering the 500-metre zone of Ekofisk 2/4-X platform and due to failure to control the vessel steer at the emergency situation, the vessel hit Ekofisk 2/4-W water injection and bridge support platform.

No physical injuries were reported [Ref. /19] from the accident either on the vessel or on the platform. However, the collision was classified as a major accident since the integrity of the hit platform was endangered. Both the vessel and the facility were seriously damaged. The vessel's bow was indented by two meters after the impact, as depicted on Figure 1-1, and consequently caused damage to several equipment.

Figure 1-1 – Damage on Big Orange XVIII after the accident (Ref. /19)

From the installation side, also from the same report, the collision caused several braces loosening from the legs, extensive bending of the water injection riser for well W-5, and dislocation of several wellheads. The bridge connecting Ekofisk 2/4-W and bridge support BS01 was also bent down and pushed away far out of position. A local deformation (buckling) was discovered on the southern leg near the cross-over to the pile. Cracks were discovered between the legs and deck on the two northern legs (northwest and northeast). The crack on the northwestern leg reached approx. 50 per cent of the circumference, and for the northeastern leg approx. two-thirds of the circumference [Ref. /19]. Part of the damage can be seen in Figure 1-2.

Figure 1-2 – Damage on Ekofisk 2/4-W platform (Ref. /19)

The consequence extended to shut down of the production platform Ekofisk 2/4-A due to lack of overpressure protection. The Ekofisk 2/4-W was removed in 2010 and consequently caused some parts of the Ekofisk field in a condition with lack of pressure support since there was less water injection capacity.

1.1 Collision by Supply Vessel

Of many types of ships travelling on the Norwegian Continental Shelf area, supply vessels are among the most frequently seen. In the 4th quarter of 2010 it was recorded to have the second most frequent arrival by the Norwegian port authorities among other types of vessels, together with tankers and bulk carriers, as summarized in Table 1-1.

Table 1-1 – Number of ship arrivals in Norwegian ports, 4th quarter of 2010 (Ref. /25)

Port Authorities	Tankers	Bulk carriers	Container	Specialized vessels	General cargo ships	Barge dry bulk	Supply vessels	Ferry in international traffic
Bergen and Omland	720	321	141	66	975	5	1025	39
Stavanger Inter-Municipal	124	248	26	10	443	7	670	92

Port Authorities	Tankers	Bulk carriers	Container	Specialized vessels	General cargo ships	Barge dry bulk	Supply vessels	Ferry in international traffic
Flora	89	102	46	42	213	0	392	0
Kristiansund and Nordmøre	162	42	2	74	580	10	282	0
Hammerfest	64	8	9	78	114	9	90	0
Karmsund Inter Municipal	250	151	7	123	1041	1	49	0
Kristiansand	36	40	91	3	72	8	21	167
Ålesund region's	168	82	111	141	398	33	20	0
Tromsø	67	26	15	20	387	3	8	0
Eigersund	19	53	18	1	48	5	5	0
Bodø	100	orm10	10	37	396	0	4	0
Molde and Romsdal	74	70	2	35	468	0	3	0
Mo i Rana	12	24	7	0	212	0	3	0
Moss	3	9	26	0	147	0	1	0
Drammen Region Inter-Municipal	15	67	10	38	159	90	1	0
Nordfjord	56	93	75	95	150	5	1	0
Brønnøy	11	3	0	4	80	0	1	0
Borg	79	11	8	0	190	29	0	31
Oslo	84	37	113	25	186	5	0	256
Tønsberg	170	19	0	0	16	4	0	0
Sandefjord	0	0	0	0	0	0	0	434
Larvik	9	5	65	0	58	6	0	163
Grenland	183	279	32	0	108	17	0	0
Bremanger	11	30	25	40	51	0	0	0
Trondheimsfjord Inter Municipal	48	58	2	1	262	1	0	0
Inner Trondheimsfjord	15	22	1	0	181	0	0	0
Narvik	2	61	1	0	79	0	0	0
Store Norske Spitsbergen Grubekompani AS	0	0	0	0	0	0	0	0
Private enterprises with own quay	2	446	0	0	242	0	0	0
Total	**2573**	**2389**	**843**	**833**	**7256**	**238**	**2576**	**1182**

On the other hand Norwegian Statistic records shows that from 2004 to 2010 the number of arrivals, particularly for supply vessels, increased from about 5700 arrivals in 2004 to 9300 arrivals in 2010. The numbers are summarized in Table 1-2.

Table 1-2 – The number of supply vessel arrival during 2004 to 2010 (Ref. /25)

Year	Domestic Arrival	Foreign Arrival	Unknown	Total
2004	5487	152	67	5706
2005	5713	188	70	5971
2006	7031	228	65	7324
2007	7245	230	43	7518
2008	8529	191	48	8768
2009	9110	258	65	9433
2010	8940	287	117	9344

From the table above, it can be concluded that there has been a positive trend line for the presented period as depicted in Figure 1-3.

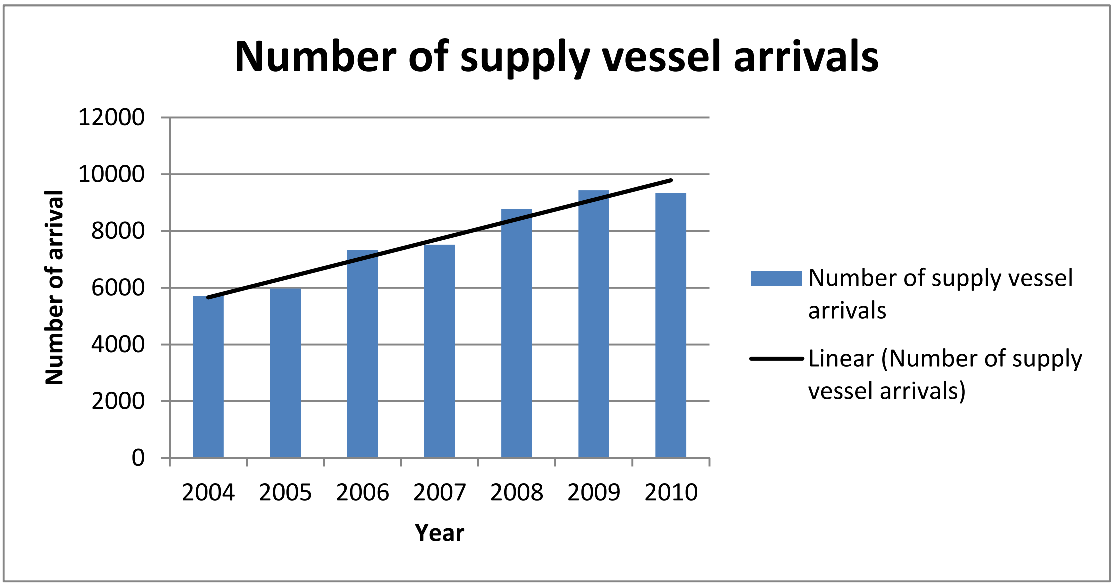

Figure 1-3 – Trend line for number of supply vessel arrivals

It can be inferred from the figure above that the number of supply vessels passing over the NCS area has become more frequent and therefore there is a higher probability of impact with offshore platforms. On the other hand, supply vessels nowadays are becoming larger in terms of displacement and consequently having higher impact energy.

1.2 Recent Collision Cases from Supply Vessel

During 2004 and 2010, The Norwegian Petroleum Safety Authority had filed collision accidents occurring on offshore platforms. Some of them were caused by impacts from supply vessels, and are listed below [Ref. /20]:

- Collision of Far Symphony with West Venture, March 2004

  The accident happened when the 4929 dead weight tons Far Symphony vessel ran towards West Venture mobile drilling unit's safety zone in autopilot mode, and none of the crews was aware of it. This ended with a collision, causing damage to both vessel and facility. The impact energy from the collision was more than 20 MJ with recorded speed is 7.3 knots at impact.

- Collision of Ocean Carrier with Ekofisk 2/4 P Bridge, June 2005

  Ocean Carrier was approaching the safety zone of the facility in calm but foggy sea. The visibility was very poor, estimated at about 100-150 meters. There were misunderstandings in navigation as the ship was entering the facility area with velocity as much as 5.5 m/s. An attempt to reduce the speed had been made but it was too late. Considerable damages were sustained to the bridge area due to the impact, as well as to the bow. The Ocean Carrier had 4679 dead weight tons and the collision energy exceeded 20 MJ.

- Collision of Bourbon Surf with Grane Jacket, July 2007

  Both the captain and the first officer left the ship bridge after the Grane facility's safety zone was passed. The crew was too late to stop the vessel but the speed was successfully reduced from 3 m/s to 1 m/s before the impact. The Bourbon Surf was a 3117 tons dead weight vessel. The impact energy was reported low but there was a large potential of causing more severe consequences.

- Collision of supply vessel Far Grimshader with Songa Dee Semisubmersible, January 2010

  Far Grimshader was carrying a task on the lee side of the Songa Dee when the accident happened. The ship was about to move to other side of the facility when its propeller was caught in a wire attached to the facility's anchoring. This caused the vessel to lose its control and hit the facility for two hours. Two columns of Songa Dee were damaged and the vessel suffered six holes on the hull and main deck, resulting in water penetration to the engine room. The vessel had 2528 dead weight tons. The collision energy was reported low, but during the hit there could have been several hundred crashes.

1.3 Objective of Analysis

Currently many installed jacket structures in the NCS area are designed to resist impact energy from supply vessel with displacement up to 5000 tons. This criterion corresponds with NORSOK standards N-004 [Ref. /24] and DNV RP C204 [Ref. /07].

However over the past 5 to 10 years the supply vessels displacement has raised. It is indeed true that the risk of colliding with offshore platforms has been managed by introducing a more reliable Dynamic Positioning (DP) system but the probability of collisions still exists however small.

The objective of the analysis is to investigate the capacity of existing jacket platforms in NCS area in terms of how much impact energy they can take during the impact with larger supply vessels.

1.4 Scope of Thesis Work

The thesis work comprises as following:

1. Literature study regarding ship collisions with jacket structures

   The work is intended for the author to capture current knowledge regarding collision analysis, knowing the basic theory, and familiarize himself with the codes, mainly DNV-RP-C204. This work will be ingredients for the author to compose Section 2 and Section 3.

2. Survey of typical supply vessels operating on the NCS

The work is intended to give the author a general view of the current development of supply vessels operating in NCS area. The result of this activity is presented in Section 4.

3. Collection and grouping of jacket structure models.

   DNV provides structural models for the thesis work, supplied by asset owners on the NCS area. However for this work, the models are made anonymous. The models then will be categorized and finite element (FE) simulation will be performed based on a prioritized sequence. The work is presented in Section 5.

4. Preparation of non-linear FE models.

   USFOS is used to perform the non-linear simulations. Therefore, the acquired structural models will be imported to USFOS as input for the analysis. Further is to apply representative loading to evaluate both local and global effect. The work is presented in Section 5.

5. Review of the results and assessment of consequences of increased impact energies on various types of jacket structures. The work is presented in Section 6.

1.5 Limitations

Due to the limited working time, the thesis work is constrained in several aspects as following:

1. Platform Type

   Only steel jacket platforms are covered for the current work. Therefore other installation types like semisubmersibles, spars and TLPs are not considered.

2. Vessel Type

   Although ship-platform collision can be caused by any types of vessel, specific for this thesis work, supply vessels are considered. Therefore collision with tankers, bulk carriers, cruise ships, etc. are out of scope. Standard non-ice strengthened bows supply vessels are considered.

3. Small diameter pipe (jacket legs and braces)

   This thesis work will investigates impact on small diameter members like jacket legs and braces. This limitation is in-line with point 1 above that only jacket structures are considered. Correspondingly impact on large columns like spars and TLP pontoons are not taken into account.

4. Norwegian Continental Shelf (NCS) Area

   The thesis work is performed over the installed platforms within NCS area only and no other areas are included.

1.6 Thesis Outline

This thesis report consists of 7 chapters as listed below:

- Chapter 1: Introduction

  Focus of this chapter is to give a description of how important it is to carry out the collision analysis. Several accident instances are also presented. This chapter also states the objective of the analysis, scope of the work, and the limitations.

- Chapter 2: Code Requirements

  This chapter presents current state of art of carrying out the collision analysis based on the applicable codes.

- Chapter 3: Plasticity Theory

  This chapter describes the plasticity theory that is being the basis for collision analysis.

- Chapter 4: Survey of Supply Vessels

  In this chapter a description of the current supply vessel profiles is provided. The chapter also discusses the energy collisions and refers to the updated NORSOK rules for collision analysis.

- Chapter 5: Methodology

  This chapter consists of methodology used in performing boat impact analysis. Simplification and limitations are also presented here. In addition, this chapter also includes modeling of structures that are analyzed for this thesis work. .

- Chapter 6: Result Analysis

  This chapter provides analysis of the results from the computerized calculation.

- Chapter 7: Summary, Conclusion, and Recommendations

  Summary and conclusion of the analysis work is presented within this chapter. Moreover, recommendations for further studies are also given here.

2 CODE REQUIREMENTS

The general provision of ship collision analysis is given in NORSOK standard N-003 section 8.1 where impact load is categorized as one of accidental actions along with, for instances, fires, explosions, drop objects, and helicopter crash. The more technical requirements regarding the impact load, also related to how the impact energy is dissipated for small tubular and large tubular steel, are briefly described in DNV-RP-C204 and NORSOK standard N-004.

In this chapter, relevant requirements for analysis of boat impact from above codes are presented.

It should be noted, however, that NORSOK N003 is under review and that larger supply vessels with higher velocities and potentially higher impact energies have to be accounted for, stated in Section 1.3 above. Therefore, the capacity of structures to take higher impact loads than required in these codes will be investigated.

2.1 Design against Accidental Loads

Accidental load design is ultimately aimed to limit the incident so that it does not extend disproportionally from the cause of origin [Ref. /07]. It can be interpreted that the structure has to perpetuate its main safety function against impairment due to design accidental loads. In general there are three main safety functions that need to be preserved after the accident; they are *usability of escape ways, integrity of shelter areas* and, *global load bearing capacity.*

Principally there are two steps of checking in design against accidental load as specified by NORSOK standard N-001 [Ref. /21]. The first step is check of structure against the accidental load. This check is aimed to ensure that the structure will not undergo instant collapse when the accident happens. The second step is the check of damaged condition of the structure with objective to investigate that the structure resistance against normal operating loads, given the local damage caused by the accident.

Particularly for the present case in this thesis report, the post-accident, i.e. after the impact, condition of the platform is not considered. The platform will rather be subjected to gradually increasing impact energy until collapse in order to investigate the maximum energy that the platform can dissipate.

The relevant limit state for accidental loads is the Accidental Limit States (ALS) which requires that the design load effect must be lower than, or equal to the design resistance (Equation 2-1). It is in accordance with Ref. /07.

$$S_d \le R_d \qquad \text{Equation 2-1}$$

where:

$$S_d = S_k \gamma_f$$

$$R_d = \frac{R_k}{\gamma_M}$$

In the ALS check, the load and material factor (γ_f and γ_M, respectively) should be taken to 1.0.

2.2 Ship Collision – General

At the event of collision, the installation is subjected to impact force generated by the kinetic energy of the ship. The magnitude of energy depends on speed and mass of the ship, taking into account the added mass of the ship. Equation 2-2 gives the formulation of impact energy for a fixed installation and is in accordance with Ref. /07 and Ref. /24.

$$E_s = \frac{1}{2}(m_s + m_a)v_s^{\,2} \qquad \text{Equation 2-2}$$

The law of conservation of energy states that energy cannot be destroyed, but it can change from one form to another. In accordance with this law, kinetic energy generated from the impact is transferred in term of elastic deformation energy. A part of the kinetic energy may remain as kinetic energy after the impact and has to be dissipated as strain energy involving plastic strains and serious structural deterioration to the installation and, the ship, or both.

Three design schemes related to distribution of energy dissipation are then specified, as depicted in Figure 2-1 [Ref. /07, /24].

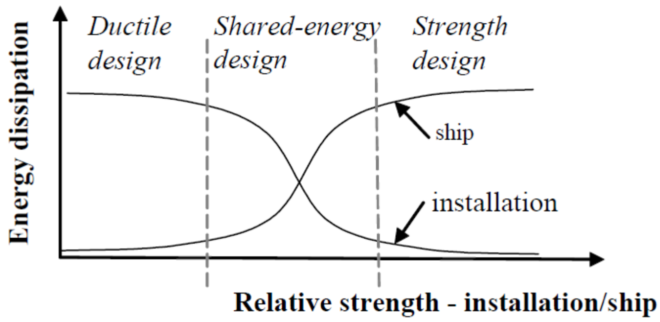

Figure 2-1 – Energy dissipation scheme (Ref. /07)

From the picture above, it can be inferred that *strength design* is when the installation is strong enough to resist the collision force with minor deformation, so that the ship is forced to deform and dissipate the major part of the energy. Strength design in some cases can be achieved with little increase in steel weight. If major part of the energy is dissipated by the platform, i.e. the ship undergoes minor deformation while the installation is forced to deform, it is called the *ductile design*.

With respect to calculation complexity the strength design or ductility design are favorable where, for both cases the response of the "soft" structure is evaluated on the basis of simple consideration of being a "rigid" structure. Meanwhile, the shared design is more complex since it includes distribution of collision forces which also depends on the deformation on both structures [Ref. /01].

In the present case the ductile design is considered as the purpose of the thesis work is to investigate ultimate strength of the jackets. It is assumed that the jacket takes all the energy and distributes the energy thorough the members (legs, braces, frames, etc.). The impact energy is given gradually until the jacket collapses. This will in particular be relevant if vessels strengthened to resist ice load is being used for supply vessels.

2.3 Strain Energy Dissipation

The strain energy dissipation is given in terms of a resistance-deformation relationship graph for both ship and the platform as illustrated in Figure 2-2. The curve is established separately assuming infinitive rigidity of the other structure. The strain energy dissipated by the ship and the structure can be evaluated by integrating the area below the curve [Ref. /07, /24].

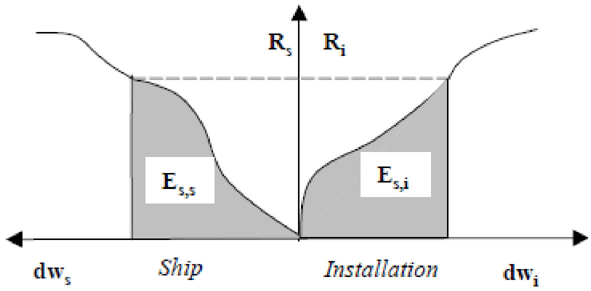

Figure 2-2 – Dissipation of strain energy in ship and platform (Ref. /07)

There are three modes of energy dissipation on which the collision effects on jacket platform analysis is based on. They are related to each other; however the analysis is carried out separately due to complexity of accounting all those effects concurrently [Ref. /01]. The three modes are as following:

1. Local denting of impacted member (cross section deformation)
2. Deformation of the structural element (bracing or leg)
3. Global deformation of the structure

If simple calculation models are used, the part of the collision energy that needs to be dissipated as strain energy can be calculated by means of the principles of conservation of momentum and conservation of energy. Plastic modes of energy dissipation shall be considered for cross sections and component/ sub-structures in direct contact with the ship [Ref. /07, /24].

2.4 Collision Forces

The interaction between impact force and structural deformation is given in Figure 2-3. The use of the curves is however limited to impact force from supply vessel with 5000 tons displacement and only for impact on jacket legs (1.5 m diameter) up to larger diameter columns (10 m diameters). Collision with smaller diameter members as jacket braces should be treated differently using different charts [Ref. /07, /24].

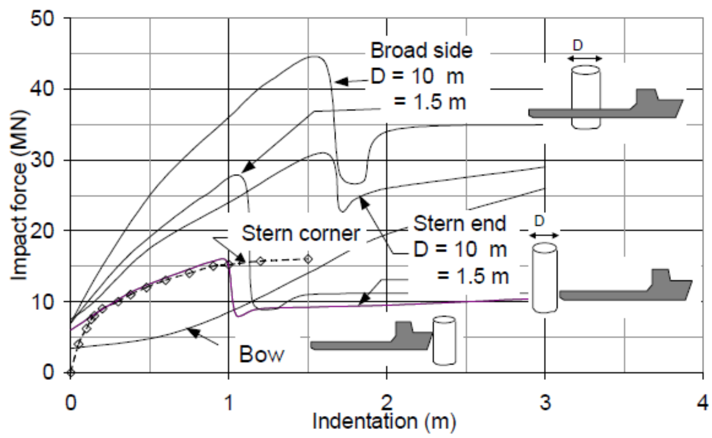

Figure 2-3 – Recommended deformation curve for beam, bow and stern impact (Ref. /07, /24)

Meanwhile, for jacket legs with diameters 1.5 m – 2.5 m the force-deformation relationship is depicted by Figure 2-4. The curves are suitable for impact of supply vessels with 2-5000 tons displacement.

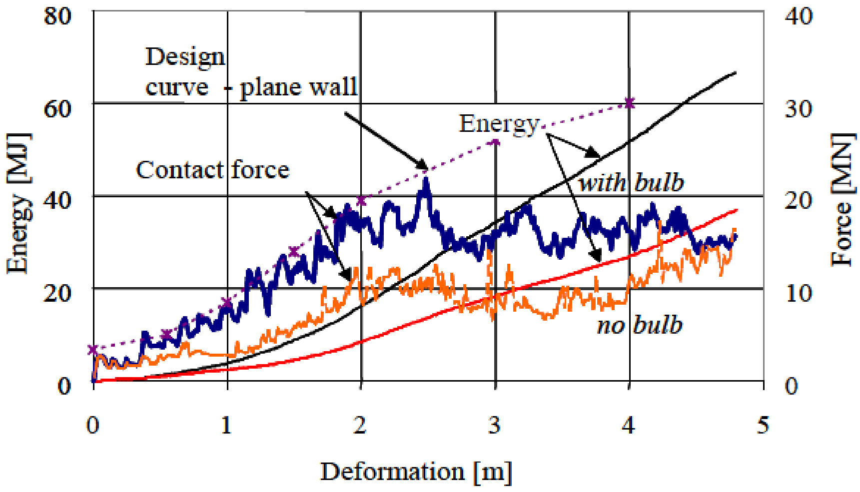

.

Figure 2-4 – Force-deformation relationship for bow with and without bulb (Ref. /07, /24)

2.5 Force – Deformation Relationship for Brace Members

The load carrying capacity of a steel beam may greatly increase due to the establishment of membrane tension forces as the beam deforms. However, in order for this to happen, it is required that the neighboring members are able to maintain connection integrity at the member ends. In other words, the joints do not fail under significant bending of the impacted member. Assuming this, the energy dissipation capacity is either limited by tension failure of the member or rupture of the connection. It is assumed that the brace dissipates the impact energy for beam, stern end, and stern corner impact.

It is quite convenient to use simple plastic methods for the analysis. The plastic force-deformation relationship for central collision (midway between nodes) for tubular members may be obtained from Figure 2-5. However, the following effects have to be given special inspection, as listed by N-004.

- Elastic flexibility of member/ adjacent structure
- Local deformation of cross section
- Local buckling
- Strength of connection
- Strength of adjacent structure
- Fracture

Taking account of the elastic axial flexibility of the member, the plastic force deformation relationship is as given by Figure 2-5.

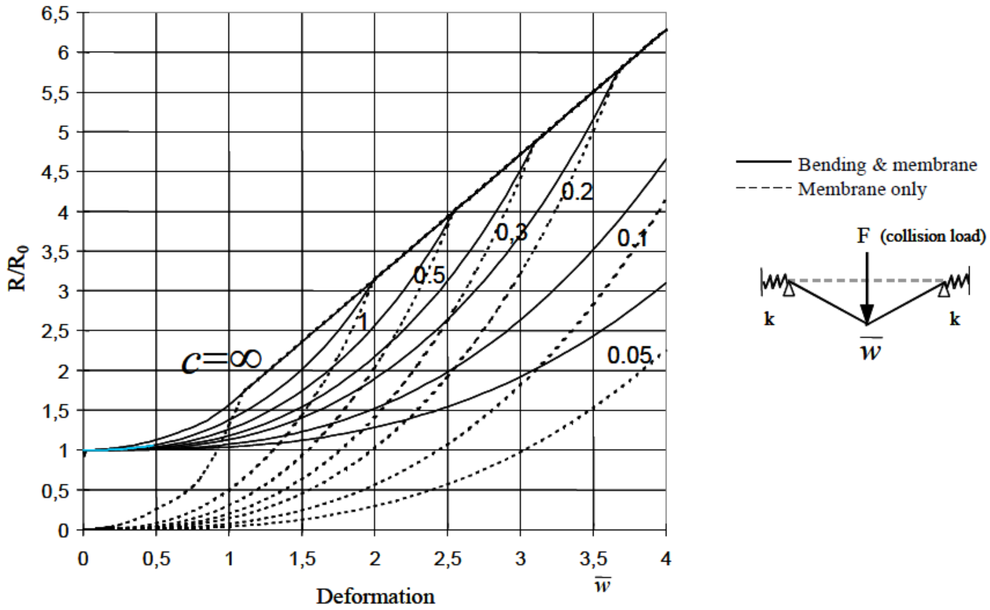

Figure 2-5 – Force-deformation relationship for tubular beam with axial flexibility (Ref. /07, /24)

Where:

$$R_0 = \frac{4c_1 M_p}{l}$$ plastic collapse resistance in bending

$$\overline{w} = \frac{w}{c_1 w_c}$$ non-dimensional deformation

$$c = \frac{4c_1 k w_c^{\,2}}{f_y A l}$$ non-dimensional spring stiffness

$$c_1 = 2$$ for clamped beam

$$c_1 = 1$$ for pinned beam

$$w_c = \frac{D}{2}$$ characteristic deformation for tubular

The effect of the elastic axial stiffness of the member is represented by k which value is determined by Equation 2-3.

$$\frac{1}{k} = \frac{1}{k_{node}} + \frac{l}{2EA}$$ Equation 2-3

The term k_{node} represents the axial stiffness of the adjacent nodes considering removal of the impacted member. In order to determine it, a unit load may be assigned at the nodes in member axial direction.

For non-central collisions the force-deformation relationship may be taken as the mean value of the force-deformation curves for central collision with member half-length equal to the smaller and the larger portion of the member length, respectively [Ref. /07]

2.6 Ductility Limit

The impacted member can take as much energy until one of the two limiting criteria is breached. The first limiting criterion is the local buckling, taking place at the compressive side of the impacted member. However the member capacity to dissipate impact energy is not simply exhausted when local buckling commences, notably for cross section Class 1 and Class 2.

If local buckling does not occur the maximum dissipated energy is limited by the second ductility limit, which is fracture. It is assumed to occur when the tensile strain exceeds the critical value due to combined effect of rotation and membrane elongation. In order to keep the moment carrying capacity during the huge plastic rotation, any member is recommended having profile proportional to Class 1 cross section. Classification of cross section class is given in DNV-OS-C101 [Ref. /08].

The ductility limits presented here are specific for tubular steel due to thesis limitation (Section 1.5). For parameter limits considering other steel profiles, such as H beam and I beam, the readers are referred to Ref. /24 section A.3.10. It should be noted that these profiles are not used in jacket design.

2.6.1 Local Buckling

The following Equation 2-4 [Ref. /07, /24] is used as criteria for a local buckling to occur. When the parameter β is less than or equal to the right-hand side of the equation, the local buckling check is not necessary.

$$\beta \le \left(\frac{14.c_f . f_y}{c_1} \left(\frac{\kappa l}{d_c} \right)^2 \right)^{\frac{1}{3}} \qquad \text{Equation 2-4}$$

The β factor and axial flexibility factor, c_f, is defined as in Equation 2-5 and Equation 2-6, respectively.

$$\beta = \frac{D/t}{235/f_y} \qquad \text{Equation 2-5}$$

$$c_f = \left(\frac{\sqrt{c}}{1+\sqrt{c}} \right)^2 \qquad \text{Equation 2-6}$$

In addition the characteristic deformation, d_c, for tubular member is defined as *diameter* of the member. Meanwhile, the value of κl is taken as the shorter length from impact point to neighboring joint. Therefore the maximum value of κl is *half* of the member length.

If the above condition is not satisfied, then local buckling is assumed to occur if the lateral deformation, w, exceeds criterion given in Equation 2-7.

$$w = \frac{d_c}{2c_f}\left(1 - \sqrt{1 - \frac{14c_f f_y}{c_1 \beta^3}\left(\frac{\kappa d}{d_c}\right)^2}\right) \qquad \text{Equation 2-7}$$

In case the axial restraint is small ($c < 0.05$) the critical deformation may be evaluated as in Equation 2-8.

$$w = \frac{3.5 d_c f_y}{c_1 \beta^3}\left(\frac{\kappa d}{d_c}\right)^2 \qquad \text{Equation 2-8}$$

2.6.2 Tensile Fracture

It is suggested in Ref. /24 that in a structure subjected to large plastic deformation, plastic strain is designed to takes place in the parent material instead of in the welded joints. This is because that the welded joints normally have defects and therefore have lower material strength than the parent material. Therefore, the value of critical strain in an axially loaded material can be used either for non-linear element analysis or simple plastic analysis, as given in Equation 2-9.

$$\varepsilon_{cr} = \left(0.02 + 0.65\frac{t}{l}\right)\frac{355}{f_y} \qquad \text{Equation 2-9}$$

In this case, l is defined as length of plastic zone. The value should be taken as equal or higher to five times of the thickness. Furthermore, rupture can be assumed to occur if deformation exceeds criterion in Equation 2-10 [Ref. /24].

$$w = \frac{d_c c_1}{2c_f}\left(\sqrt{1 + \frac{4c_w c_f \varepsilon_{cr}}{c_1}} - 1\right) \qquad \text{Equation 2-10}$$

The value of displacement factor, c_w, is calculated using Equation 2-11.

$$c_w = \frac{1}{c_1}\left(c_{lp}\left(1 - \frac{1}{3}c_{lp}\right) + 4\left(1 - \frac{W}{W_p}\right)\frac{\varepsilon_y}{\varepsilon_{cr}}\right)\left(\frac{\kappa d}{d_c}\right)^2 \qquad \text{Equation 2-11}$$

The plastic zone length factor, c_{lp}, can be determined using Equation 2-12.

$$c_{lp} = \frac{\left(\frac{\varepsilon_{cr}}{\varepsilon_y} - 1\right)\frac{W}{W_p}H}{\left(\frac{\varepsilon_{cr}}{\varepsilon_y} - 1\right)\frac{W}{W_p}H + 1} \qquad \text{Equation 2-12}$$

The parameter W and W_p denote elastic and plastic modulus, respectively. The non-dimensional plastic stiffness, H, is computed using Equation 2-13.

$$H = \frac{E_p}{E} = \frac{1}{E}\left(\frac{f_{cr} - f_y}{\varepsilon_{cr} - \varepsilon_y}\right)$$ Equation 2-13

For certain steel grades the value of ε_{cr} and H have been proposed by N-004 as presented in Table 2-1.

Table 2-1 – Proposed Value of Critical Strain and Plastic Stiffness (Ref. /24)

Steel Grade	Critical strain (ε_{cr})	Plastic Stiffness (H)
S 235	20 %	0.0022
S 355	15 %	0.0034
S 460	10 %	0.0034

3 PLASTICITY THEORY

The accidental loads often involve a high level of energy which should be dissipated by the structure and cause it to sustain deformations out of range of elastic theory. Therefore elastic analysis is no longer applicable. On the other hand, steel material has ductility character. It has the ability to resist stress larger than its yield strength and to deform on certain level of strain beyond the level of elastic strain. Consequently, plastic design method should be used as it gives more convenient approach to calculate the ultimate structural strength after yielding.

In addition, the plastic design may provide a more economically beneficial structural design. Structures analyzed using plastic methods can have significantly larger capacity to take load than those which are designed using elastic method. This results in smaller section design which eventually is resulting in less steel required [Ref. /11].

The basic theory of plasticity is presented within this chapter. It encompasses discussion about steel ductility, yield criteria, steel behavior after yielding, derivation of plastic moment capacity, hinge formation at plastic section, and “beam mechanism” several support conditions.

3.1 Material Ductility

The plastic method is used to investigate the total resistance of a cross section against a given load. Unlike the elastic method where the structural strength analysis is carried out until the first yield of the cross section occurs, the plastic method continues the evaluation of capacity until the whole cross section yields. This is due to the fact that when the cross section yields the structure does not instantly collapse. In addition, Caprani (2010) wrote that an indeterminate structure may still be able to carry load larger than the load that causes first yield at any point in the cross section. The load then will be distributed to other parts of the cross section which has not yielded yet and the structure can still stand as long as it can find redundancies to yield. When all redundancies have been exhausted, the structure cannot take any more loads. The continuation of loading will cause the structure to fail.

The above explanation becomes viable because of the special character of steel material called *ductility*; the theory plasticity is based on. This special behavior enables steel to elongate to a certain degree beyond the yield strain. The elongation can be very large without creating any fracture. In order to illustrate the principal of ductility, a typical idealized stress-strain relationship is depicted in Figure 3-1.

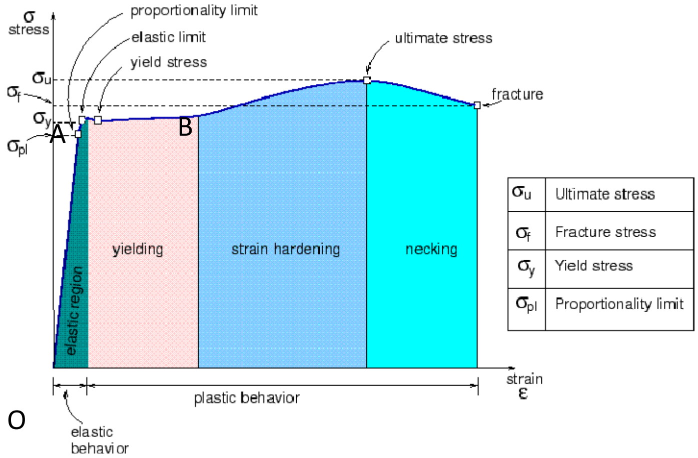

Figure 3-1 – Typical stress-strain relationship for steel in tension (Ref. /13)

From the figure above it can be seen that the steel starts to deform in linear elastic relationship from point O up to point A, known as yield point. At this point yield stress (σ_y) occurs and results in corresponding yield strain (ε_y). Within this region the strain grows proportionally with the given stress. When the load is taken off, the structure will deform back into its initial condition (point O).

Beyond point A, the steel continues to deform even if the stress remains constant or almost constant as showed in the Figure 3-1. The stress from this point equals to yield stress. The elongation extends up to point B where the minimum strain level at this point is ten times the yield strain at point A [Ref. /11]. After point B, in order to stretch the steel even further more stress is required and physically this means that the structure is capable to carry more loads. Strain hardening will commences as load is given beyond point B and may continue up to peak point where the ultimate stress occurs. Due to ductility property, the stress may continue until the fracture point is reached and the failure stress occurs.

3.2 Yield Criteria

Five main yielding criteria are described by Boresi (2003) in Ref. /04 as listed below:

- Maximum principal stress criterion

  The criterion is also known as Rankie's criterion. It states that yielding starts when the principal stress (whether tension or compression) at one point in the member reaches the level of yield stress. The illustration of principal stress acting at a point is given in Figure 3-2.

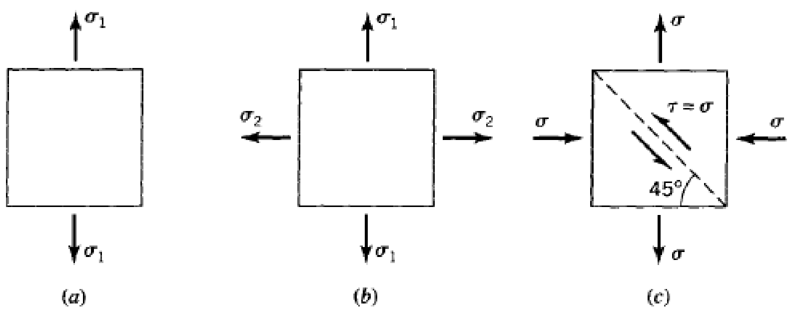

Figure 3-2 – Principal stresses at a point (Ref. /04)

A condition of uniaxial stress is represented in Figure 3-2a with a non-zero principal stress σ_1 acting at a point of a steel structure. Based on this criteria, the point starts to yield when the value of σ_1 equals the value of yield stress σ_Y. Meanwhile, a condition of biaxial stress is given in Figure 3-2b where another principal stress σ_2 exists. In case the value of σ_1 is greater than σ_2, yielding starts when σ_1 balances the yield stress of the material, regardless the presence of σ_2 and vice versa. If the magnitude of σ_2 equals to σ_1 but in opposite direction, a shear stress (τ) will occur in direction of the diagonal, as depicted in Figure 3-2c. The value of shear stress is equal to σ_1. This means that the value of yield shear stress τ_Y is also equal to σ_Y which is unrealistic for ductile material.

For tri-axial stress condition, the maximum principal stress criterion can be expressed the yield function as in Equation 3-1, and is illustrated in Figure 3-3.

$$f = \sigma_e - \sigma_Y \qquad \text{Equation 3-1}$$

Where;

$$\sigma_e = \max(|\sigma_1|, |\sigma_2|, |\sigma_3|) \qquad \text{Equation 3-2}$$

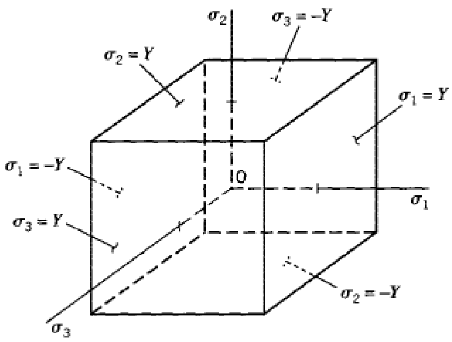

Figure 3-3 – Illustration of principle stress criterion in six-plane surface[1] (Ref. /04)

- Maximum principal strain criterion

This criterion is also known as St. Venant's criterion and has similar principle as previous criterion. It states that yielding begins to occur when the value of maximum principal strain at one point in a structure equals the yield strain of the material. The stress – strain relationship at yield condition is given in Equation 3-3.

$$\varepsilon_Y = \frac{\sigma_Y}{E} \qquad \text{Equation 3-3}$$

Hence, from Figure 3-2a it can be inferred that yielding starts when the value of σ_1 equals σ_Y which means that ε_1 equals ε_Y. Considering an isotropic material under biaxial stress as in Figure 3-2b, the maximum principal strain criterion is expressed as in Equation 3-4.

[1] Yield stress is symbolized with Y in the reference while in this thesis report yield stress is symbolized with σ_Y

$$\varepsilon_1 = \frac{\sigma_1}{E} - \upsilon\left(\frac{\sigma_2}{E}\right)$$ Equation 3-4

From the equation above it can be inferred that if the second principal stress (σ_2) is positive (tension), yielding starts at the value of the first principal stress which is larger than the yield stress ($\sigma_1 > \sigma_Y$). On the other hand, if the second stress is negative (compression), yielding starts at the value below the yield stress.

In order to express the principal strain criteria in form of yield stress function, both sides of Equation 3-4 are multiplied with modulus elasticity (E) and becomes Equation 3-5, assuming ε_1 is larger than ε_2 and associating it with yield strain $(\varepsilon_1 \equiv \varepsilon_Y)$.

$$\sigma_Y = \sigma_1 - \upsilon\sigma_2$$ Equation 3-5

Therefore, the yield function can be expressed as in Equation 3-6, with expression of effective stress is given by Equation 3-7.

$$f = \sigma_e - \sigma_Y$$ Equation 3-6

$$\sigma_e = \max_{i \neq j}\left|\sigma_i - \upsilon\sigma_j\right|$$ Equation 3-7

Figure 3-4 illustrates yield surface for principal strain criterion under biaxial stress state.

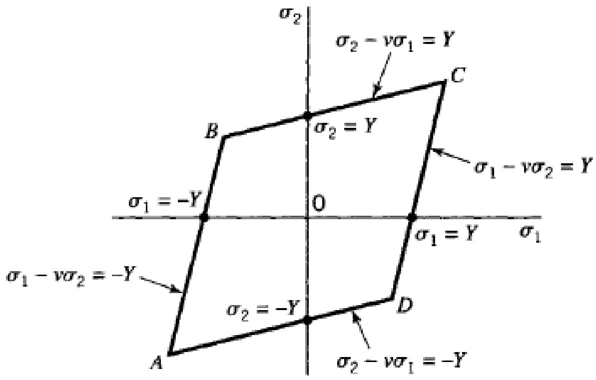

Figure 3-4 – Surface of principal strain criterion under biaxial stress state (Ref. /04)

- Strain-energy density criterion

  Under this criterion, yielding is predicted to occur at a point if the strain-energy density at the point is equal to energy density at yield in uniaxial stress (tension or compression). The formula of strain energy density in terms of principal stresses is given in Equation 3-8[2].

$$U_0 = \frac{1}{2E}\left[\sigma_1^2 + \sigma_2^2 + \sigma_3^2 - 2\upsilon\left(\sigma_1\sigma_2 + \sigma_1\sigma_3 + \sigma_2\sigma_3\right)\right] > 0$$ Equation 3-8

[2] For complete derivation of this equation, readers are referred to Boresi, Ref. /04 chapter 3.3.2

The strain-energy density criterion requires Equation 3-8 to be equal with Equation 3-9 and so becomes Equation 3-10.

$$U_{0Y} = \frac{1}{2E}\sigma_Y^{\ 2} \qquad \text{Equation 3-9}$$

$$\sigma_Y^{\ 2} = \left[\sigma_1^{\ 2} + \sigma_2^{\ 2} + \sigma_3^{\ 2} - 2\upsilon\left(\sigma_1\sigma_2 + \sigma_1\sigma_3 + \sigma_2\sigma_3\right)\right] \qquad \text{Equation 3-10}$$

Therefore, yield function can be expressed by Equation 3-11 with effective stress is as given in Equation 3-12.

$$f = \sigma_e^{\ 2} - \sigma_Y^{\ 2} \qquad \text{Equation 3-11}$$

$$\sigma_e = \sqrt{\sigma_1^{\ 2} + \sigma_2^{\ 2} + \sigma_3^{\ 2} - 2\upsilon\left(\sigma_1\sigma_2 + \sigma_1\sigma_3 + \sigma_2\sigma_3\right)} \qquad \text{Equation 3-12}$$

In state of biaxial stress, the strain energy density yield surface is depicted in Figure 3-5.

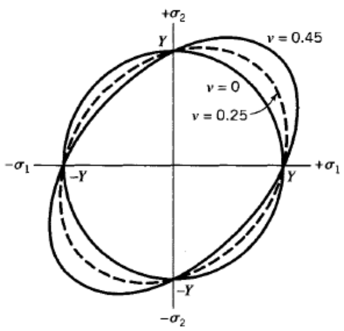

Figure 3-5 – Yield surface of strain-energy density in biaxial state (Ref. /04)

- Maximum shear-stress criterion

This criterion is also known as *Tresca criterion*, which states that yielding commences when maximum shear stress at a point equals yield shear stress in uniaxial stress state. The expression of maximum shear stress in multiaxial and uniaxial stress is given by Equation 3-13 and Equation 3-14, respectively.

$$\tau_{\max} = \frac{\sigma_{\max} - \sigma_{\min}}{2} \qquad \text{Equation 3-13}$$

$$\tau_{\max - uni} = \frac{\sigma_Y}{2} \qquad \text{Equation 3-14}$$

Furthermore, equating the above equations results the yield stress function of Tresca criterion as expressed in Equation 3-15. It should be noted that the maximum and minimum stress in Equation 3-13 correspond to the largest and smallest principal stress, respectively. It can be inferred also from the equation that the effective stress σ_e is represented by the maximum shear stress $\tau_{\max}$.

$$f = \tau_{\max} - \frac{\sigma_Y}{2}$$ Equation 3-15

- Distortional energy density criterion

  The strain energy density in Equation 3-8 can be decomposed into two parts as expressed in Equation 3-16[3]. The first part of the equation causes volumetric change (U_v) and the second part of the equation causes distortion (U_D). The distortional energy density criterion, known also as *von Mises' criterion* states that "yielding starts when distortional strain energy density at a point equals the distortional strain-energy density at yield in uniaxial stress" (Boresi, p.120).

$$U_0 = \frac{\left(\sigma_1^{\,2} + \sigma_2^{\,2} + \sigma_3^{\,2}\right)^2}{\dfrac{6E}{1-2\upsilon}} + \frac{(\sigma_1 - \sigma_2)^2 + (\sigma_2 - \sigma_3)^2 + (\sigma_3 - \sigma_1)^2}{\dfrac{6E}{1+\upsilon}}$$ Equation 3-16

Introducing shear modulus as in Equation 3-17, distortional strain energy density can be expressed as in Equation 3-18.

$$G = \frac{E}{2(1+\upsilon)}$$ Equation 3-17

$$U_D = \frac{(\sigma_1 - \sigma_2)^2 + (\sigma_2 - \sigma_3)^2 + (\sigma_3 - \sigma_1)^2}{12G}$$ Equation 3-18

For uniaxial state, U_D is expressed as in Equation 3-19.

$$U_{D-uni} = \frac{\sigma_Y^{\,2}}{6G}$$ Equation 3-19

In short[4], the yield stress function given by this criterion is expressed by Equation 3-20, and the effective stress is given by Equation 3-21.

$$f = \sigma_e^{\,2} - \sigma_Y^{\,2}$$ Equation 3-20

$$\sigma_e = \sqrt{\frac{1}{2}\left[(\sigma_1 - \sigma_2)^2 + (\sigma_2 - \sigma_3)^2 + (\sigma_3 - \sigma_1)^2\right]}$$ Equation 3-21

The illustration of Tresca and von Misses criterion is given in Figure 3-6.

[3] Complete derivation of this equation can be found in Ref. /17
[4] For complete derivation, the readers are referred to Boresi, p. 120 – p.121.

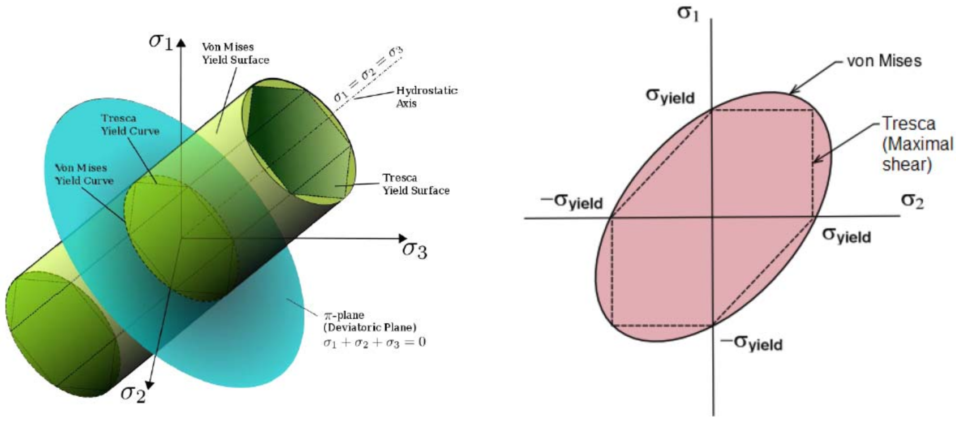

Figure 3-6 – Yield surface for Tresca and von Misses criterion (Ref. /12)

3.3 Material Behaviour during Application of Bending

Cross section of a structure subjected to a bending moment behaves differently following the applied bending level. Caprani (2011) described this behavior in 5 stages as listed below:

1. Elastic stage

   During this stage bending stress is less than yield stress. Material behaves elastically.

2. Yielding stage

   If condition in stage 1 continues and bending stress is increased, the outermost fibers of the cross section start to yield. Meanwhile, the other fiber on the cross section have not yield yet and still behave elastically.

3. Elastic-plastic stage

   If bending from stage 2 increases above the level of yield stress, yielding will spread to other part of the cross section towards the neutral axis. Neutral axis is defined as imaginary line separating the region of tensile stress and compressive stress on the cross section. At this stage, plastic and elastic region exist subsequently on the cross section.

4. Plastic stage

   At this stage, all cross section have become plastic. “Any attempt at increasing the moment at this point simply results in more rotation, once the cross-section has sufficient ductility. Therefore in steel members the cross section classification must be plastic” (Caprani, 2011, p.8 – p.9).

5. Strain hardening stage

   Two things happen when the load is continued to be given to a steel material after the yield point is reached. “As the material is loaded beyond its yield stress, it maintains an ability to resist additional strain with an increase in stress. This response is called strain hardening. At the same time the material loses cross sectional area owing to its elongation. This area reduction has a softening (strength loss) effect, measured in terms of initial area” (Boresi, 2003, p. 11). From point B up to the ultimate stress point, the strain hardening is more dominant than the softening effect (Figure 3-1). However, after the ultimate stress point is exceeded, the softening effect becomes greater and thereby decrease the load carrying capacity until the structure fails at the fracture point.

3.4 Elastic-plastic Moment Capacity and Shape Factor

The derivation of elastic-plastic moment capacity is based on the assumption that the material behaves elastic-perfectly plastic when subjected to a bending moment. Illustration of stress-strain relationship for an elastic-perfectly plastic material is given in Figure 3-7. "Perfectly plastic materials follow Hook's law upto the limit of proportionality.The slopes of stress-strain diagrams in compression and tension i.e. the values of Young's modulus of elasticity of the material, are equal. Also the values of yield stresses in tension and compression are equal. The strains upto the strain hardening in tension and compression are also equal. The stress strain curves show horizontal plateau both in tension and compression" [INSDAG, p.35-2].

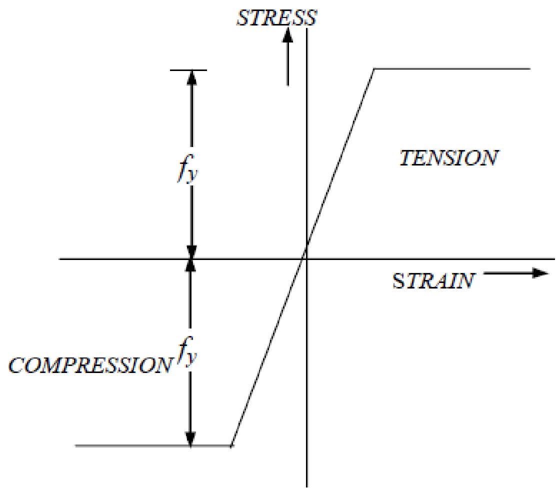

Figure 3-7 – Stress – strain relationship for an elastic-perfectly plastic material (Ref. /11)

The moment capacity of elastic-plastic material is simply an addition of moment capacity of the plastic region to moment capacity of the elastic region, as expressed in Equation 3-22. In addition, a rectangular cross section is chosen for simplification of deriving the elastic-plastic moment capacity, as depicted in Figure 3-8.

$$M_{EP} = M_{elastic} + M_{plastic} \qquad \text{Equation 3-22}$$

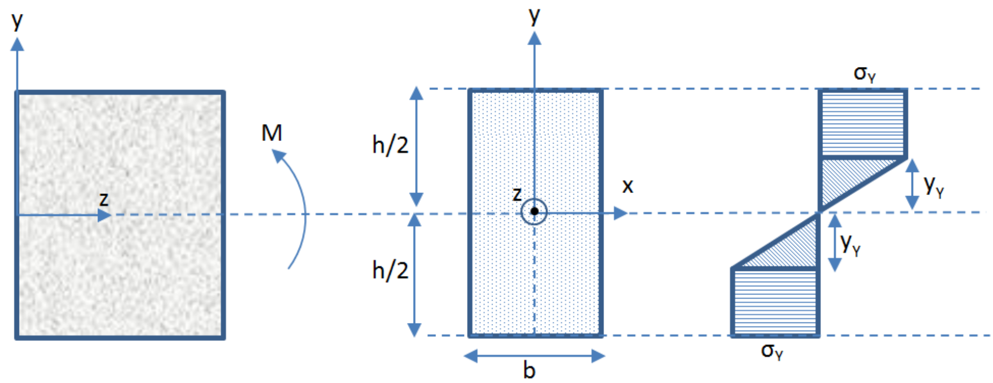

Figure 3-8 – Elastic-plastic diagram for a rectangular cross section

The figure above shows a beam having rectangular cross section with height (h) and width (b), subjected to a bending moment working around the x-axis (left side of the picture). The applied bending moment causes a stress perpendicular to cross section (σ_{zz})[5]. The elastic-plastic stress diagram is shown by picture in the right. Assuming elastic-perfectly plastic material property, the tension on the lower part of cross section equals the compression on the upper part of the beam. In addition, elastic and plastic region on the compression side have same area with those in tension side. The border between elastic and plastic area is shown by y_Y. Taking moment equilibrium around *x-axis*, equation of elastic-plastic moment capacity in Equation 3-22 can be expanded into Equation 3-23.

$$M_{EP} = 2\int_{0}^{y_Y} y \cdot \sigma_{zz} dA + 2\int_{y_Y}^{\frac{h}{2}} y \cdot \sigma_Y dA \qquad \text{Equation 3-23}$$

The perpendicular stress in elastic region (σ_{zz}) can be expressed in term of yield stress (σ_Y) using the similar triangle principle as shown in Figure 3-9.

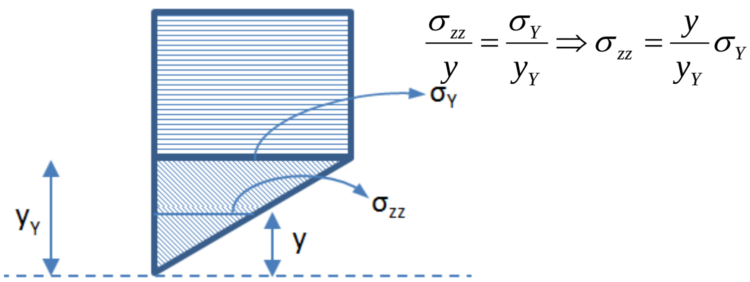

Figure 3-9 – Similar triangle principle

By substitution of σ_{zz} from figure above to Equation 3-23, and by evaluating the integral, the elastic plastic moment is expressed as in Equation 3-24.

$$M_{EP} = 2\sigma_Y b\left(\frac{h^2}{8} - \frac{{y_Y}^2}{6}\right) \qquad \text{Equation 3-24}$$

Therefore, plastic moment (at $y_Y = 0$) and moment at initiation of yielding (at $y_Y = \frac{h}{2}$) is given by Equation 3-25 and Equation 3-26, respectively.

$$M_P = \frac{1}{4}\sigma_Y bh^2 \qquad \text{Equation 3-25}$$

$$M_Y = \frac{1}{4}\sigma_Y bh^2 \frac{2}{3} \qquad \text{Equation 3-26}$$

Apparently, it can be seen the relation between plastic moment and yielding moment as expressed in Equation 3-27.

[5] The naming of the stress component follows convention as in Boresi, Ref. /04.

$$M_P = \frac{3}{2} M_Y \qquad \text{Equation 3-27}$$

In a more general form, the relation of yield-plastic moment capacity can be expressed as in Equation 3-28 , with α denotes shape factor.

$$M_P = \alpha \cdot M_Y \qquad \text{Equation 3-28}$$

Plastic moment capacity can also be derived in terms of *plastic modulus section (Z)* by re-arranging Equation 3-25 into Equation 3-29.

$M_P = Z\sigma_Y$; where Equation 3-29

$$Z = \frac{1}{4} bh^2 \qquad \text{Equation 3-30}$$

Similarly, moment at initiation of yielding can also be presented in terms of *elastic modulus section (W)* as in Equation 3-31.

$M_Y = W\sigma_Y$; where Equation 3-31

$$W = \frac{1}{6} bh^2 \qquad \text{Equation 3-32}$$

Shape factor can also be derived by taking ratio between *plastic and elastic modulus section* as in Equation 3-33.

$\alpha = \frac{Z}{W}$; where Equation 3-33

For rectangular cross section, the shape factor is 1.5. The values of shape factor for other cross sections are listed in Table 3-1.

Table 3-1 – Several values of shape factor for different cross sections (Ref. /26)

Cross section	α
Square Tube	1.125
Rigid Circular	1.70
Circular Tube	1.27
I-Beam	1.10 – 1.17

3.5 Plastic Hinge Formation

"At the plastic hinge an infinitely large rotation can occur under a constant moment equal to the plastic moment of the section. Plastic hinge is defined as a yielded zone due to bending in a structural member at which an infinite rotation can take place at a constant plastic moment M_p of the section. The number of hinges necessary for failure does not vary for a particular structure subject to a given loading condition, although a part of a structure may fail independently by the formation of a smaller number of hinges. The member or structure behaves in the manner of a hinged mechanism and in doing so adjacent hinges rotate in opposite directions" (INSDAG, p.35-8).

A simply supported beam is used to illustrate the formation of plastic hinge in a member structure as depicted in Figure 3-10. The beam has rectangular cross section and subjected to a point load *W* at the middle of the span. The total length of the beam is denoted with *L*.

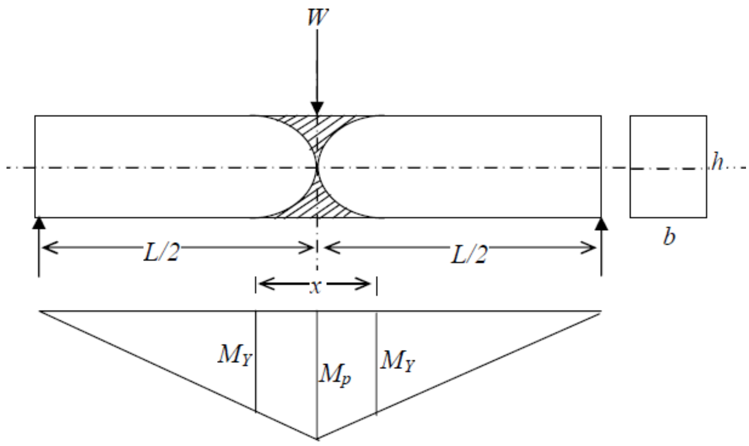

Figure 3-10 – Plastic hinge formation in a simply supported beam (Ref. /11)

As the load *W* increases, the section in-line with the direction of load will be the first that reaches full plastic moment. In the figure above, since the point load is applied precisely at the center of the beam, the largest bending moment occurs in there and therefore the first plastic hinge will be formed at *L/2*. *Length of plastic zone* is denoted by *x*.

The length of the plastic zone can be determined using the similar triangle principle for Figure 3-10, as expressed in Equation 3-34.

$$\frac{M_Y}{\frac{L}{2}-\frac{x}{2}}=\frac{M_p}{\frac{L}{2}}$$ Equation 3-34

Hence;

$$\frac{M_Y}{M_p}=\frac{\frac{L}{2}-\frac{x}{2}}{\frac{L}{2}}\Rightarrow\frac{M_Y}{M_p}=1-\frac{x}{L}$$

$$(L-x)M_p=L\cdot M_Y$$ Equation 3-35

For rectangular cross section, yield moment is two-third of the plastic moment (Equation 3-27), so Equation 3-35 can be written as in Equation 3-36. Therefore, the length of the plasticity zone is given by Equation 3-37.

$$(L-x)M_p=L\cdot\frac{2}{3}\cdot M_p$$ Equation 3-36

$$x = \frac{1}{3}L$$ Equation 3-37

In more general form, Equation 3-35 can be expanded by inserting the value of plastic moment as in Equation 3-28 and result in Equation 3-38. Therefore the length of the plasticity zone in terms of shape factor is expressed in Equation 3-39.

$$(L - x) \cdot \alpha \cdot M_Y = L \cdot M_Y$$ Equation 3-38

$$x = \frac{L \cdot (\alpha - 1)}{\alpha}$$ Equation 3-39

3.6 Beam Mechanism

A *mechanism* is defined as condition where there is no more resistance against rotation in the structure. The formation of mechanism marks the collapse resistance of a structure [Ref. /11]. The illustration of mechanism formation on a beam loaded with a point load is given by Figure 3-11.

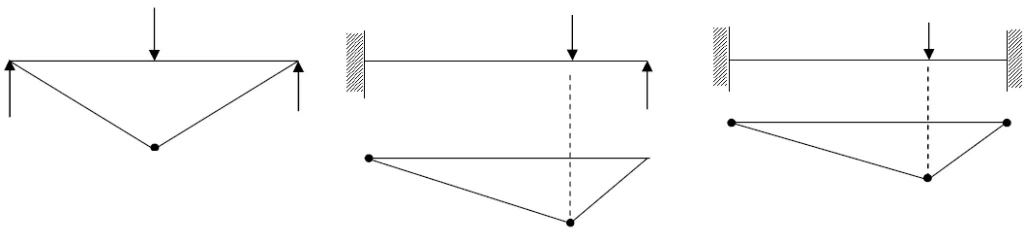

Figure 3-11 – Beam mechanism for several support conditions (Ref. /11)

The left-hand part of the picture above shows mechanism for a simply supported beam loaded with point load at any point through the length of the member. Maximum bending occurs at the point where the load is applied, and in addition, the cross section at this point will be the first part of the structure that becomes plastic (plastic hinge formed). Once the cross section becomes plastic, a large rotation will occur at the support. However, simple supports cannot take moment so they are not available to resist rotations. On the other words, it can be said that the structure fails. Therefore a simply supported structure has no redundancy; it fails immediately as one hinge is formed.

The figure at the middle shows a beam structure with fix support at one end and simple support at the other end. The loading condition is the same as the figure in the left. Depending on the location of the point load, the first plastic hinge formation occurs either at the point of loading or at the fixed end. If one hinge is formed “below” the load level, for example at the point of loading, then the “remaining” of the load is transferred to the fixed end. At this level, the structure is not collapse yet because the rotation can still be resisted by the fixed end. Only if the loading is continued until the fixed end is plasticized and therefore another plastic hinge is formed, the structure is said to be collapse. The load level causing these two plastic hinges to form is called the collapse load. This type of structure is called to have 1 redundancy. Two plastic hinges are needed to collapse the structure.

The figure at the right hand side of the picture above shows a beam structure with fixed support at both ends. The loading condition is the same as the previously described. In this case, the structure has two redundancies at the end supports. Therefore 3 hinges are needed to make the structure collapse.

4 SURVEY OF SUPPLY VESSELS

The NCS, mainly North Sea and Norwegian Sea area, is a busy maritime area with many vessels travelling every day, not only supply vessels, but also other types of vessel such as tankers, fishing vessels, and cruise ship. Figure 4-1 gives a description of the marine activities on NCS. It is important to notice that the figure only gives an illustration of marine traffic conditions at one specific time. The condition may be very different at other times because the figure was taken from a screen capture of a live map, giving real time position of the vessels.

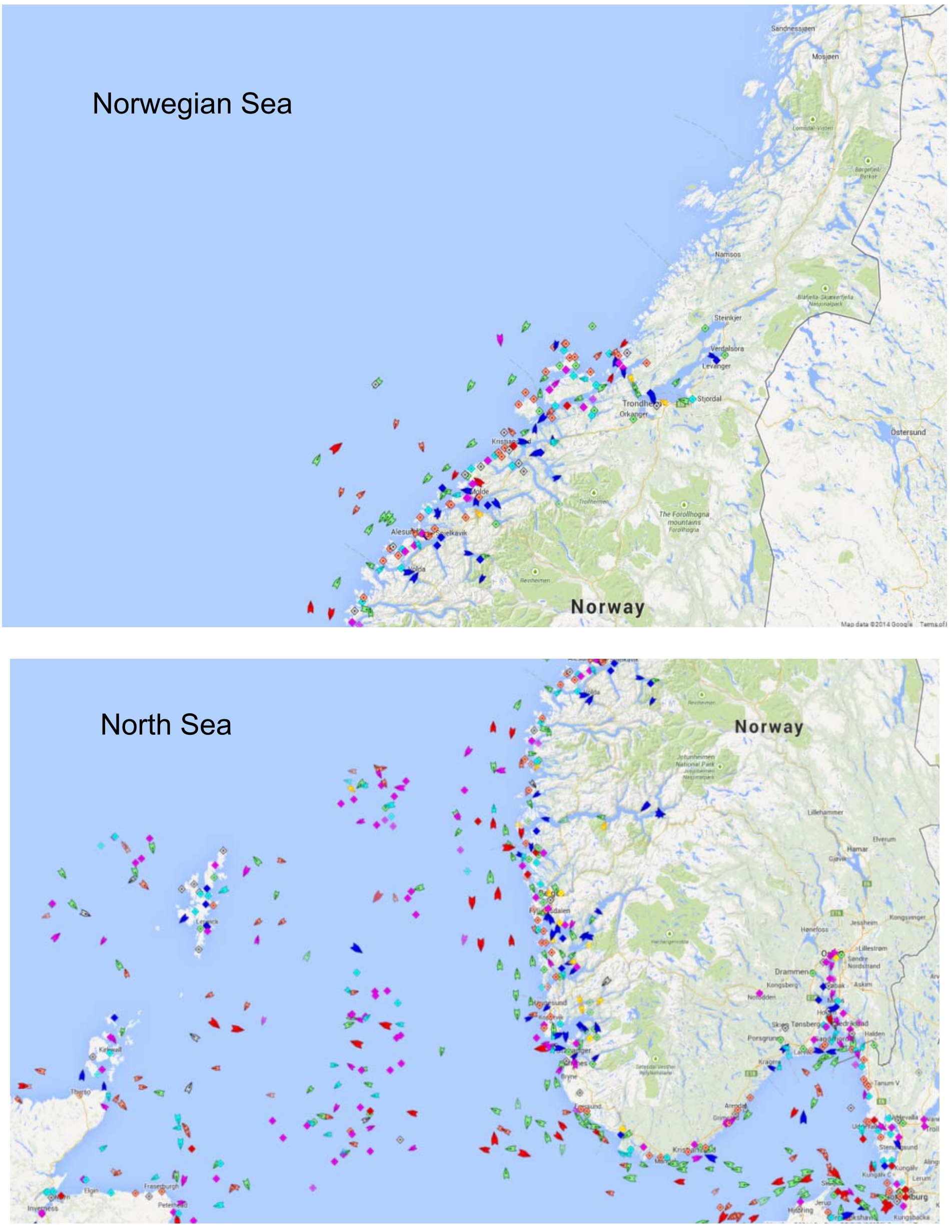

Figure 4-1 – Maritime Activities in Norwegian Continental Shelf (Ref. /28)

Different colors on the figure above denote type of ship. Supply ships belong into the same group as cargo ship, and are denoted green. Red and blue triangles denote tankers and passenger vessels, respectively.

A survey of supply vessels has been carried out and the result is presented within this chapter. The area of survey is NCS which encompasses North Sea and Norwegian Sea. The survey is intended to investigate the latest development of supply vessel in terms of deadweight.

Collision characteristic is discussed in the first part of this section. Several impact scenarios are described within. Further, the result of the survey is presented in the forms of a scatter diagram and a pie chart. In the last section of this chapter, the impact energy is evaluated for several vessel velocities. The results are presented also in form of scatter diagrams.

4.1 Collision Characteristics

According to IAOGP [Ref. /10], the collisions may be categorized as *powered collision* and *drifting collision*. "Powered collisions include navigational/ maneuvering errors, watch keeping failure, and bad visibility/ ineffective radar use. A drifting vessel is a vessel that has lost its propulsion or steerage, or has experienced a progressive failure of anchor lines or towline and is drifting only under influence of environmental forces" (IAOGP, 2010).

The collision of supply vessel is most likely to happen in splash zone [Ref. /27] with scenario as following:

- Broadside impact on one of the legs
- Bow impact on braces
- Stern impact on braces

Figure 4-2 illustrates impact scenario for stern (a), bow (b), and side (broadside) (c) impact.

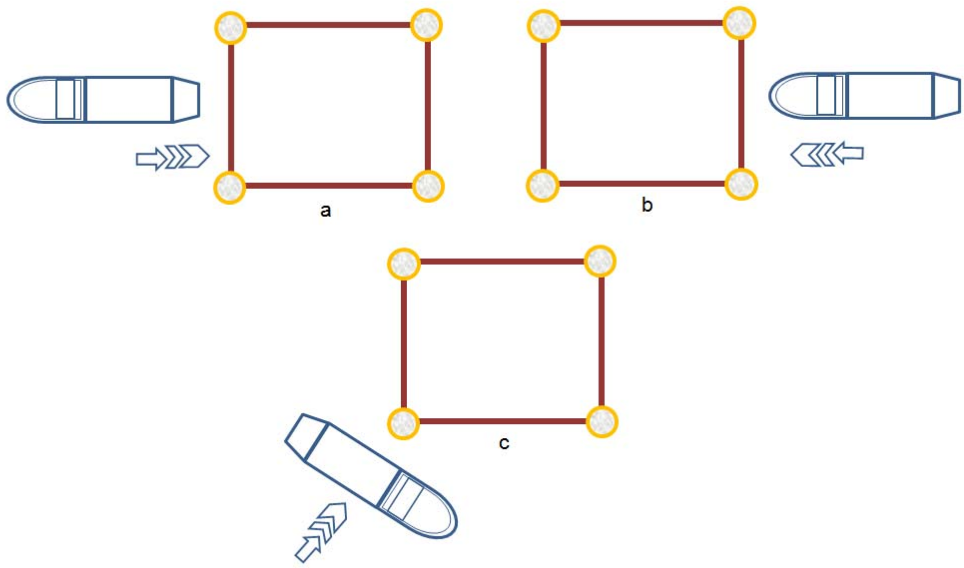

Figure 4-2 – Illustration of Impact Scenarios

In this thesis, the structures will be subjected to high impact energy to see how much impact energy a platform can withstand before it collapses, disregarding whether the energy is due to bow, stern, or broadside impact. The only differentiating situation is the location of impact; jacket brace or leg, and whether the ship will hit the member at the mid span (weak point) or at the joint (strong point).

4.2 Trend of Supply Vessels in NCS

The data for the survey is gathered from *marinetraffic.com* [Ref. /29] which provides real time position of various types of vessel operating throughout the globe, as well as physical data of each vessel. There are 115 vessels operating in the North Sea and Norwegian Sea area encompassed in the survey. Verification has been made for each supply vessel to ensure that one particular vessel operate in North Sea or Norwegian Sea.

The survey result is represented in a graph in Figure 4-3, showing deadweight development of supply vessels as function of year of construction. It should be noted also that there are very few vessel built before 1995. One of the reasons is that they are no longer in operation. The more complete survey result, comprising vessel name and dimensions, is tabulated in APPENDIX A.

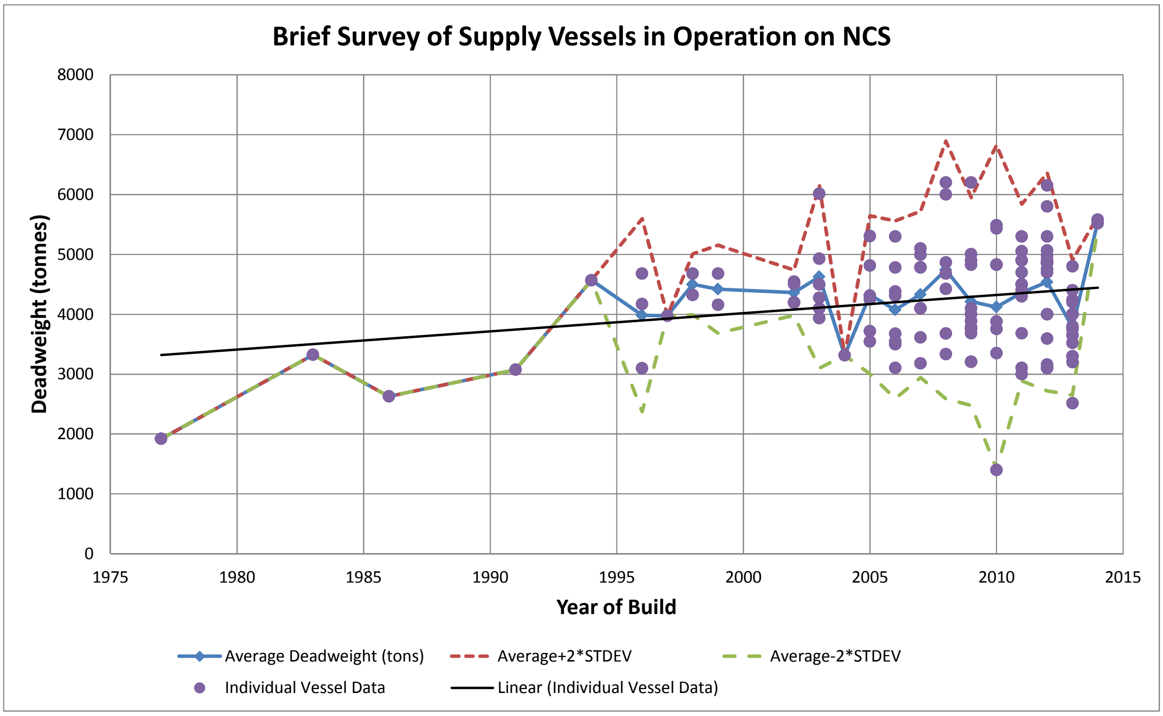

Figure 4-3 – Weight development of supply vessels in North Sea and Norwegian Sea

From the Figure 4-3 above, it is obvious that over the past 40 years, there has been an increase of large supply vessels on the NCS. Most of the vessels have *deadweight tonnages* (DWT) between 4000 tons and 5000 tons, mainly after the millennium. Their number is 54 vessels. This corresponds to 47% of the data. However, there is a quite high percentage of supply vessel having DWT more than 5000 tons. Their number is as much as 15% or equivalent to 17 vessels out of 115 vessels. The rest of the vessels have DWT less than 4000 tons. Figure 4-4 describes the distribution of supply vessels with respect to DWT. Numbers 1, 2, and 3 represent DWT range above 5000 tons, 4000 – 5000 tons, and below 4000 tons, respectively.

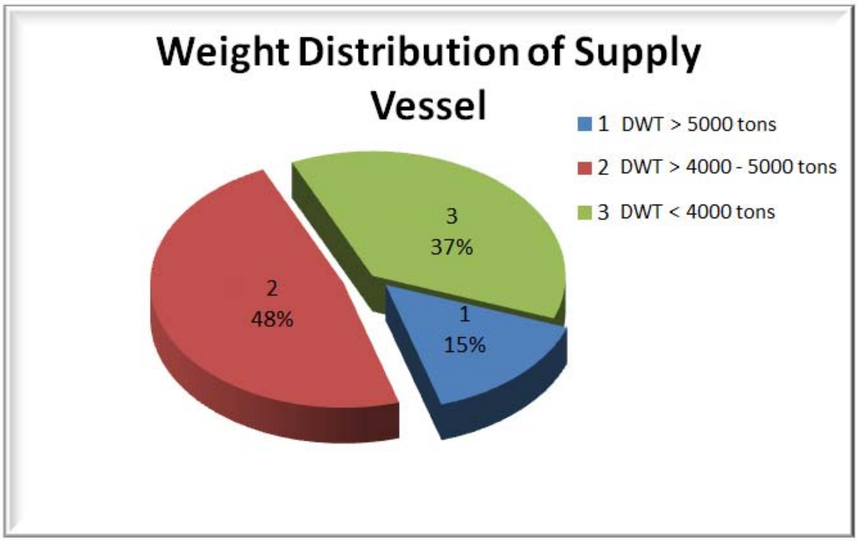

Figure 4-4 – Weight Distribution of Supply Vessels

Viking Lady and Skandi Seven are two of the surveyed vessels having the largest DWT. They have 6200 tons and 6000 tons DWT, respectively. Both vessels operate in North Sea. Photos of Viking Lady and Skandi Seven are depicted in Figure 4-5.

Figure 4-5 – Photo of Viking Lady and Skandi Seven (Ref. /28)

4.3 Evaluation of Impact Energy

The impact energy is expressed in kinetic energy and should be transferred in forms of absorbed energy by vessel (E_v), platform (E_s), and fendering system (E_f). In mathematical form, this relation is expressed by Equation 4-1.

$$E_k = E_s + E_v + E_f \qquad \text{Equation 4-1}$$

Normally a jacket platform is equipped with a fendering system in the boat landing area. This system is provided to resist design impact energy due to approaching vessels in regular basis during the operating phase. However, it is not common for jacket platforms in NCS to be outfitted with fendering system. In addition, this thesis focuses on the accidental case where the vessel hit the jacket at random locations. Hence, it is reasonable to exclude the contribution of fendering system in terms of its capacity to absorb impact energy. The last term of Equation 4-1 (E_f) can therefore be omitted.

In general, the impact energy will be shared between the installation and the vessel. It is due to the fact that in some degree part of the ship (bow, stern, or broadside, depends on the impact situation) can be crushed and undergoes huge deformation. Picture of Big Orange XVIII in Figure 1-1 can be referred as example. However the amount of energy that the ship has to dissipate is hard to determine. There is also a big uncertainty in terms of how large the vessel that will hit the jacket. Therefore it is assumed in this thesis that all kinetic energy will be taken by the installation. This assumption makes the analysis even more conservative but for the sake of safety, it is worth to assume.

According to the explanation in above paragraph, the absorbed energy by vessel (E_v) can also be omitted from Equation 4-1. This leaves the equation of kinetic energy with only one last term which is the energy absorption by the platform (E_s), which can be evaluated using equation of kinetic energy in Section 2.2. From there it is obvious that there are two important aspects in regard with kinetic energy of the collision. The first aspect is velocity at impact and the second one is added mass. NORSOK N003 states that for ALS design check, the impact speed should be taken 2 m/s as minimum and the added mass is taken 10% for bow and stern impact and 40% for broad side impact.

Nowadays, some supply vessels operating in North Sea are equipped with ice strengthening bow. Classified as DNV's ICE-C vessels, they are designed to be able to operate in light ice condition. Example of such vessels are Skandi Seven (Figure 4-5), Rem Fortress, and Rem Leader (Figure 4-6). This emphasizes that, due to a very strong bow, the impact energy will all be absorbed by the structure.

Figure 4-6 – Photo of Rem Fortress and Rem Leader (Ref. /31)

Using minimum NORSOK criteria as above, the impact energy for Viking Lady and Skandi Seven is tabulated in Table 4-1.

Table 4-1 – Impact Energy for Viking Lady and Skandi Seven

Vessel	Impact Energy Bow/ Stern Impact (MJ)	Impact Energy Broadside Impact (MJ)
Viking Lady	13.6	17.4
Skandi Seven	13.2	16.8

However, taking only the minimum speed is quite overconfident. In a real accident case the speed may be higher like in Big Orange XVIII and Far Symphony case. The recorded speed at impact was 9.3 knots (4.8 m/s) and 7.3 knots (3.8 m/s), respectively. In consequence, the resulting impact energy may become much higher. The impact energy evaluated for surveyed supply vessel for velocity 2 m/s, 3.8 m/s, and 4.8 m/s are presented in

Figure 4-7.

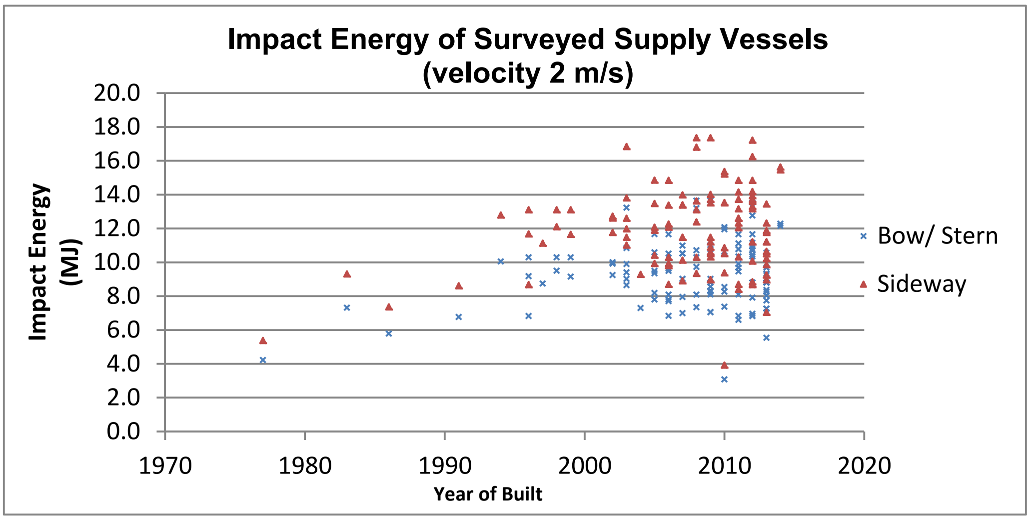

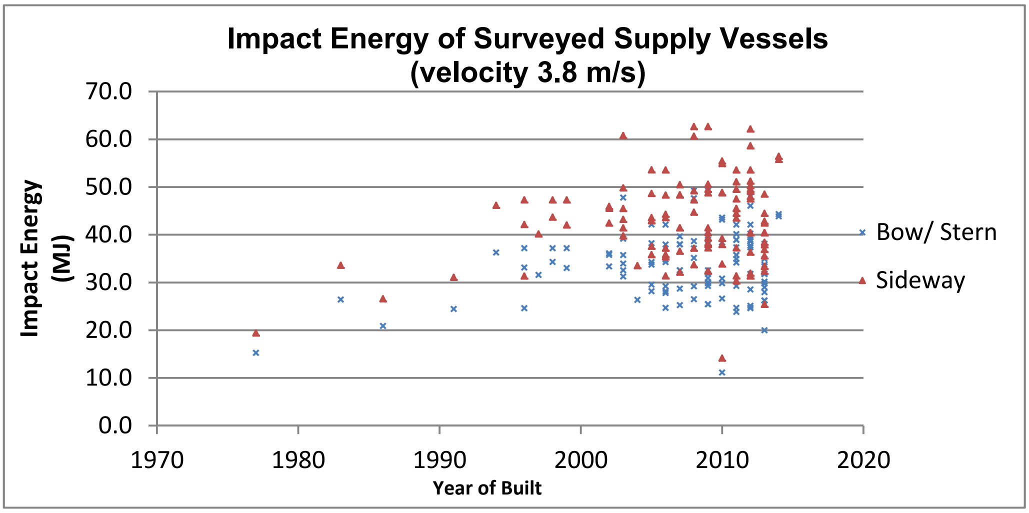

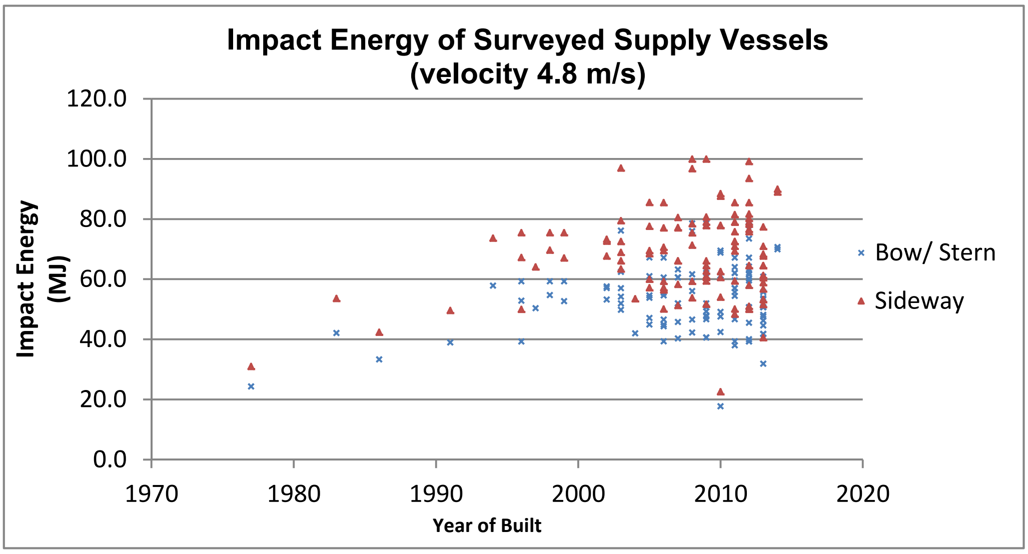

Figure 4-7 – Impact Energy of Supply Vessels for several Impact Velocities

5 METHODOLOGY

The boat impact analysis is carried out based on the quasi-static non-linear approach. This is the industry standard approach for boat impact analysis. The approach is acceptable since the time of accident when a boat hits a jacket is very short while structural response Eigen period relatively long. Therefore the global response of the structure under and after impact may be neglected. That is why normally boat impact cases cause damages limited to neighboring members of impact area, and therefore global response of the structural system is not observed.

Another approach is to run dynamic time domain analysis. This type of analysis may be important for some single cases, for example slender jackets, sensitive to global dynamic response. However for standard jackets such approach is normally not used due to required time for analysis. The quasi static approach gives sufficient accuracy with saving of analysis time.

The third method which could be of use is to perform evaluation based on manual calculations. NORSOK N-004 provides some basic tools to perform such analysis; however such analyses by definition are limited to single elements and are based on simplified models. Therefore such approach was not considered to be good enough and was used only for simplified quality assurance.

In this thesis report, the effect of high impact energy is evaluated for four jacket platforms. They are real platforms that are now operating on NCS. Due to request from asset owner, the platform names are made anonymous. They are named Platform A, Platform B, Platform C, and Platform D. All of them have conductor inside the jackets as depicted in Figure 5-3.

5.1 Bottom Boundary Condition

A fixed boundary condition is defined for each jacket. With the jacked fixed at its bottom entire jacket is somehow stiffer than with use of piles. As noted before normally boat impact causes local effect damaging neighboring members of the impacted area. When the jacket is fixed the global overall stiffness is higher and the impacted area will absorb energy.

By applying the pile supports (additional spring supports) the system may absorb some more impact energy (global effects) before the corresponding damage happens at the impacted area. Therefore the evaluation with fixed bottom is normal practice since one wants to evaluate impacted area – damage of impacted area may lead to overall collapse of structure (topside).

It is to be noted that no big difference is expected between these two boundary condition cases, unless the pile support is quite flexible. Of course the capacity of the pile supports are to be verified against the reaction forces in fixed supports.

5.2 Pile and Grouting

All jackets have pile sleeves and therefore the pile is not taken into account in calculation of leg resistance against impact energy. The legs are also assumed ungrouted.

5.3 Impact Scenario

Single impact scenarios are simulated for leg, braces, and can on each jacket. The purpose of simulating single impact scenarios is to evaluate the capacity of a single element. However, except for the leg, failure in one single element does not necessarily mean collapse of the jackets. Therefore, several single impacts are simulated sequentially to form multiple impacts scenario to investigate the capacity of the jacket beyond the capacity of each single element. The number of impact scenario may be different from one jacket to another, depending on the configuration of the bracing system of each jacket.

5.4 Topside Weight

The topside frame is modeled in the software to account for its stiffness contribution to the entire platform system. However, the steel frame is modeled with zero density. The total weight of the topside, consisting of steel weight and operating weight is modeled as a point mass which is distributed equally on top of each jacket.

5.5 Application of Impact Energy

The impact energy is applied to a point in the specified leg and brace. From this initial input, USFOS will transform the energy into load which will be gradually incremented until the limit is exceeded. Limiting criteria are given in Section 5.6.

5.6 Limiting Criteria

The calculation of absorbed energy in an element of the jacket structures is limited when one of the following criteria as described below is reached.

1. Fracture

   Fracture limitation is set to the impacted member based on the yield property of the element. This means that fracture is assumed to occur when the plastic strain in the impacted member reaches a specific value and thus, the analysis will stop. The energy level when fracture occurs will then be reported as the result. The value of the maximum strain for various yield stress properties is given in Table 2-1.

2. Joint Failure

   The strength of the adjacent joints of the impacted member is accounted in the analysis. The calculation procedure for strength of the joints refers to Ref. /24 section 6.4 and is carried out by internal commands in the software.

3. Denting of member

   Denting of member contributes to the strain energy absorption. However, limitation is set for how much a member can be indented due to the impact. For a leg, failure of the member is assumed if the ratio between the depth of the denting and the outer diameter of the leg equal or higher than a half ($\frac{w_d}{D} \geq 0.5$). For the brace, the member is assumed failed if the ratio $\frac{w_d}{D} \geq 0.7$. The calculation of denting depth in each step is carried out internally by the software.

4. Contact with conductor

   The ship impact cases are considered to take place at the jacket face nearest to the conductors. If the braces constructing the face fail, then it is assumed that there is nothing more to stop the ship from going inside the jacket and hit the conductors.

Contact of ship with conductors / raisers is normally not allowed (standard design practice).

5.7 Computer Modeling with Finite Element Program

GeniE and USFOS are two main finite element programs used in this thesis. GeniE is part of the SESAM package and is a tool for designing marine and offshore structures. Independently it can take care of all modeling, analysis, and presentation of the result in the same user interface [Ref. /09]. However, in this thesis GeniE is used specifically to generate 3D modeling of jacket structures. No load is specified in GeniE.

USFOS is a program that is specifically developed to perform progressive collapse analysis of space frame based structures. The basic philosophy in USFOS is to create a coarse mesh of the structural model. It is also capable of taking into account nonlinearities in the model such as nonlinearity in material properties and structural geometry [Ref. /15]. This is important due to the involvement of a great amount of energy in the boat impact case that will require evaluation of the strength of the structure beyond its linear – elastic limit. The initial impact energy is introduced to the structures in USFOS, as well as fracture criteria and inelastic material properties.

GeniE and USFOS are related one to each other through SESAM Interface Files. This enables the model that has been developed in GeniE to be used in USFOS. The interface between GeniE and USFOS is described in Figure 5-1.

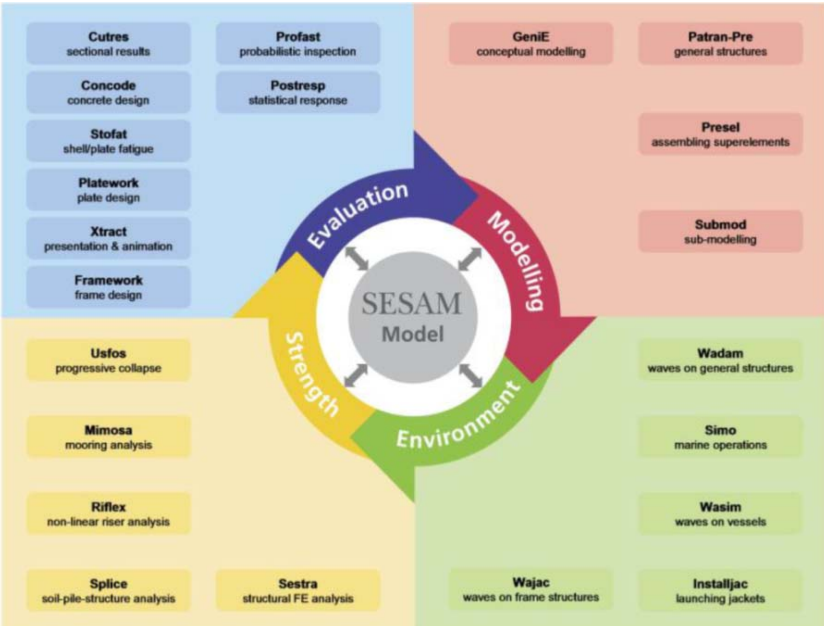

Figure 5-1 – Interface among SESAM programs
(Ref. /09)

However, the structural model from GeniE cannot be directly used in USFOS. Therefore there should be something in between that can act as interconnecting device so that USFOS can read input from GeniE. USFOS is equipped with a Structural File Manipulator (StruMan) utility by which the structural models from GeniE are “translated” so they can be read by USFOS and further be processed for boat impact analysis. The relation between GeniE, StruMan, and USFOS is described in Figure 5-2.

Figure 5-2 – Relation between GeniE and USFOS

The structural models in USFOS, as depicted in Figure 5-3, are not scaled. More detailed information for each platform is given in the next subsections 5.7.1 to 5.7.4.

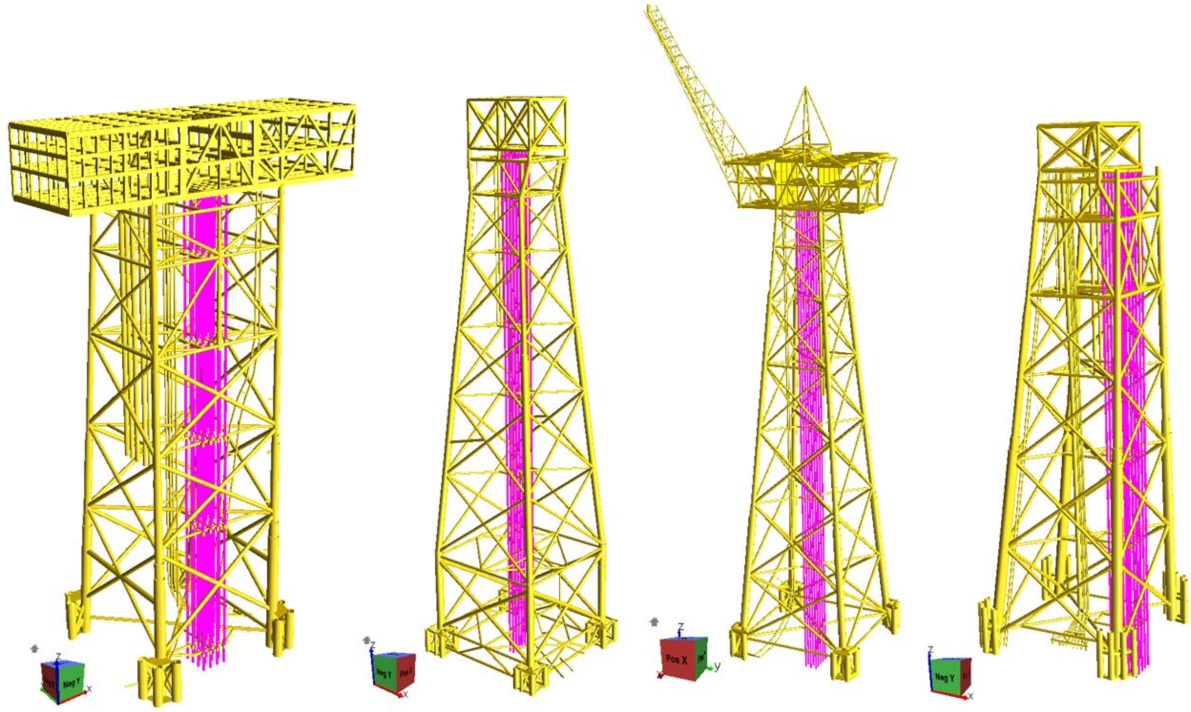

Figure 5-3 – Model of jacket platforms in USFOS – the conductors are marked by roseate highlight (unscaled)

For all jackets, the impact energy will be implemented in the range between 10 m below low astronomical tide (LAT) and 13 m above high astronomical tide (HAT) as suggested by Ref. /23. The impact is set to the side which is closest to conductors as this is considered to be the most critical part with respect to ship collision.

5.7.1 Platform A

Platform A is located in 109 m water depth (relative to MSL) in the North Sea area. The topside has an operating weight of 19000 tons and is equipped with process facility for partial stabilization of oil and gas. The jacket weights 7400 tons and is equipped with 3 pile sleeves at each leg. The leg is battered in one direction and as much as 16 conductors are installed inside the jacket, located near the straight (unbattered) face of the jacket. The general view of Platform A is depicted in Figure 5-4.

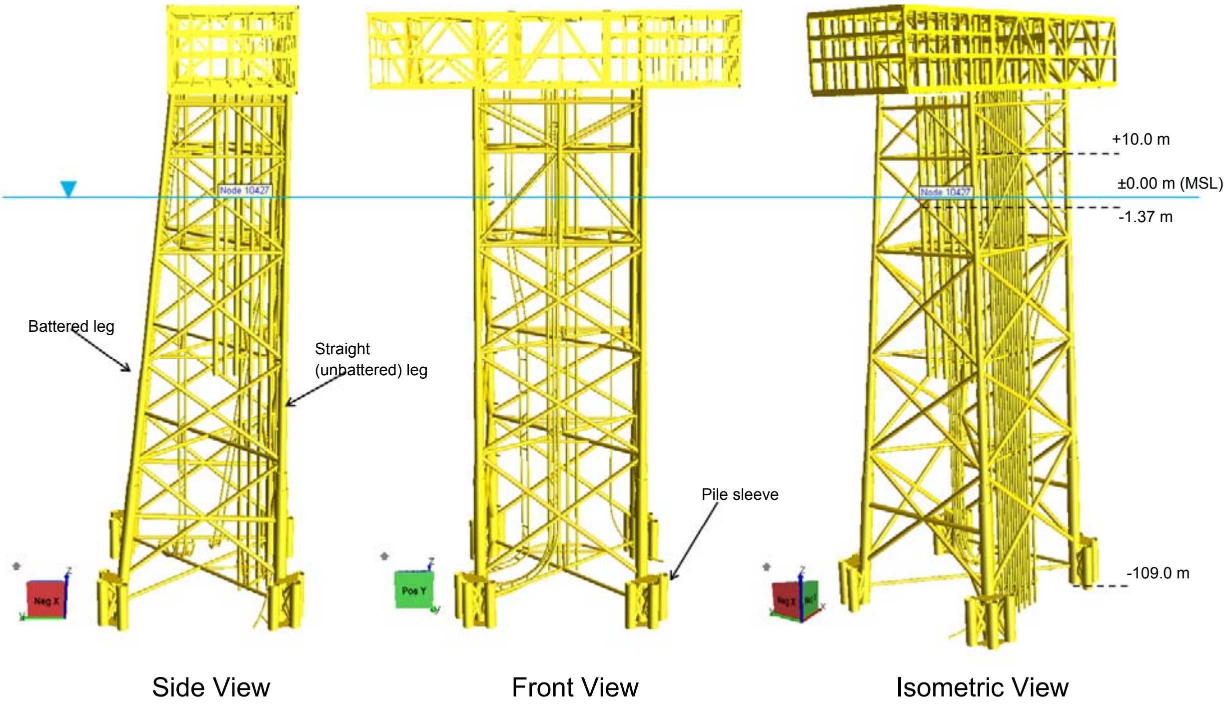

Figure 5-4 – General view of Platform A

The impact cases for Platform A are assigned at the unbattered face, which is the nearest face to the conductors, between elevations -1.37 m and +10.0 m. Figure 5-5 gives description of basic impact cases for Platform A.

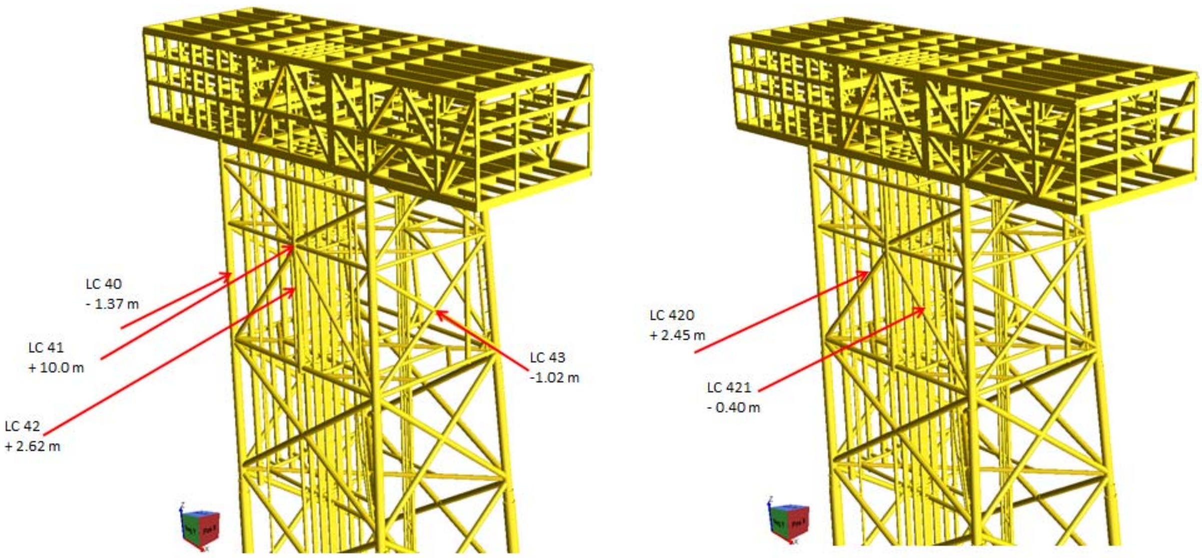

Figure 5-5 – Basic impact cases for Platform A

The explanation of each case is given in Table 5-1.

Table 5-1 – Basic impact cases for Platform A

Case No	Description	Member Profile (mm)	SMYS (MPa)	Member length (m)
40	Impact on leg	Ø 1600 x 70	420	23
41	Impact on brace can	Ø 1400 x 75	420	35.2
42	Impact on vertical brace	Ø 970 x 50	420	12.3

Case No	Description	Member Profile (mm)	SMYS (MPa)	Member length (m)
43	Impact on intersection of X–brace	Ø 930 x 45	420	2.7
420	Dummy load case representing impact on diagonal brace	Ø 900 x 40	420	20.0
421	Dummy load case representing impact on diagonal brace	Ø 900 x 40	420	27.8

In addition to single impact cases as described above, one multiple impact is also simulated in the boat impact analysis for Platform A. This multiple impact involves impact on a vertical brace and impact two diagonal braces. First impact with an initial amount of energy made on the vertical brace until the brace fails. If the member fails before all energy is absorbed, the remaining energy then will be transferred to the diagonal braces using two dummy load cases (420 and 421) sequentially. This dummy load case means that it has no initial energy, rather than taking the remaining energy from the previous impact case. The purpose of creating these dummy load cases is only to help simulating multiple impact scenarios. Then fracture will limit the absorption of the impact energy. The combination for multiple impact case for Platform A is given in Table 5-2.

Table 5-2 – Multiple impact cases for Platform A

Case No	Description	LC 40	LC 41	LC 42	LC 43	LC 420	LC 421
A01	Multiple impact on Vertical brace and diagonal braces	-	-	1	-	+	+

It should be noted from the table above that the first impact is denoted by “1”, and the following impact is denoted by “+”. Load cases denoted by “+” are dummy load case, which means that they do not have initial impact energy. Dummy cases are assigned to take the remaining energy from the previous impact case.

5.7.2 Platform B

Platform B is located in North Sea area in 190 m water depth, relative to MSL. The topside is equipped with integrated accommodation, drilling, and processing facility and has 24000 tons maximum weight in operating condition. The jacket leg is double-battered and equipped with 4 pile sleeves at each leg. As many as 16 conductor slots are installed inside the jacket. In addition, the jacket has identic bracing configuration for all four sides. A general view of Platform B is depicted in Figure 5-6.

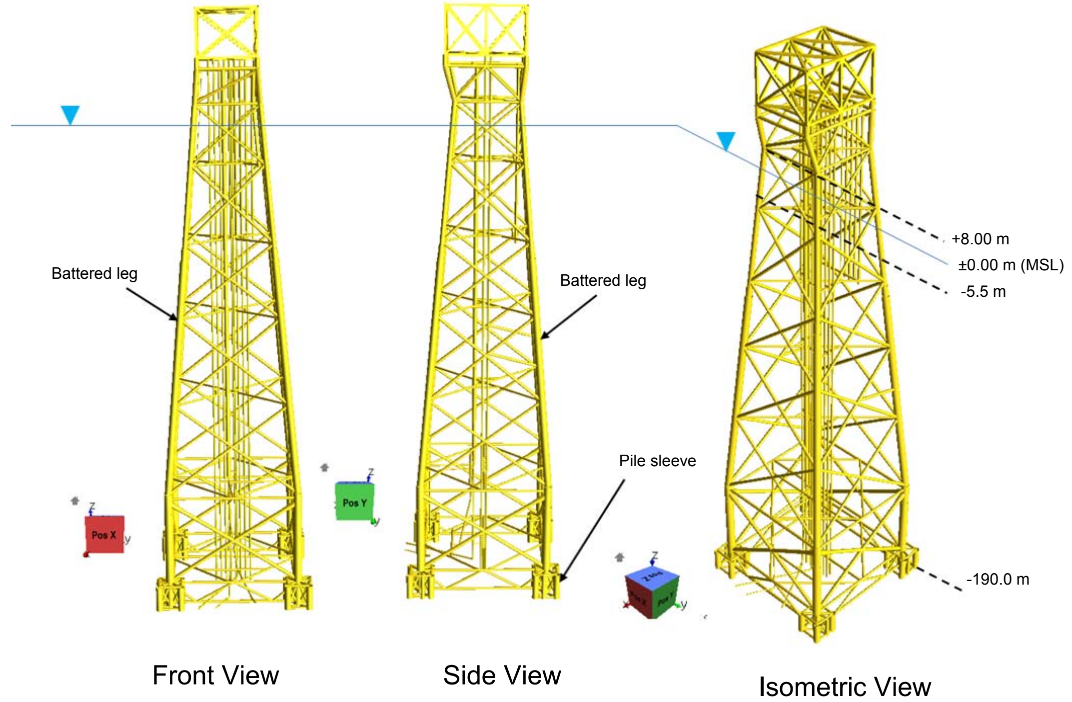

Figure 5-6 – General view of Platform B

Basic impact cases for Platform B are assigned between elevation -5.5 m to elevation + 8.00 m, as depicted in Figure 5-7. Five basic cases are assigned comprising impact on leg and braces.

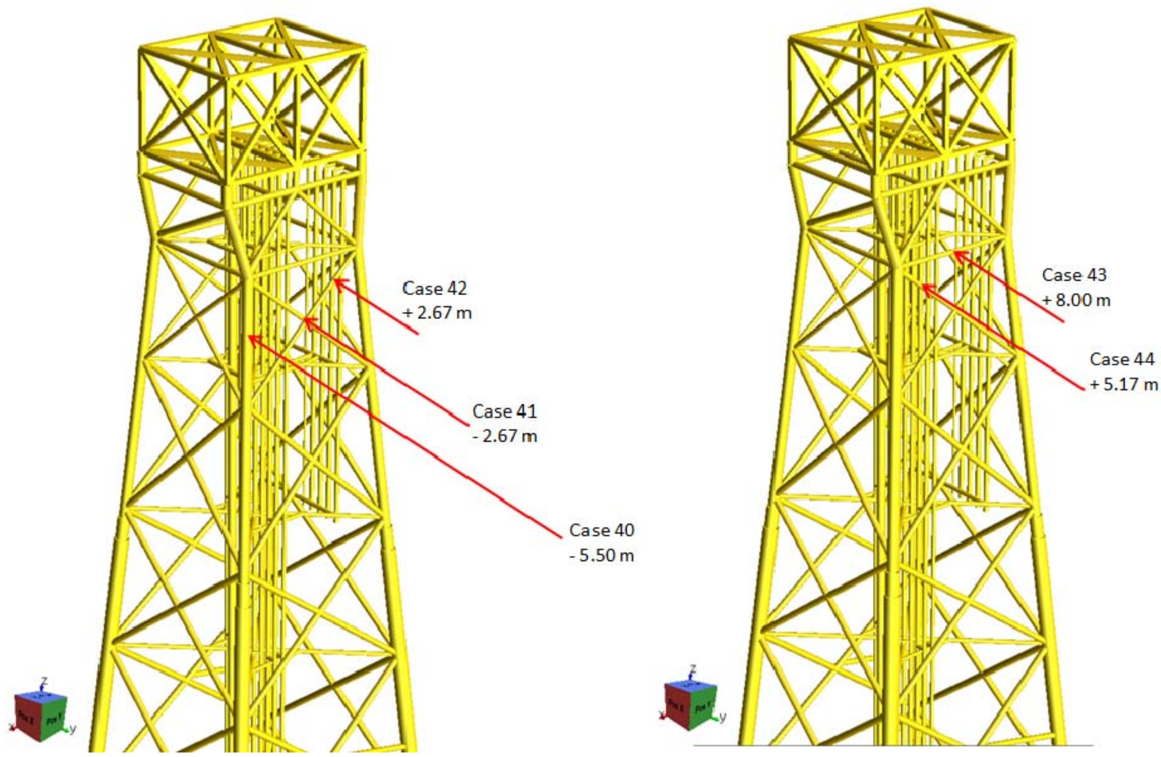

Figure 5-7 – Basic impact cases for Platform B

Description of each load case is given in Table 5-3 below.

Table 5-3 – Basic impact cases for Platform B

Case No	Description	Member Profile (mm)	SMYS (MPa)	Member length (m)
40	Impact on leg	Ø 2000 x 85	420	23.1
41	Impact on intersection of X–brace	Ø 900 x 65	420	35.2
42	Impact on diagonal brace	Ø 900 x 65	420	16.3
43	Impact on horizontal brace	Ø 950 x 60	420	24.7
44	Impact on diagonal brace	Ø 900 x 65	420	16.3

One multiple impacts scenario is simulated for Platform B, involving two basic impacts on a diagonal brace (LC 42 and LC 44). The first impact is given by load case 42 with fracture limit criterion set for the member. If the member fails before all energy is absorbed, the remaining energy is transferred to another diagonal brace under load case 44. The combination for multiple impact case for Platform B is given in Table 5-4.

Table 5-4 – Multiple impact cases for Platform B

Case No	Description	LC 40	LC 41	LC 42	LC 43	LC 44
B01	Multiple impact on two diagonal braces	-	-	1	-	+

5.7.3 Platform C

Platform C is located in the North Sea area in 157 m water depth, relative to MSL. The platform is equipped with an integrated accommodation, drilling, and production facility with equipment for first phase processing. The maximum of the topside weight in operating condition is 13090 tons. The topside is supported by a four legged jacket, configured with X-bracing arrangement, identical for all four faces. The jacket is supported by three piles in each corner, which are stabbed to seabed through pile sleeves. Grouting is used to fill the gaps between the piles and the sleeves. The legs are battered in two directions. A total of 15 conductors are installed in the middle of the jacket. Total weight of the jacket is 7100 tons, including pile sleeves, anodes, and other appurtenances. General view of Platform C is given in Figure 5-8.

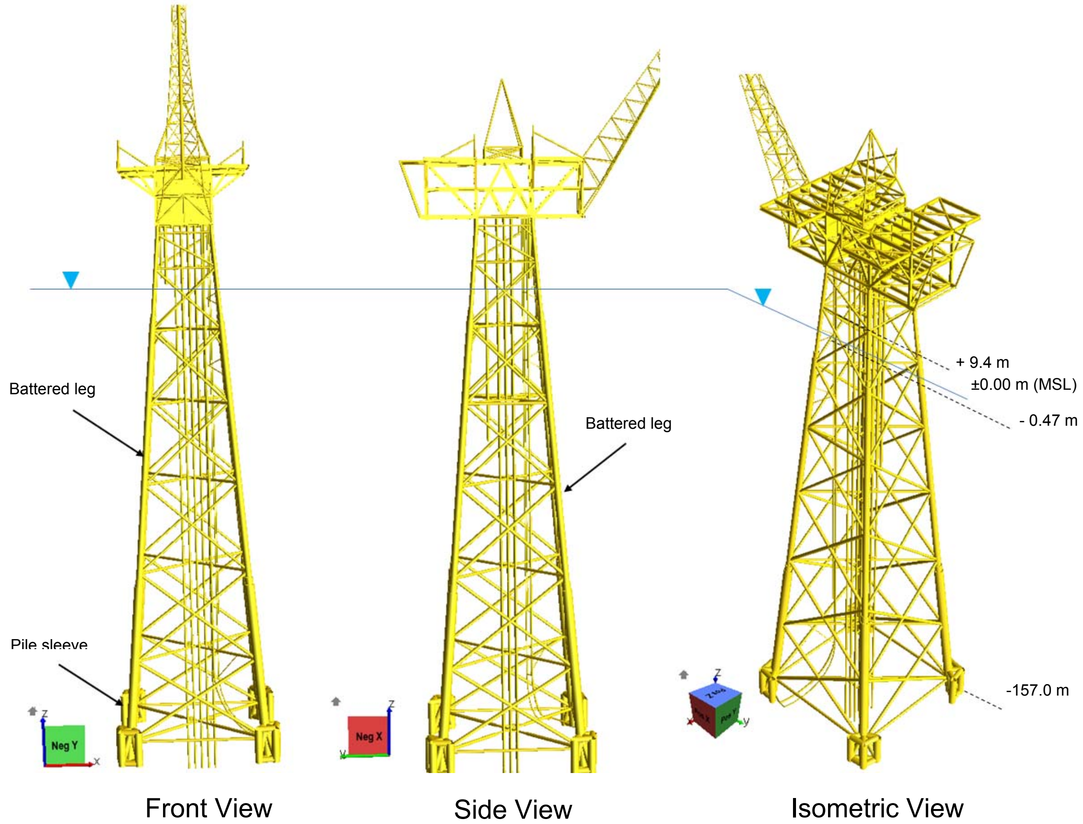

Figure 5-8 – General view of Platform C

Basic impact cases for Platform C are assigned between elevations -0.47 m to elevation + 9.40 m, as depicted in Figure 5-9. Five basic impact cases are assigned comprising impact on leg and braces.

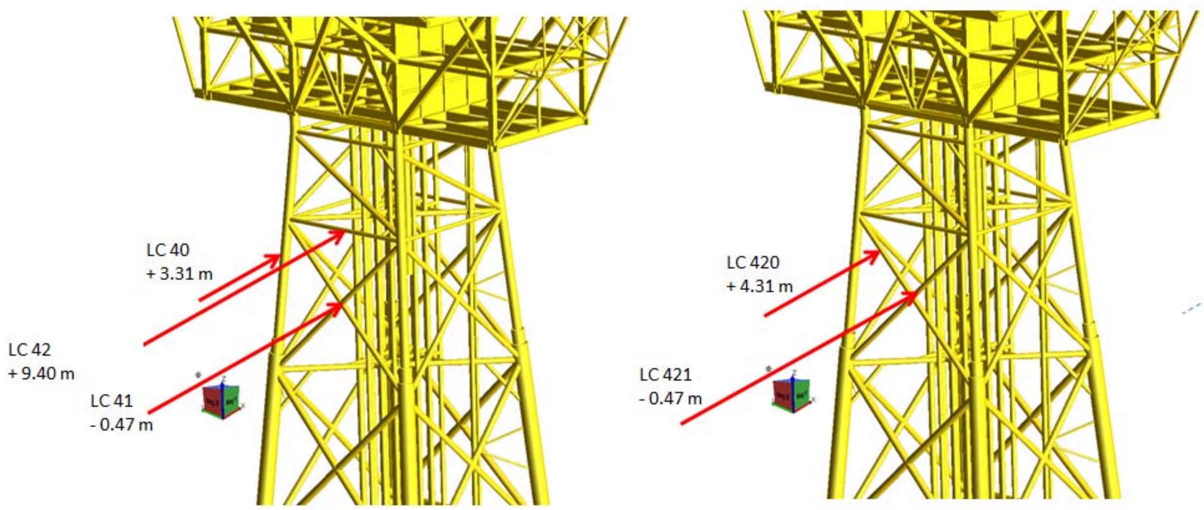

Figure 5-9 – Basic impact cases for Platform C

Description of each case is given in Table 5-5.

Table 5-5 – Basic impact cases for Platform C

Case No	Description	Member Profile (mm)	SMYS (MPa)	Member length (m)
40	Impact on leg	Ø 1308 x 74	420	16.6

Case No	Description	Member Profile (mm)	SMYS (MPa)	Member length (m)
41	Impact on intersection of X–brace	Ø 798 x 44	420	30.1
42	Impact on horizontal brace	Ø 600 x 30	420	19.9
420	Dummy impact on diagonal brace	Ø 788 x 39	420	9.5
421	Dummy impact on intersection of X–brace	Ø 798 x 44	420	1.4

Two dummy load cases are defined for Platform C in order to simulate the multiple impact case. This multiple impact case involves impact on the horizontal brace, followed by impact on a diagonal brace and impact at the intersection of X-brace, sequentially. Initial energy is given under load case 42 with fracture limit set for the impacted members. If the member fails before all initial energy is absorbed, the remaining energy will first go to diagonal brace (load case 420) and then to the intersection of the X-brace members (load case 421).

The combination for multiple impact case for Platform C is given in Table 5-6.

Table 5-6 – Multiple impact cases for Platform C

Case No	Description	LC 40	LC 41	LC 42	LC 43	LC 420	LC 421
C01	Multiple impact on horizontal brace and diagonal braces	-	-	1	-	+	+

5.7.4 Platform D

Platform D is located in North Sea, in water depth of 153 m, relative to MSL. The topside is equipped with living quarter and separation facilities for gas, condensate, and water. Total weight of the topside in the operating condition is 12500 tons. The jacket leg is battered in one direction, and supported with 4 piles at each corner. The piles are stabbed to seabed through pile sleeves. General view of Platform D is given in Figure 5-10.

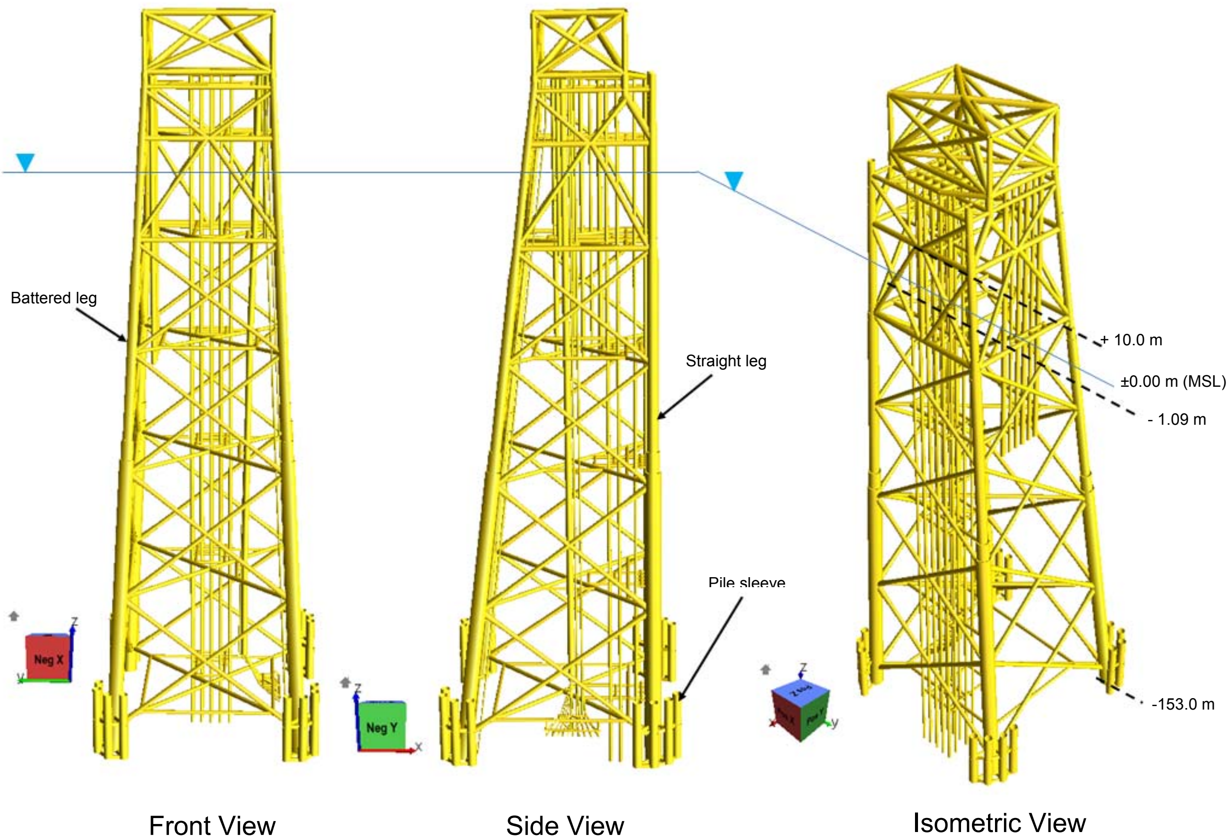

Figure 5-10 – General view of Platform D

Platform D has a more complex bracing system in the splash zone, compared with previous platforms. The impact scenarios are simulated at the straight face of the jacket, which is closer to the conductors, between elevations –1.09 m to elevation +10.0 m. Figure 5-11 gives a description of the basic impact cases for Platform D.

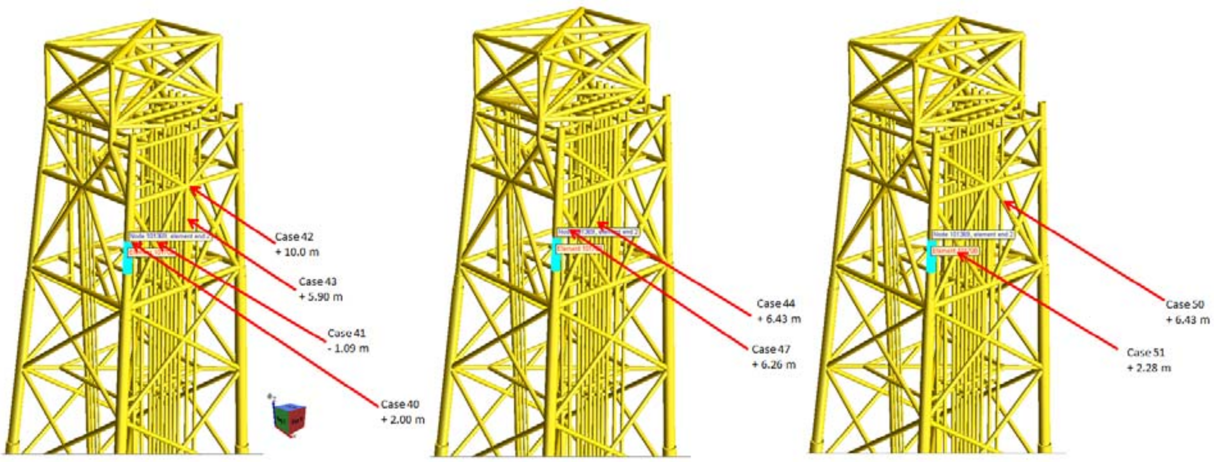

Figure 5-11 – Basic impact cases for Platform D

Due to the complexity of bracing system at the impacted side, more basic cases can be assigned for Platform D. Description of each basic case is given in Table 5-7.

Table 5-7 – Basic impact cases for Platform D

Case No	Description	Member Profile (mm)	SMYS (MPa)	Member length (m)
40	Impact on leg	Ø 1984 x 52	480	20.8
41	Impact on intersection of X–brace	Ø 1484 x 52	480	27.8
42	Impact on brace can	Ø 1400 x 100	480	7.5
43	Impact on vertical brace	Ø 1300 x 50	480	23.0
44	Impact on diagonal brace	Ø 1200 x 60	480	9.8
47	Dummy impact on diagonal brace	Ø 1200 x 60	480	9.8
50	Dummy impact on diagonal brace	Ø 1200 x 60	480	9.8
51	Dummy impact on diagonal brace near intersection	Ø 1485 x 92	480	1.7

In addition to the basic impact cases above, 3 multiple impact cases are simulated for Platform D. The description of the multiple impact cases for Platform D is given in Table 5-8.

Table 5-8 – Multiple impact cases for Platform D

Case No	Description	LC 41	LC 43	LC 44	LC 47	LC 50	LC 51
D01	Multiple impact on two diagonal brace	-	-	1	+	-	-
D02	Multiple impact on Intersection of X-brace, followed by diagonal brace	1	-	-	-	-	+
D03	Multiple impact on vertical brace and two diagonal brace	-	1	+	-	+	-

6 RESULT OF ANALYSIS

6.1 Impact on Jacket Leg

The case of an impact on jacket legs is simulated for all platforms. The results show that the legs of Platform A and Platform C dissipate a relatively lower impact energy compared to Platform B and Platform D. The dissipated impact energy for the case of impact on the legs is 33 MJ and 27 MJ for Platform A and Platform C, respectively. On the other hand, Platform B and Platform D absorb more energy, which is 54 MJ and 44 MJ, respectively. The summary result for this case for each platform is tabulated in Table 6-1, and the description of each platform when fracture occurs is depicted in Figure 6-1 and Figure 6-2.

Table 6-1 – Summary results for case of impact on leg

Platform Name	Leg Profile (mm)	Span of Impacted Leg (m)	SMYS (MPa)	Absorbed Energy (MJ)	Failure criteria
A	Ø 1600 x 70	23.0	420	33	Fracture
B	Ø 2000 x 85	23.1	420	54	Fracture
C	Ø 1308 x 74	16.6	420	27	Fracture
D	Ø 1984 x 52	20.8	480	44	Denting

It can be seen from the table that, except for Platform D, the maximum energy dissipation is limited by fracture of the member, which is assumed to occur in case of impact on jacket legs. The summary result shows that plastic strain in the impacted member reaches 12%. The value is taken from interpolation of the proposed critical strain values in Table 2-1.

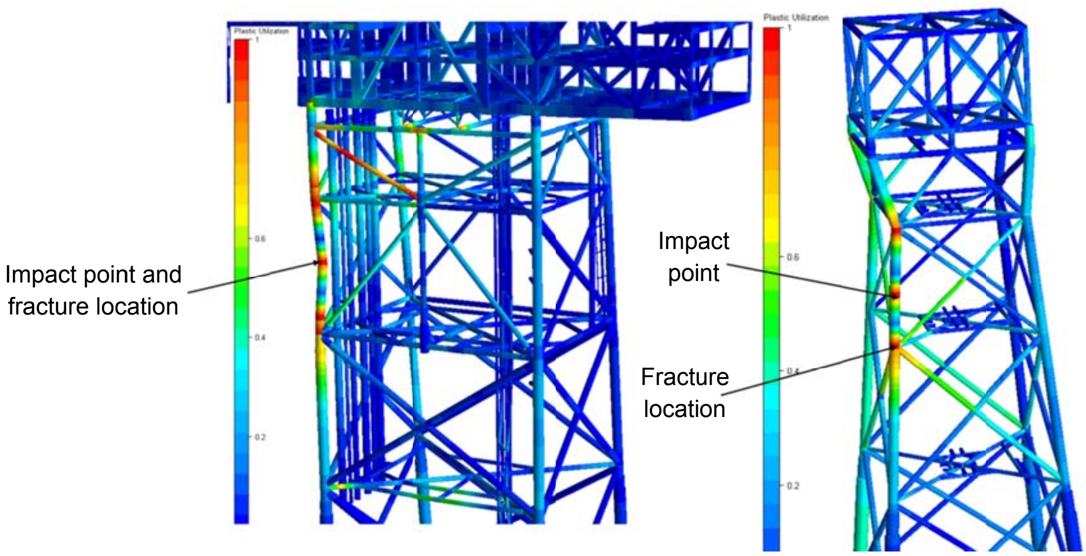

Figure 6-1 – Condition of Platform A and Platform B when fracture occurs

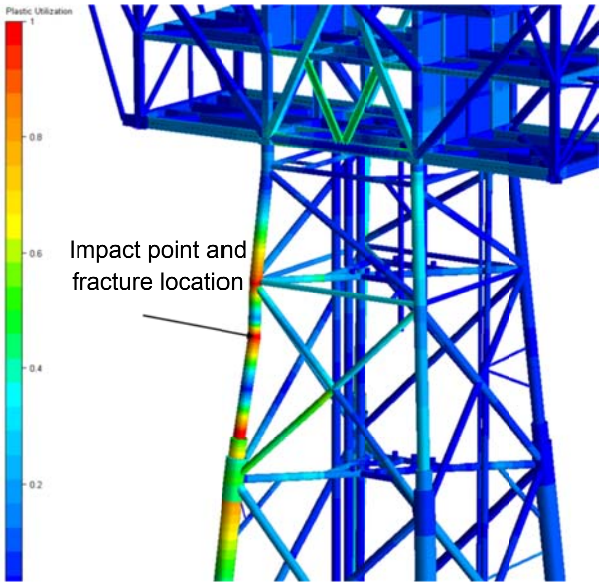

Figure 6-2 – Condition of Platform C when fracture occurs

Actually, Platform D can dissipate energy as much as 54 MJ until fracture occurs (at step number 82) at the impacted member. At this level, the tubular wall of the impacted member undergoes a 1 m indentation. Ratio of the indentation to outer diameter of the leg is more than 0.5, which is assumed as the collapse criteria for the leg due to denting. It is therefore considered that maximum absorbed energy for Platform D is lower than 54 MJ, which is observed 44 MJ (step number 79). At this level of energy, the indentation of tube wall of the impacted member is 0.96 m, which gives denting ratio less than 0.5. The comparison between the two steps is tabulated in Table 6-2 and the platform condition is given in Figure 6-3.

Table 6-2 – Energy level of Platform D at two different step numbers

Step No	Energy Level (MJ)	Tube Indentation (m)	Denting Ratio
79	44	0.96	0.48
82	53	1.03	0.52

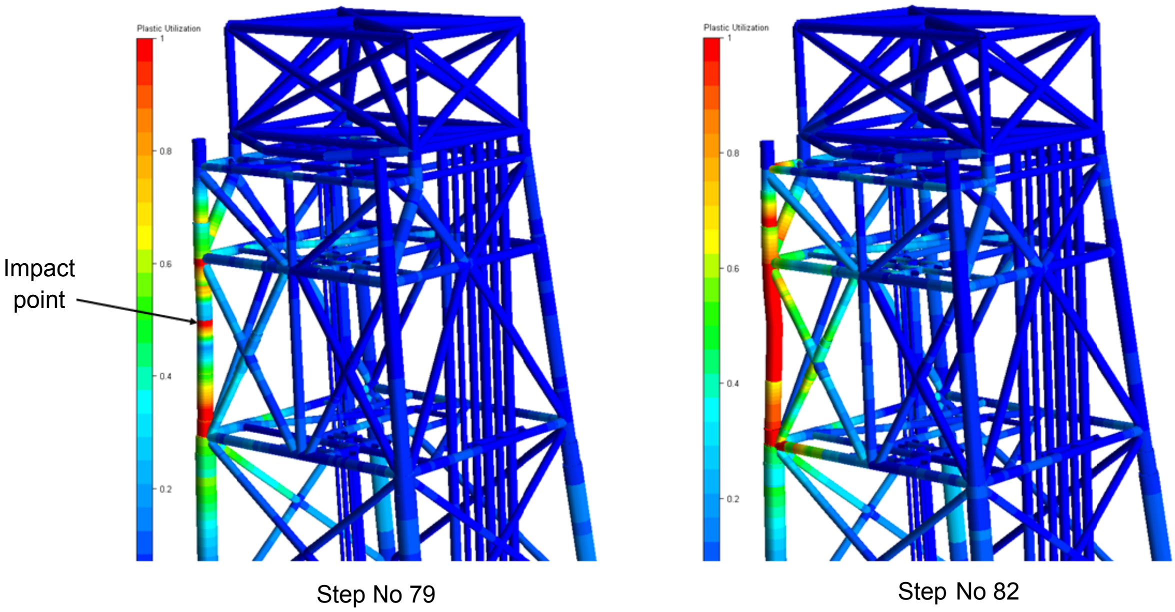

Figure 6-3 – Condition of Platform D in two different steps

6.2 Impact on X Brace Intersection

It is mentioned in Ref. /21 that this case is very favorable in terms of energy absorption due to the large ratio of length/diameter. In addition, the impact energy is also distributed to the two braces constituting the X-brace. The case of an impact on the intersection of the X brace is simulated for all platforms. The results show that energy dissipation for this case falls at almost the same level for all platforms, as tabulated in Table 6-3.

Table 6-3 – Summary results for case of impact on X-brace intersection

Platform Name	X brace Profile (mm)	Effective length (m)	SMYS (MPa)	Absorbed Energy (MJ)	Failure criteria	L / D
A	Ø 930 x 45	35.2	420	42	Fracture	38
B	Ø 900 x 65	35.2	420	42	Fracture	39
C	Ø 798 x 44	30.1	420	45	Fracture	38
D	Ø 1484 x 52	27.8	480	46	Fracture	19

It can be seen also that the absorbed energy for each platform is limited by fracture. The condition of each platform when fracture occurs is depicted in Figure 6-4.

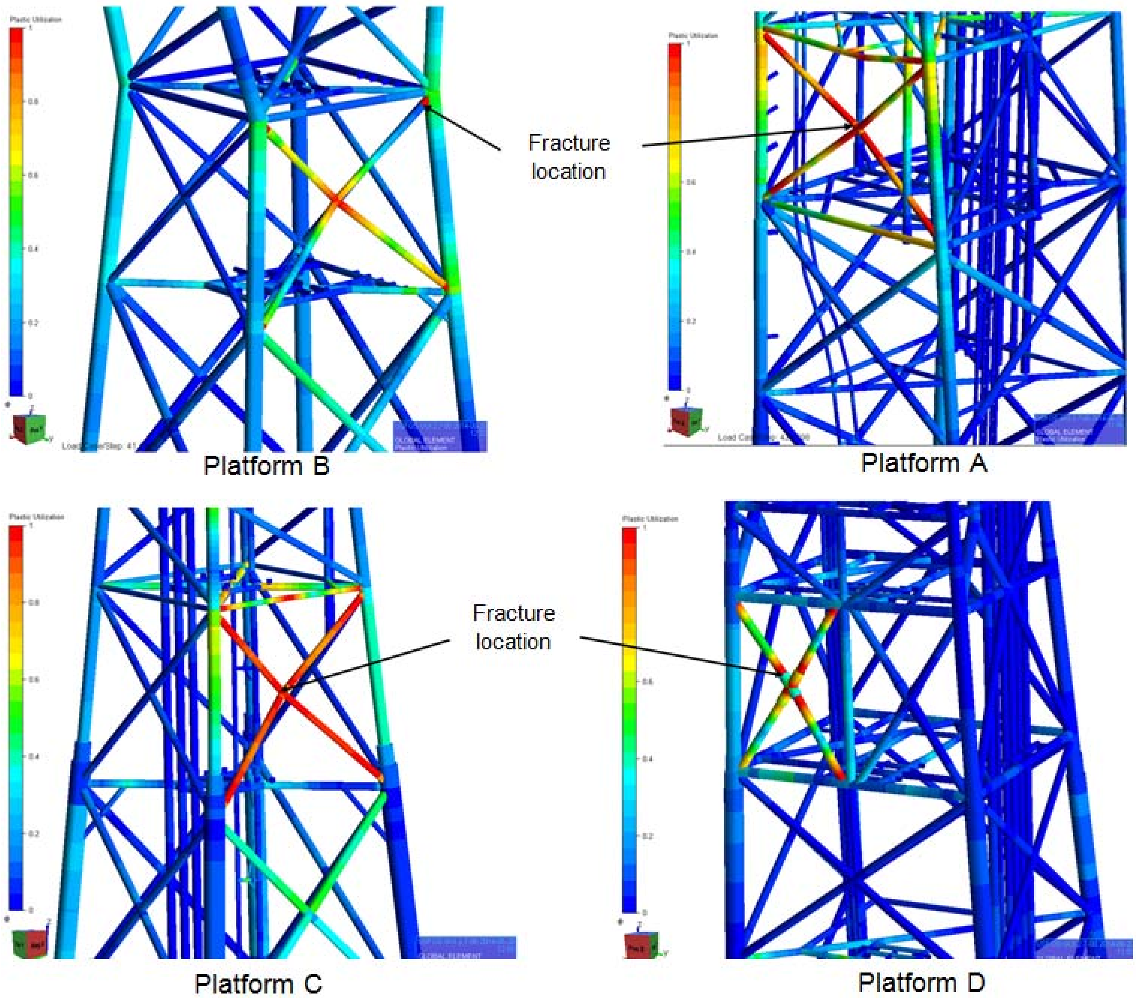

Figure 6-4 – Condition of the platforms when fracture occurs for case impact on X-brace intersection

For comparative study, it is important to mention the same impact case which is described in Ref. /21. The length/ diameter ratio for the impacted X brace in Ref. /21 is around 30. The total absorbed impact energy is approximately 54 MJ, which is higher than the result for the platforms presented in Table 6-3. This is understandable since the case in Ref. /21 considers 15% strain limit as collapse criteria while in this report 12% strain limit is used. However, no attempt has been made in this report to examine the level energy absorption if the strain limit is increased from 12% to 15%.

6.3 Impact on Brace Can

In this report, a brace can refer to a can connecting many braces in one specific joint. This case is of interest since the can is considered a strong point. Moreover, since the can connects many braces, the energy given to the can is propagated prevalently to the surrounding members. Hence, this case may give a good picture of collapse of the jacket since many members will fail at certain levels of energy.

In this thesis, only Platform A and Platform D have brace cans. Due to the strength of the cans, the energy absorption is not limited by the fracture at the tubular wall. However, USFOS stops its calculation when instability in the model is encountered, which is caused by failure of one or several joints nearby the impacted can. At this condition, it is assumed that the jacket cannot take any more energy. The results are summarized in Table 6-4.

Table 6-4 – Summary results for case of impact on brace can

Platform Name	Can Profile (mm)	SMYS (MPa)	Absorbed Energy (MJ)	Calculation Step
A	Ø 1400 x 75	420	28	244
D	Ø 1400 x 100	480	76	103

From Table 6-4 above, it can be seen that Platform D takes more energy than Platform A. It is understandable since Platform D has thicker can wall than Platform A.

For Platform A, the maximum energy that can be absorbed is limited at calculation step 244. The condition of the brace can of Platform A at calculation step 244 and 249 (last step) is given in Figure 6-5.

From the graph in the up-right side of Figure 6-5, it is obvious that step 244 represents the peak of the impact energy curve. Beyond this step the impact energy curve lowers down. This can be interpreted that the jacket cannot take more energy. Therefore, the level energy at calculation step 244 is considered as maximum absorbed energy. Step 249 is the last step where USFOS is able to carry out the calculation due to instability of the model. At the last step, more members near the impact point have been highly utilized, which is considered as collapse of the jacket.

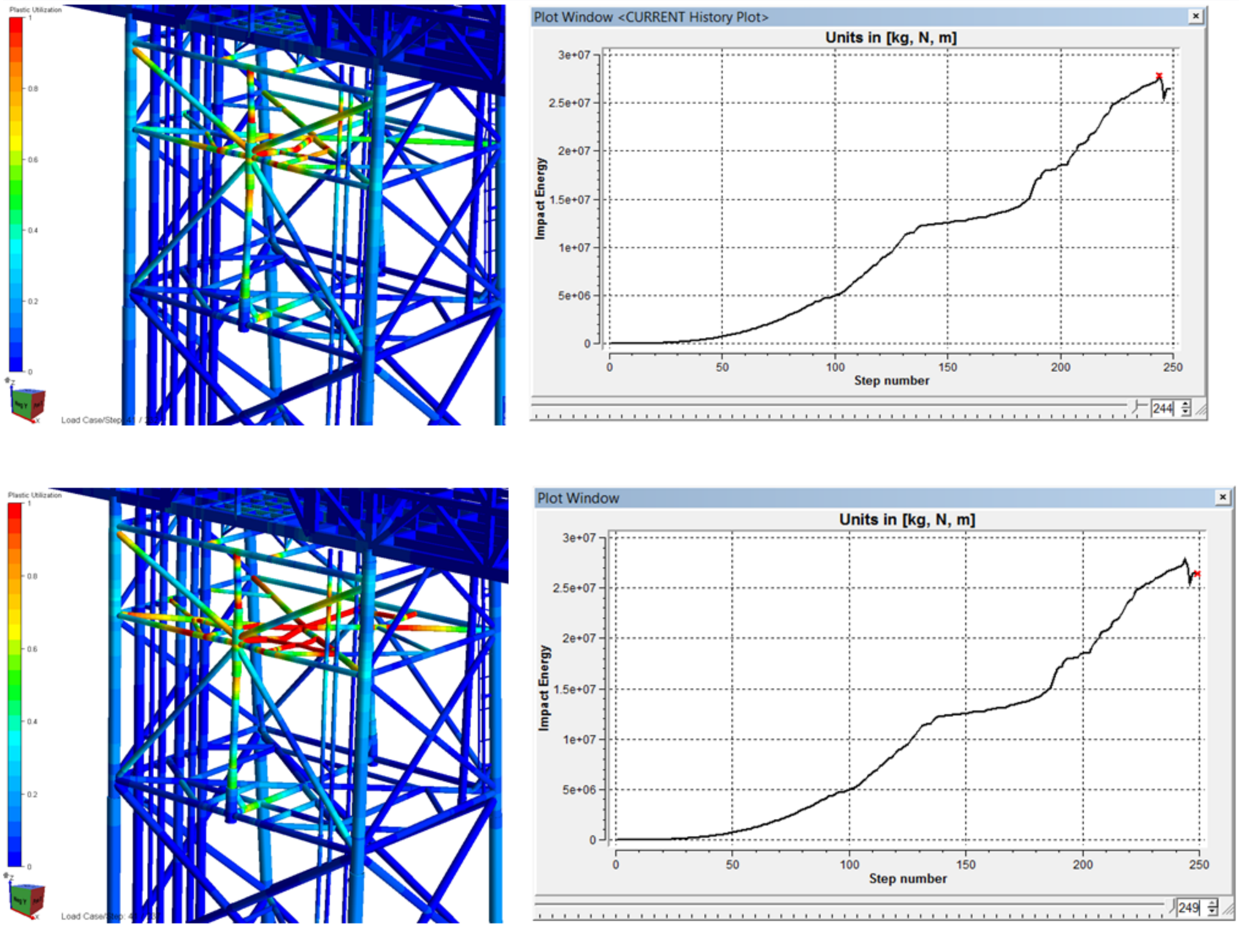

Figure 6-5 – Platform A at calculation steps 244 and 249

Platform D is considered to reach its capacity in terms of impact energy absorption at step 103 when 76 MJ energy has been dissipated by the jacket. The condition of Platform D at calculation step 103 is depicted in Figure 6-6.

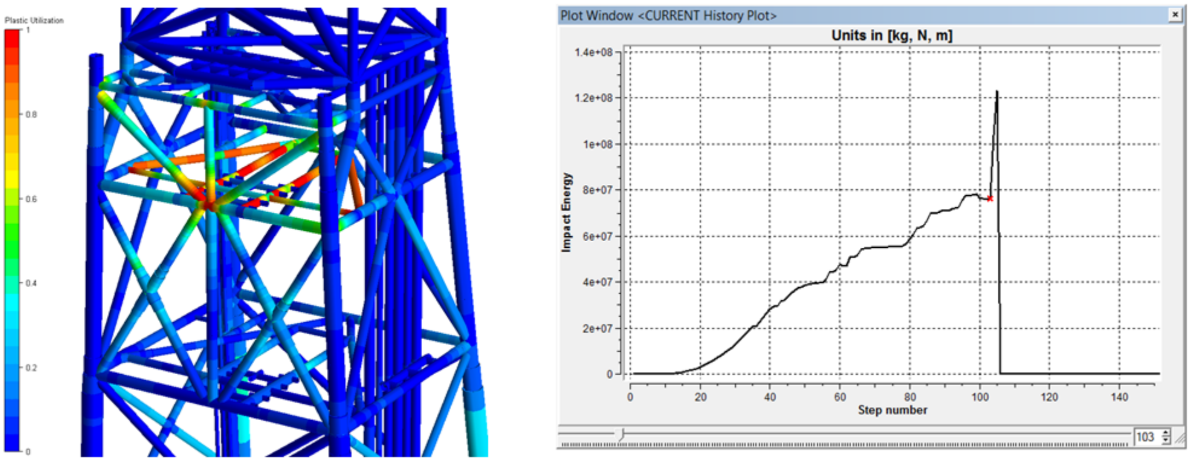

Figure 6-6 – Platform D at calculation step 103

Instability occurs in the model after step 103 and results in “jump” in impact energy curve between step 104 and step 105. Afterwards the curve drops down to zero level of impact energy. This means that the jacket cannot take more impact energy. The condition of Platform D beyond calculation step 103 is given in Figure 6-7.

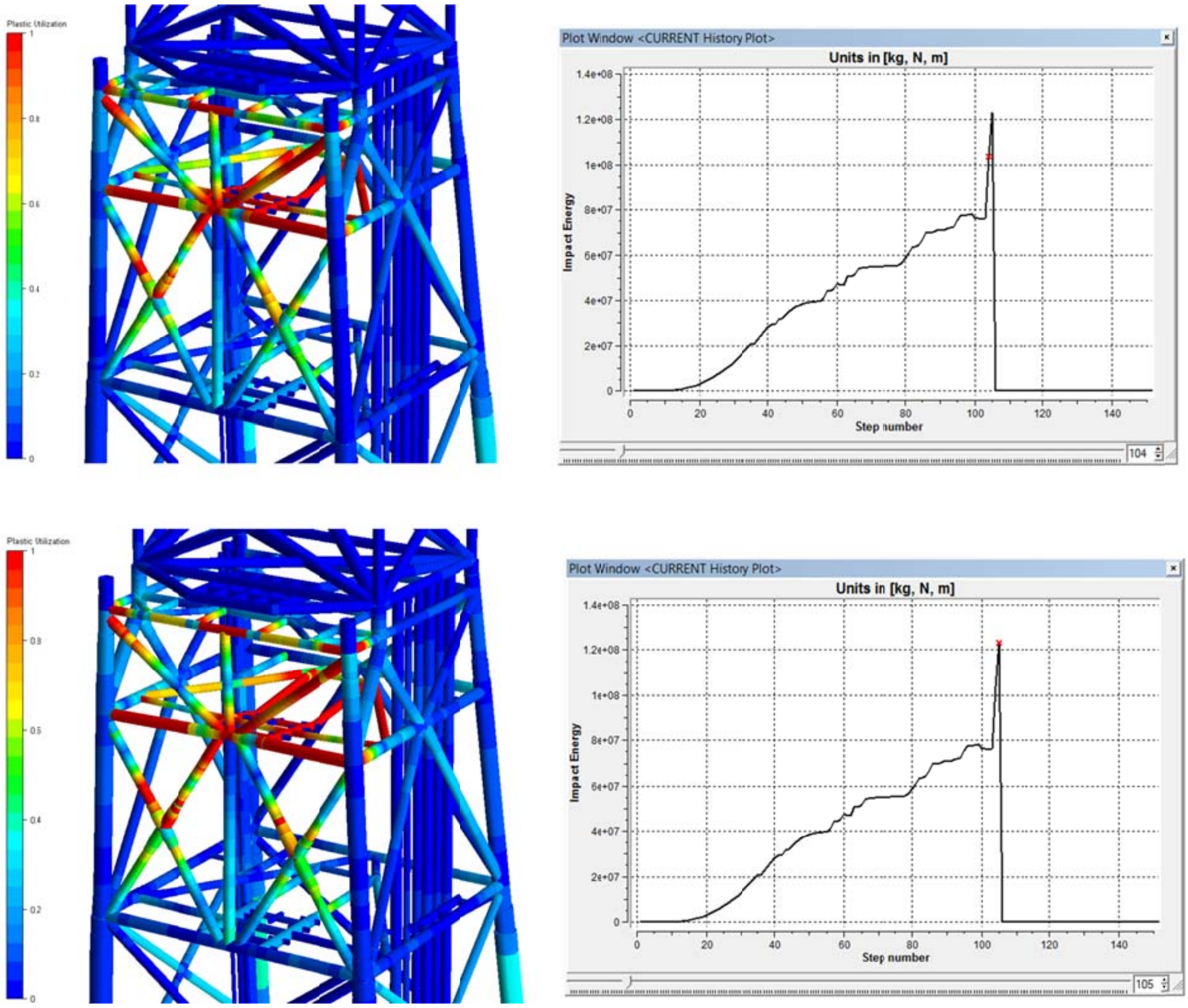

Figure 6-7 – Condition of Platform D beyond calculation step 103

6.4 Impact on Single Brace

This case is simulated for the vertical brace in Platform A and Platform D, and for the horizontal brace in Platform B and Platform C, and also for a diagonal brace in Platform C. Reference about locations of impact can be made to Figure 5-5, Figure 5-7, Figure 5-9, and Figure 5-11. The purpose of carrying out simulation on single brace impact is to investigate the capacity of braces as basis for simulating multiple impacts which will be explained in next section. All impacts are set at the midspan of each brace. The resulting summary for impact on a single brace is tabulated in Table 6-5.

Table 6-5 – Summary results for case of impact on single brace

Platform Name	Scenario	Leg Profile (mm)	Span of Brace (m)	SMYS (MPa)	Absorbed Energy (MJ)	Failure criteria
A	Single impact on vertical brace	Ø 970 x 50	23.0	420	18	Fracture
B	Single impact on diagonal brace	Ø 900 x 65	16.3	420	14	Fracture
	Single impact on horizontal brace	Ø 950 x 60	24.7	420	21	Fracture
C	Single impact on horizontal brace	Ø 600 x 30	20.0	420	7	Fracture

Platform Name	Scenario	Leg Profile (mm)	Span of Brace (m)	SMYS (MPa)	Absorbed Energy (MJ)	Failure criteria
D	Single impact on vertical brace	Ø 1300 x 50	23.0	480	16	Fracture

For all platforms, the energy dissipation is limited by fracture occurring either at the midspan of the brace or at the joint. It can be seen from Table 6-5 that the horizontal brace of Platform B can take the most impact energy while the horizontal brace of platform C takes the least energy. This is due to that the horizontal member in Platform C has the smallest profile compared to the other platforms. The conditions of the braces of two platforms at failure are depicted in Figure 6-8.

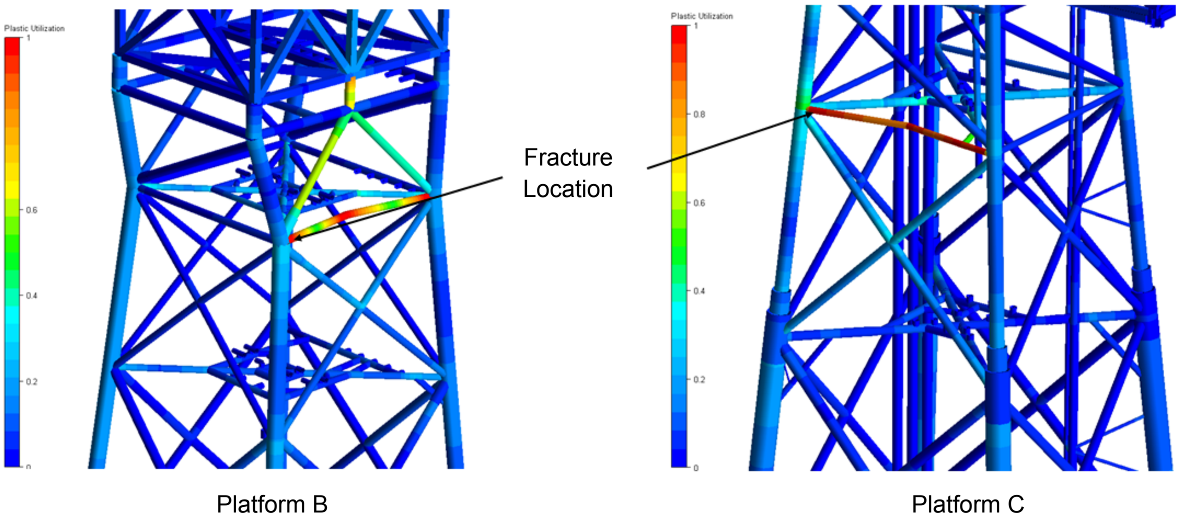

Figure 6-8 – The brace condition at fracture of Platform B and Platform C

The maximum energy for other single brace impact cases falls at almost the same level, which is 14 MJ to 18 MJ. The vertical brace in Platform D has larger diameter than that in Platform A, yet the absorbed energy is smaller compared to Platform A. It can be understood that the increase in outer diameter (D) does not give additional resistance against rupture. What is more important in this case is the wall thickness, t. It can be seen also that for such a big outer diameter- (1300 mm), the wall thickness of the member is relatively small (50 mm). It must be recognized that the D/t ratio is important and a higher D/t ratio gives less resistance to collapse. Moreover, the yield stress of the vertical brace of Platform D is higher than the yield stress of vertical brace of Platform A. Consequently, the brace in Platform D is subjected to lower strain limitation, which is 10%, while the vertical brace in Platform A is subjected to 12% strain limitation. The conditions of the platforms at fracture for this case are given in Figure 6-9.

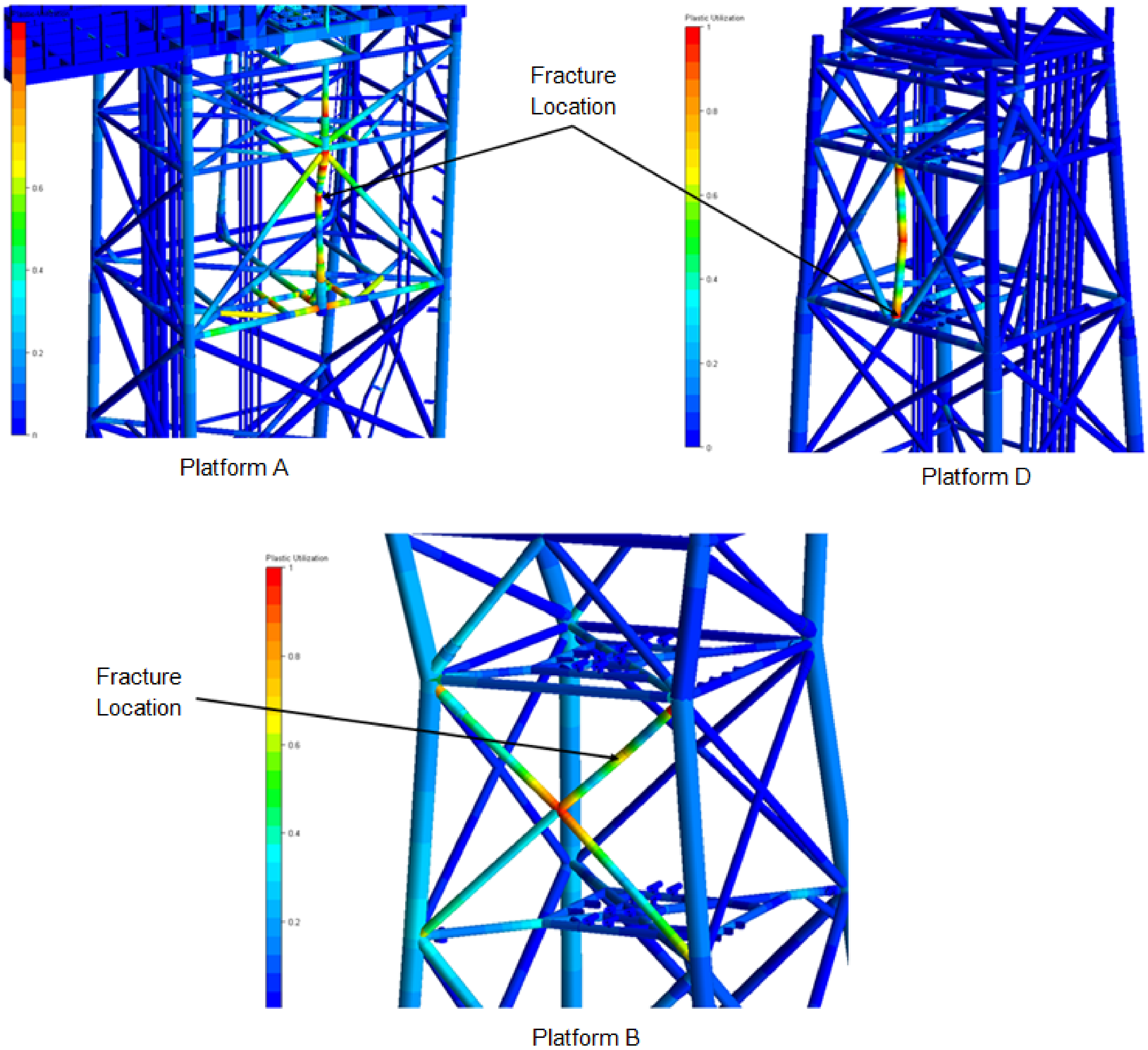

Figure 6-9 – The brace condition at fracture of Platform A, Platform B, and Platform D

6.5 Multiple Impacts

6.5.1 Multiple impact scenario on Platform A

The first impact on the vertical brace (LC 42) results in 18 MJ impact energy when fracture occurs at the impact point. Then the remaining energy is transferred to the diagonal braces under load case 420 and load case 421 sequentially and results in the addition of 7 MJ and 22 MJ impact energy, respectively. The total absorbed energy by Platform A under this multiple impact scenario is 47 MJ. The condition of Platform A after the first impact on vertical brace is as presented in Figure 6-9. The condition of Platform A after the second and third impact on diagonal braces is given in Figure 6-10. Table 6-6 tabulates the results from the multiple impact scenarios for Platform A.

Table 6-6 – Result from multiple impact scenario for Platform A

Case No	First Impact LC 42 (MJ)	Second Impact LC 420 (MJ)	Third Impact LC 421 (MJ)	Total Energy (MJ)
A01	18	7	22	47

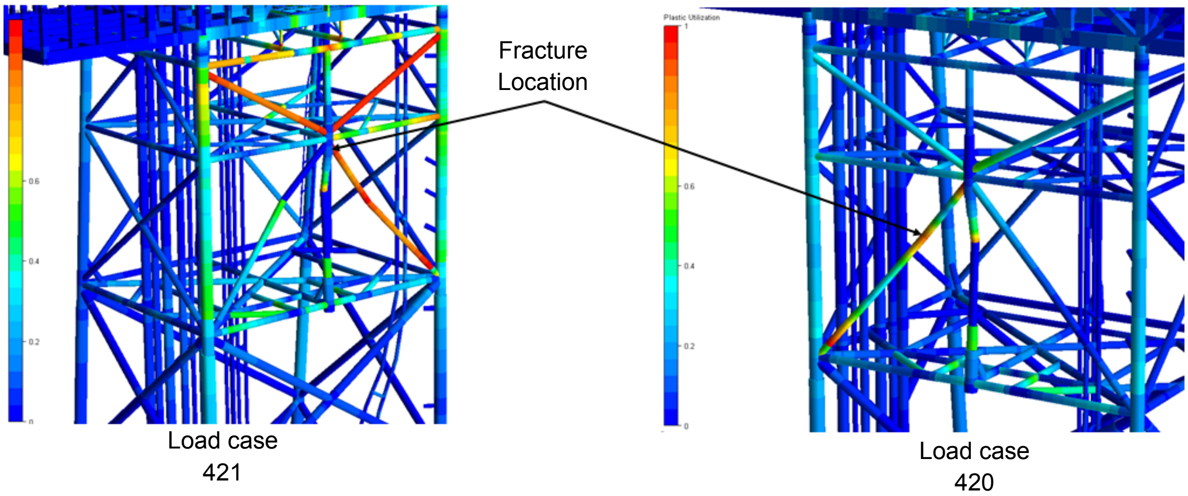

Figure 6-10 – Condition of Platform A after multiple impact case A01

This stage is considered as representing the ultimate jacket strength in terms of capacity to absorb impact energy. As can be seen in the figure above, many braces near the impact point have been highly utilized and are assumed failing. On the other hand, these braces are there in order to protect the conductors. If these braces fail then the conductor is exposed and most likely will be hit by the ship. This is a catastrophic event which may lead to injuries and fatalities since the conductors may leak explosive hydrocarbons.

6.5.2 Multiple impact scenario on Platform B

The first impact (load case 42) on the diagonal brace results in 14 MJ impact energy when fracture occurs at the member. Then the remaining impact energy is transferred to the other diagonal brace (load case 44) and results in an additional 32 MJ energy absorption until fracture occurs. Therefore, under this scenario the maximum absorbed energy of Platform B is 46 MJ. The condition of the diagonal brace after first impact is as given in Figure 6-9, while the condition after the second impact is given in Figure 6-11.

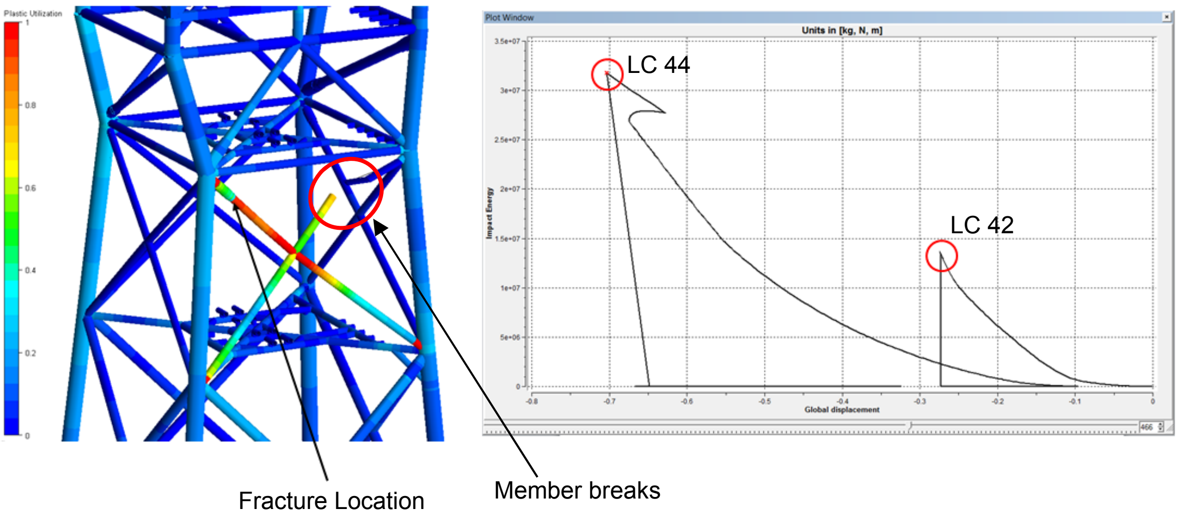

Figure 6-11 – Condition of Platform B after multiple impact case B01

It can be seen from the Figure 6-11 above that the first impacted member breaks and the second diagonal brace fractures due to the multiple impact. At this stage, it is assumed that the X-brace has failed. Physically this means that the remaining lower part of the X brace behaves as a cantilever and cannot stop the bow's penetration into the jacket. The conductors are assumed to be damaged either by the ship's bow or by the inward shifting of the lower part of the X-brace. The graph at the right side of Figure 6-11 shows the level of impact energy for each case. Table 6-7 tabulates the result from multiple impact scenarios for Platform B.

Table 6-7 – Result from multiple impact scenario for Platform B

Case No	First Impact LC 42 (MJ)	Second Impact LC 44 (MJ)	Total Energy (MJ)
B01	14	32	46

6.5.3 Multiple impact scenario on Platform C

The first impact is on the horizontal brace at Elev. + 9.40 m and results in 7 MJ impact energy when fracture occurs, as given in Table 6-5. The platform condition can also be referred to Figure 6-8. Then the second impact at the diagonal brace and the third impact at the X-brace intersection result 16 MJ and 35 MJ impact energy when fractures occur, respectively. The platform condition after multiple impact scenarios is depicted in Figure 6-12.

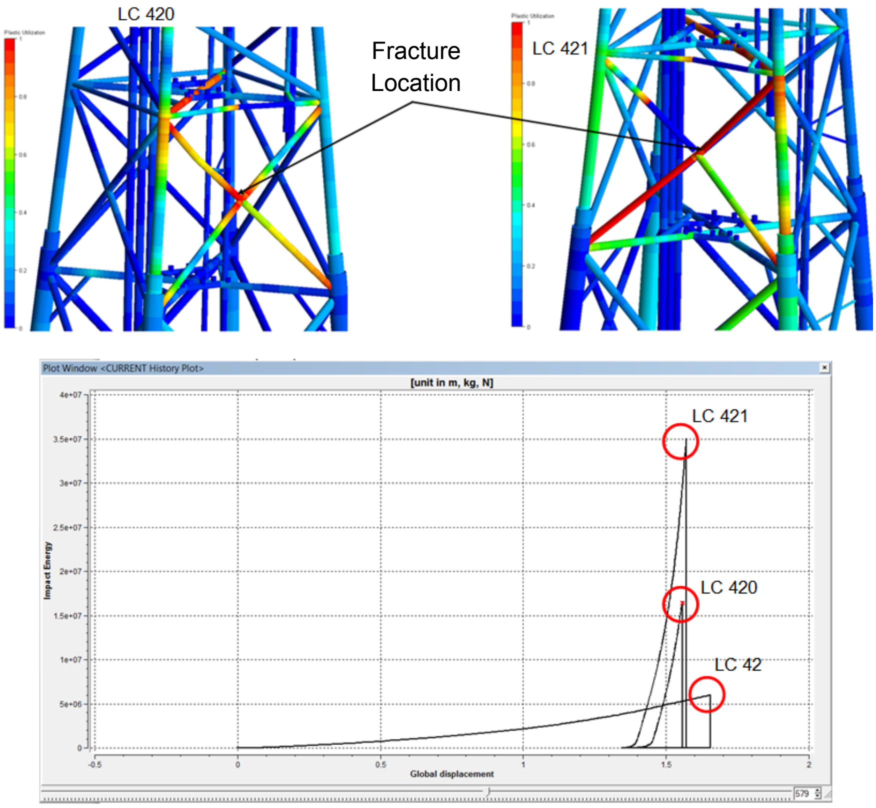

Figure 6-12 – Condition of Platform C after multiple impact case C01

It can be seen from Figure 6-12 above that the braces have been highly utilized. Moreover, the whole diagonal brace fails in load case 421. It can be inferred that the braces have collapse and therefore the ship may go inside the jacket and hit conductors. Then the total energy resulting from this scenario can be considered as the maximum energy that the platform can take before collapse. The results are tabulated in Table 6-8.

Table 6-8 – Result from multiple impact scenario for Platform C

Case No	First Impact LC 42 (MJ)	Second Impact LC 420 (MJ)	Third Impact LC 421 (MJ)	Total Energy (MJ)
C01	7	16	35	58

6.5.4 Multiple impact scenario on Platform D

Due to the complexity of the bracing configuration, many multiple impact scenarios can be simulated. In this report, three multiple impact cases are chosen. The first multiple impact case (D01) involves impact at two diagonal braces which are denoted by load case 44 and load case 47. The location of impact is as depicted in Figure 5-11 and the description of each load case is given in Table 5-7. The first impact results in 15 MJ energy absorption when fracture occurs and the second impact results in less impact energy, which is 9 MJ. Therefore the total impact energy is 24 MJ. The condition of Platform D after the first multiple impact scenarios is depicted in Figure 6-13.

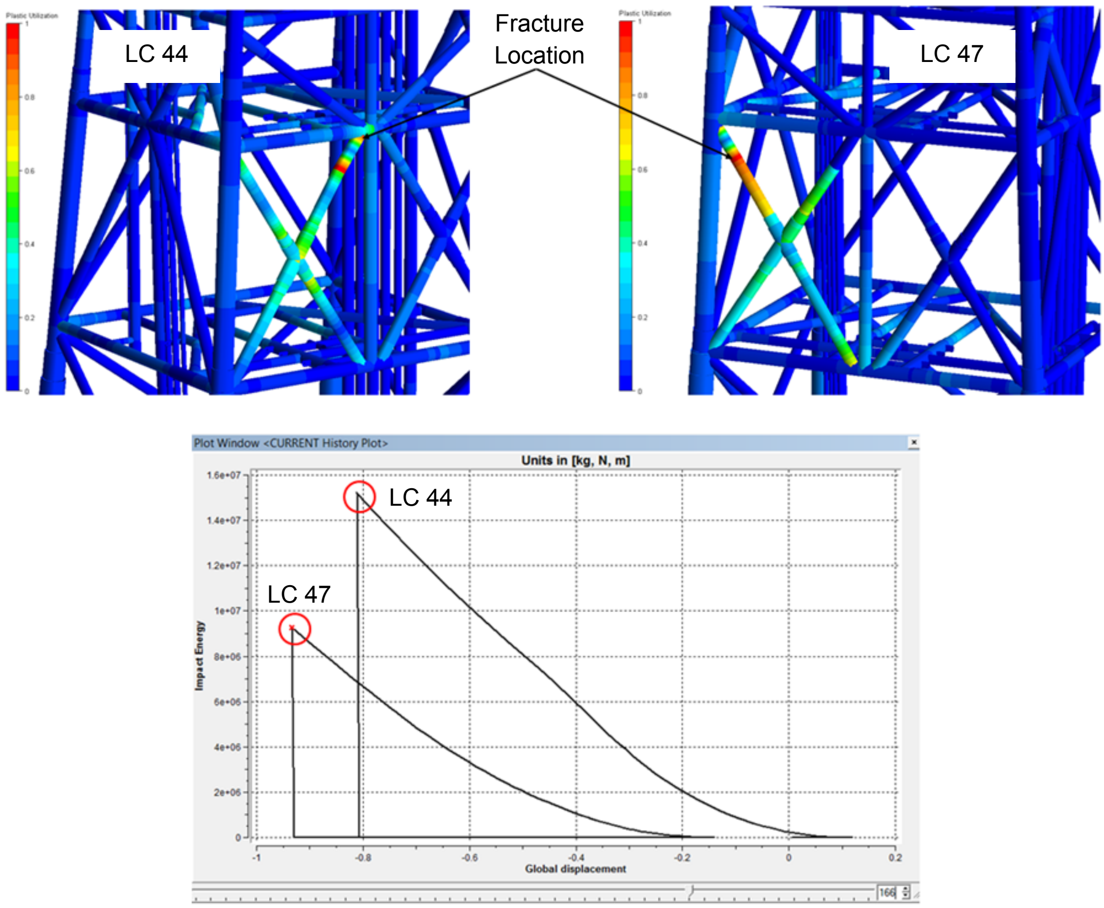

Figure 6-13 – Condition of Platform D after multiple impact case D01

The second impact case (D02) involves impact on the X-brace intersection (LC 41) and a diagonal member nearby (LC 51). From the first impact, the energy when fracture occurs is 16 MJ and from the second impact the energy is 15 MJ. Therefore the total absorbed energy is 31 MJ. The condition of Platform D after the multiple impact case D02 is depicted in Figure 6-14.

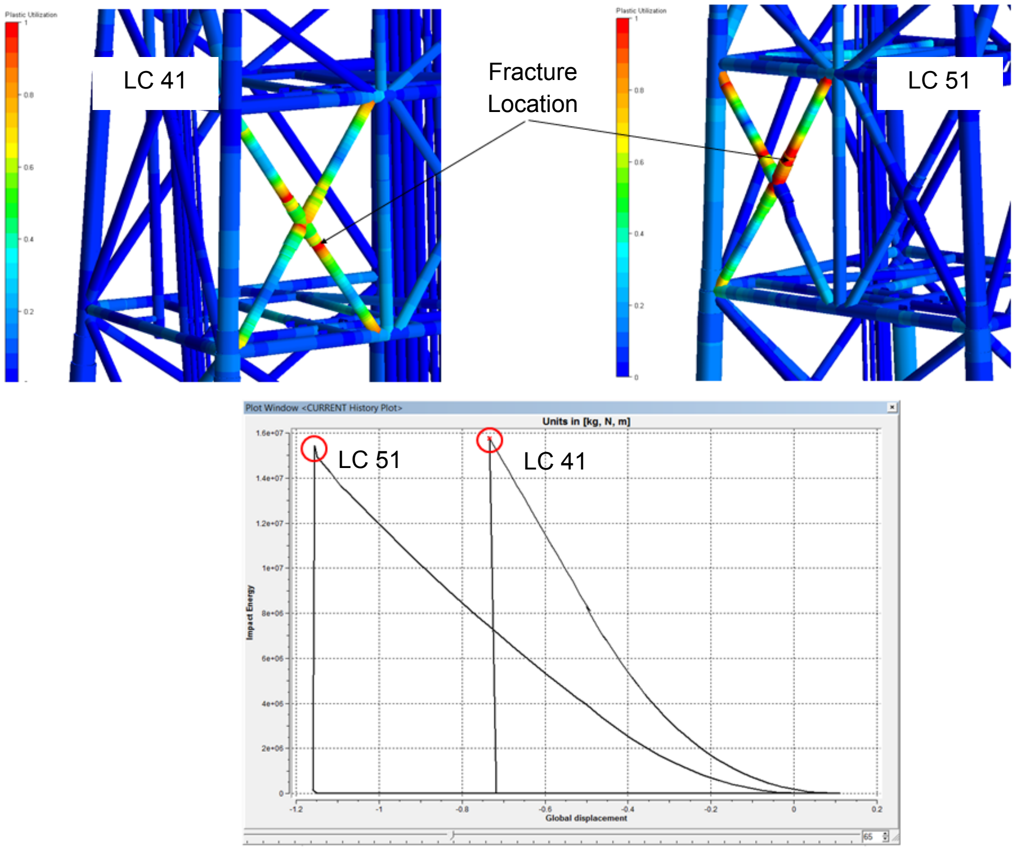

Figure 6-14 – Condition of Platform D after multiple impact case D02

The third impact case (D03) involves impact on vertical brace (LC 43), followed by impact on two diagonal braces (LC 44 and LC 50) subsequently. The description of each load case can be referred to Figure 5-11 and Table 5-7. From the first, second, and third impact the absorbed energy is 11 MJ, 14 MJ, and 13 MJ, respectively. Therefore, the total absorbed energy for this case is 38 MJ. The condition of Platform D after the multiple impact case D03 is depicted in Figure 6-15. The result of the three multiple impact cases is tabulated in Table 6-9.

Table 6-9 – Result from multiple impact scenario for Platform D

Load Case	Fisrt Impact (MJ)	Second Impact (MJ)	Third Impact (MJ)	Total (MJ)
D01	15	9	-	24
D02	16	15	-	31
D03	11	14	13	38

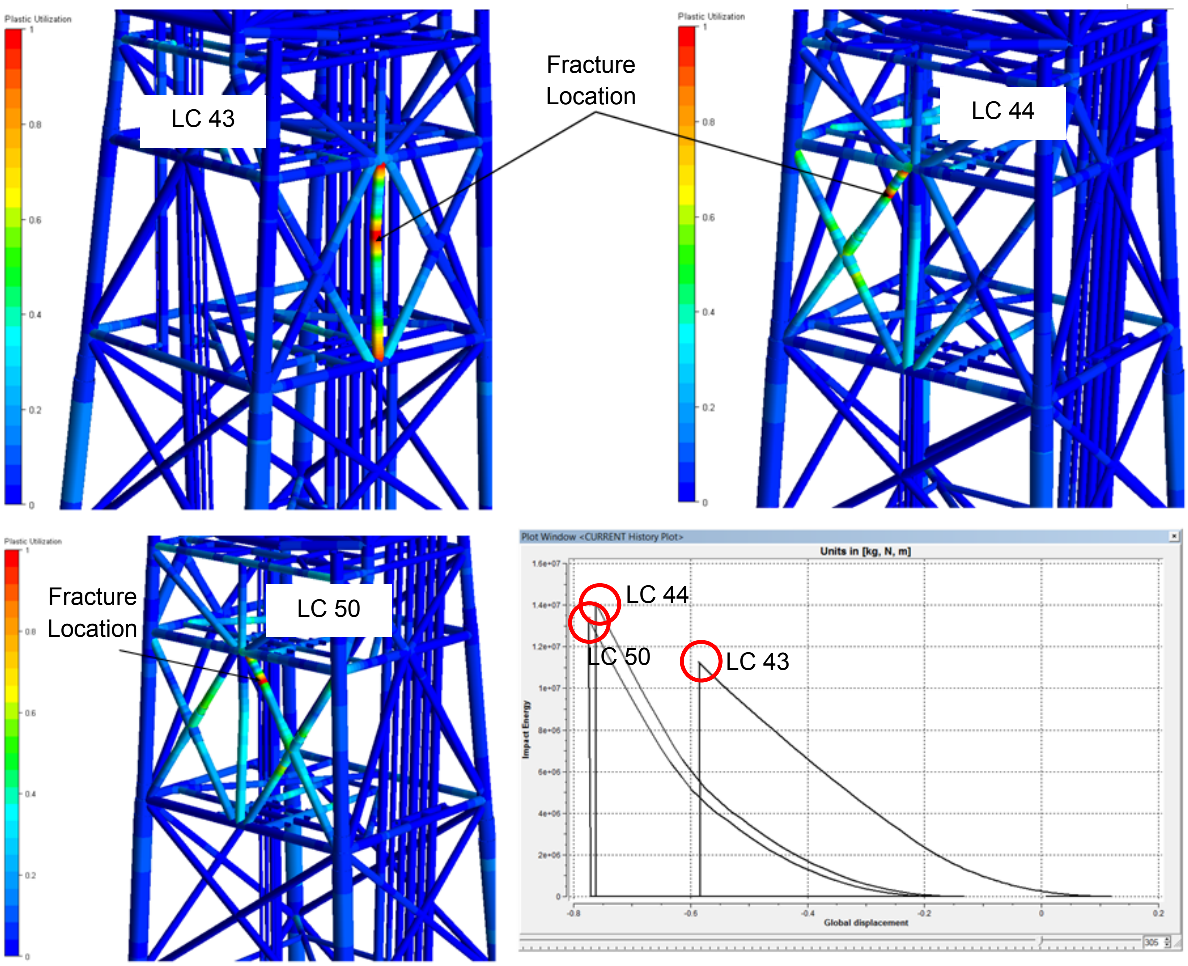

Figure 6-15 – Condition of Platform D after multiple impact case D03

6.6 Discussion on Diameter/wall thickness Ratio

The relation between D/t ratio and member capacity to absorb energy is not straightforward. In order to evaluate that, it should be recalled that the ship impact energy is dissipated by following:

- Plastic hinge formation
- Fracture
- Denting

For above points, the D/t evaluation against member strength would be more straightforward if one of the two parameters (either D or t) varies while the other parameters are kept constant, including local boundary condition the member, stiffness of adjacent joints, member length, material properties, etc. It is clear that, for example, if D/t ratio decreases for a constant D, the following properties of member will be affected:

- Cross section area increases, therefore capacity to take axial stress increases.
- Moment inertia and modulus section increases, therefore capacity to take bending moment increases.
- Local denting capacity increases, therefore the member is harder to dent and literally more energy can be absorbed by denting formation.

Due to time limitation, such study is not carried out within this thesis. However, the relation between D/t ratio and energy capacity may still be investigated using the normalization of axial member capacity and normalization of energy capacity. In order to do that, the case of impact on the legs is used as example.

The actual energy absorption for each jacket leg is given in Table 6-1. These values however do not describe the capacity of the leg against impact force. The reason is that before the leg is impacted by a vessel it has been utilized due to the selfweight, which causes compressive stress in the leg. To evaluate the capacity of the legs in terms of energy absorption, an additional simulation run needs to be made involving only the impact load (and therefore neglecting selfweight). On the other hand, the capacity of legs against compressive loads is also investigated. The appropriate formula is as given in NORSOK N004 [Ref. /24]. The detailed calculation is given in APPENDIX D. The results of such simulations and the calculations of the axial capacity of the legs are tabulated in Table 6-12.

Table 6-10 – Capacity of Platform Legs

Platfom Leg	Energy Capacity, E_{rd} (MJ)	Axial Capacity (compressive), N_{rd} (MN)
Leg of Platform A	75	110
Leg of Platform B	58	174
Leg of Platform C	53	96
Leg of Platform D	62	124

The actual compressive load on the legs is investigated by running simulations for each platform involving only selfweight. The selfweight is factored 1.0 and 1.5. This does not refer to any standard or certain criterion. The purpose of adding different factors for selfweight is merely add more data points to plot the relation chart. In addition, the impact on leg scenario is also simulated for selfweight factor 1.5. The results are summarized in Table 6-11.

Table 6-11 – Actual compressive load, N_{sd}, on the legs

Platfom Leg	N_{sd} with selfweight factor 1.0 (MN)	N_{sd} with selfweight factor 1.5 (MN)	Actual energy absorption, E_{sd}, with selfweight factor 1.5 (MJ)
Leg of Platform A	49	77	12
Leg of Platform B	62	93	40
Leg of Platform C	33	50	17
Leg of Platform D	21	27	44

The relation between axial capacity and energy capacity can be seen by taking the normalization of actual compressive load and energy actual absorbed energy to capacity of each, for selfweight factors of 1.0 and 1.5. The plot is given in Figure 6-16.

From Figure 6-16, the red dots mark the idealized relation between ratio of actual axial force to axial capacity of a member (N_{sd}/N_{rd}) and ratio of actual energy to capacity of energy absorption (E_{sd}/E_{rd}). The linear line between two red dots denotes the relation that generally exists for a general tubular member. If a member has been exhausted by axial load, showed by high ratio of N_{sd}/N_{rd}, then its capacity to take impact energy becomes lower, and vice versa.

It can be concluded therefore that since lower of D/t may increase the member axial capacity, then the ratio of N_{sd}/N_{rd} becomes smaller. Consequently, the capacity of the member to take the energy becomes higher.

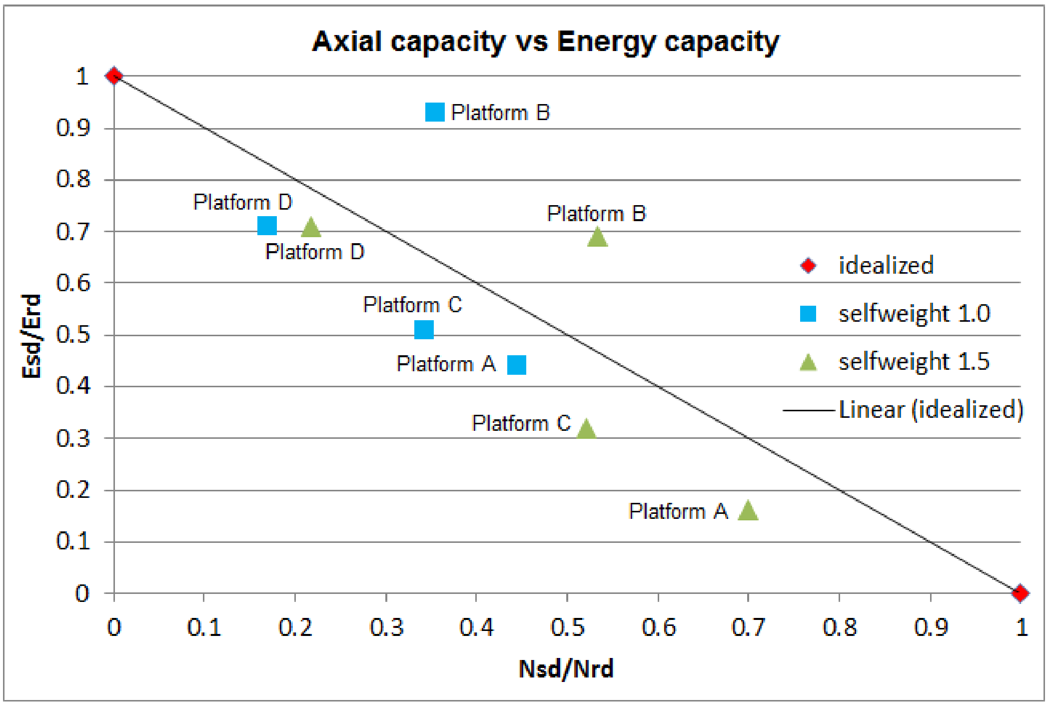

Figure 6-16 – Axial capacity plot against energy capacity

The ratio of actual axial force to axial capacity of member is (N_{sd}/N_{rd})
The ratio of actual energy to capacity of energy absorption is (E_{sd}/E_{rd})

It should be noted also that the profiles of the impacted member varies. This may result in different capacity of the member to absorb energy. In addition to that the energy absorption capacity is also affected by other factors such as member length, strength of adjacent joints, configuration of joint supports, material properties, etc. In this respect we can notice that the results of all impact scenarios described in the previous section are tabulated in Table 6-12.

Table 6-12 – Results summary for all impact scenarios

Impact Scenario	Range of Impact Energy before Failure (MJ)
Impact on jacket leg	27 – 54
Impact on X-brace intersection	42 – 46
Impact on brace can	28 – 76
Impact on single brace	7 – 21
Multiple impact	24 – 58

7 SUMMARY, CONCLUSION, AND RECOMMENDATIONS

7.1 Summary

The purpose of this thesis work is to investigate the strength of existing jacket platforms on NCS against collision from larger supply vessels which may involve high amount of impact energy. In order to do so, a survey of supply vessels has been done to give a view of the size of supply vessels operating on the NCS. The size is proportional to the kinetic energy, if there is an event when a vessel collides with a jacket platform accidentally. Depending to the mass of the vessels and the velocity at the time of impact, the kinetic energy may be very high and may cause the jacket platform to collapse.

A total of 115 vessels have been surveyed. The maximum tonnage of the supply vessels is 6200 tons, which corresponds to 14 MJ and 17 MJ kinetic energy for bow/ stern impact and broadside impact, respectively, at an impact speed of 2 m/s. The calculation of kinetic energy is based on suggested added mass value and minimum impact velocity as stated in NORSOK N-003 [Ref. /23]. However the impact speed may be higher and results in higher kinetic energy. In this thesis, the maximum investigated impact energy is around 80 MJ and 100 MJ for bow/ stern impact and broadside impact, respectively for collision speed of 4.8 m/s.

In this thesis an analysis of jacket platforms in terms of their capacity to absorb impact energy has been done. Four platforms have been analyzed based on a non-linear static method with assistance of a non-linear computer program to simulate various impact scenarios. The maximum energy absorption is limited either by fracture, denting, or failure of the joints.

For a single brace impact, the maximum absorbed energy is 21 MJ. However, this result does not cause the collapse of a platform. It is shown from Figure 6-8 and that the damage due to a single impact on a brace is localized only at the impacted member.

The impact on a jacket leg is considered as a critical scenario. Failure of one leg may lead to a severe damage of the whole platform since the load carrying capacity of the jacket will be reduced substantially. In this report, the maximum impact energy that can be taken by a leg is 54 MJ.

From the various impact scenarios that have been simulated in this thesis, the maximum capacity of energy absorption of the jacket is 76 MJ. This occurs if the ship hits jacket can. However, this case is less critical since impacts on jacket cans have lower likelihood compared with impact on jacket legs.

In a real collision event, the supply vessel may hit a jacket at a random location. In order to represent that, impacts at an X-brace intersection with multiple further impact scenarios are simulated. The results of analysis show that the maximum impact energy that can be taken by a jacket platform is 46 MJ and 58 MJ for X-brace impact and multiple impacts, respectively. This however refers to the strongest jacket discussed in the thesis (Platform D for X-brace impact and Platform C for multiple impact case).

For the case of impact at an X-brace intersection, other platforms have slightly lower impact energy. Platforms A and B have the same impact energy which is 42 MJ, and platform C has impact energy which is 45 MJ.

For multiple impact case, the result of energy absorption quite varies; particularly for Platform D which has impact energy at range of 24 MJ – 38 MJ for the simulated multiple impact scenarios. Moreover, Platform A and Platform B have similar capacity under multiple impact case, which is 47 MJ and 46 MJ, respectively. It is important to highlight that the results may be different if other impact scenarios are to be simulated in further work.

The relation between D/t ratio and member capacity to dissipate impact energy has also been investigated. Although the relation is not straightforward, it still can be seen that a higher D/t ratio gives a higher capacity to absorb impact energy.

7.2 Conclusion

Recalling NORSOK N-003 criteria for calculating kinetic energy of a vessel, the recommended ship velocity at impact to be taken is 2 m/s as minimum, with 10% and 40% added mass for bow/ stern impact and broadside impact, respectively. If these criteria are to be used, then from the analysis, it can be concluded that the platforms capacity in terms of energy absorption is far greater than the impact energy from the biggest vessel that has been surveyed (6200 tons).

If the calculation is taken all the other way around, considering the maximum absorption energy of 58 MJ (for multiple impact case) and keeping the criteria of minimum speed and added mass, the platform can take impact from supply vessels having 20000 tons and 26000 tons displacement for broadside impact and bow/ stern impact, respectively.

It should be noted that in this thesis the platforms are assumed to take all impact energy. This is very conservative since in real collision accident, some parts of impact energy are also dissipated by the ship. Therefore the energy absorption capacity of the jacket platforms is actually higher than what has been presented here, and they can withstand the collision from heavier supply vessels.

7.3 Recommendation for Future Work

Due to constraints of time and availability of supporting data, some assumptions were made during the completion of this thesis work. More improvements can be made in order to make the analysis more representative to the real condition of the platforms and thus the results of the analysis would give more accurate description of what would happen to the platforms after a real impact accident. The author suggests several recommendations for further work as following:

- The structural model should be verified against the supporting documents such as drawings, design basis, design brief, etc. USFOS models used in this analysis are transformed from a GeniE model. During the transformation some errors may occur; material profiles, cross section profile, etc. may differ from the GeniE model. Verification is needed to ensure that the models used in USFOS do not deviate from the original design.
- The USFOS model should be made as coarse as possible. The models used in USFOS were taken from GeniE models, which may have as original purpose to carry out analyses other than non-linear analysis. Too fine mesh in the model is not good for calculation with USFOS. In USFOS, every component has the same importance. One detail may disturb the solution, causing singularities, and in the end may give inappropriate calculation results. Therefore tiny details in the model should be avoided.
- A pile model could be used instead of a fixed bottom boundary condition. Additionally for slender jackets one may evaluate the use of a dynamic approach, in which the flexibility of the bottom support affects the global dynamic response. Since the Platform B jacket is relatively slender, a dynamic run could be applied in order to verify the impact result. For this, a pile model should be used instead of a fixed

bottom boundary condition. The non-linearity of pile-soil interaction will affect the structural response for high energy boat impact loads, in particular where piles' capacities will be below the global impact load and piles will be damaged. That situation is normally assumed not to be probable; however it was not verified in this report.

- More multiple impact scenarios should be simulated. More multiple impact scenarios may cover more possibilities of studying collision accidents in terms of location of impact.

In addition, the analysis covered in this thesis report may also be used as basis of the following works:

- Risk evaluation including an investigation of operational limits for vessel operations around a jacket platform. The results in this report can be used to give input to risk matrices regarding consequences of the accidental event.
- Evaluation of effect of impact from vessels for other types of jackets. The analysis may be expanded to investigate the capacity of tripods, 6-legged jacket platforms, 8-legged jacket platforms, etc. With similar methodology that has been used in this thesis, the analysis may also be used to investigate the capacity of other offshore platforms such as jack up rigs.

REFERENCES

/01 Amdahl, J., 1983. *Energy Absorption in Ship-Platform Impacts.* Trondheim: Marine Technology Center.

/02 Amdahl, J. and Johansen, A., 2001. *High-Energy Ship Collision with Jacket Legs.* Paper on International Offshore and Polar Engineering Conference. Stavanger: The International Society of Offshore and Polar Engineer.

/03 Aven, T., 2012. *Fundamentals about Risk and Probability*. Presentation Slides on Risk Analysis Lecture at University of Stavanger-August 22nd 2012. Available online at itslearning: https://www.itslearning.com/ContentArea/ContentArea.aspx?LocationID=15491&LocationType=1

Accessed date: 4th February 2014.

/04 Boresi, A.P. and Schmidt, R.J., 2003. *Advanced Mechanics of Materials.*6th ed. John Wiley & Sons.

/05 Caprani, C., 2010. Lecture notes on Plastic Analysis. Available online at: http://www.colincaprani.com/files/notes/SAIII/Plastic%20Analysis%201011.pdf

Accessed date: 31th March 2014

/06 Det Norske Veritas, 2013. *DNV-OS-A101 Safety Principles and Arrangements.* Høvik: Det Norske Veritas.

/07 Det Norske Veritas, 2010. *DNV-RP-C204 Design against Accidental Loads.* Høvik: Det Norske Veritas.

/08 Det Norske Veritas, 2011. *DNV-OS-C101 Design of Offshore Steel Structure, General (LRFD Method).* Høvik: Det Norske Veritas.

/09 Det Norske Veritas Software, 2013. *SESAM User Manual GeniE Vol.1 – Concept design and analysis of offshore structures.* Høvik: Det Norske Veritas Software.

/10 International Association of Oil & Gas Producers (IAOGP), 2010. *Risk Assessment Data Directory – Ship/ Installation Collision, Report No. 434-16.*

/11 Institute for Steel Development & Growth (INSDAG). Teaching Material on Plastic Analysis (Chapter 35). Version II. Available online at: http://www.steel-insdag.org/TeachingMaterial/chapter35.pdf

Accessed date: 25th March 2014.

/12 Johansen, A., 2013. *Basic Theory – Plasticity and Yield Hinges.* Presentation notes on USFOS Course on 19-20 June 2013. Høvik: Det Norske Veritas.

/13 Learn Easy. *Properties of Materials*. Available online at: http://www.learneasy.info/MDME/MEMmods/MEM30007A/properties/Properties.html

Accessed date: 26th March 2014.

/14 Lubliner, J., 2005. *Plasticity Theory*. Revised Edition. University of California at Berkeley.

/15 Marintek, 1999. *USFOS User's Manual – Program Concepts.* Sandsli: SINTEF Marintek.

/16 Oltedal, H. A., 2012. *Ship-Platform Collisions in the North Sea*. Helsinki: The Annual European Safety and Reliability Conference (ESREL).

/17 Oosterkamp, L. D., 2013. *Plasticity*. Lecture notes on Advanced Mechanics of Materials course. Available online at: https://www.itslearning.com/ContentArea/ContentArea.aspx?LocationID=16305&LocationType=1.

Accessed on: 28th March 2014

/18 Petroleum Safety Authority, 2011. *Collision between vessels and installations: Averting Unwanted Contact*. Online web page available at: http://www.ptil.no/structural-integrity/collisions-between-vessels-and-installations-averting-unwanted-contact-article7670-901.html

Accessed date: 30th January 2014.

/19 Petroleum Safety Authority, 2009. *Investigation of Big Orange XVII's collision with Ekofisk 2/4-W 8th June 2009.* Petroleum Safety Authority Norway.

/20 Petroleum Safety Authority, 2011. *Risk of Collision with Visiting Vessels.* Online web page available at: http://www.ptil.no/structural-integrity/risk-of-collisions-with-visiting-vessels-article7524-901.html

Accessed date: 3rd February 2014

/21 Skallerud, B., and Amdahl, J. 2002. *Nonlinear Analysis of Offshore Structures.* Hertfordshire: Research Studies Press.

/22 Standards Norway, 2004. *NORSOK Standard N-001 Structural Design.* Lysaker: Standards Norway.

/23 Standards Norway, 2007. *NORSOK Standard N-003 Actions and Action Effects.* Lysaker: Standards Norway.

/24 Standards Norway., 2013. *NORSOK Standard N-004 Design of Steel Structure*. Annex A.3 Ship Collision. Lysaker: Standards Norway.

/25 Statistic Norway on Maritime Transport. Online web page available at: https://www.ssb.no/en/transport-og-reiseliv/statistikker/havn/kvartal/2014-01-23?fane=tabell#content

Accessed date: 28th January 2014

/26 Søreide, T. H., 1981. *Ultimate Load Analysis of Marine Structures*. Trondheim: Tapir.

/27 Viser, W., 2004. *Ship Collision and Capacity of Brace Members of Fixed Steel Offshore Platforms.* Houten: Health & Safety Executive.

/28 Marine Traffic. Live map of supply vessels operating in North Sea and Norwegian Sea.

http://www.marinetraffic.com/

Accessed date: 9th April 2014

/29 Norwegian Petroleum Directorate, 2013. *Map of the Norwegian Continental Shelf.* Available online at: http://www.npd.no/en/Maps/Map-of-the-NCS/

Accessed date: 10th April 2014.

/30 Det Norske Veritas, 2000. Class classification. Available online at: https://exchange.dnv.com/exchange/en/mainclass.html

Accessed date: 15th April 2014.

/31 REM Offshore. *Vessel Fleet*. Available online at: http://www.rem-offshore.no/fleet

Accessed Date: 15th April 2014

APPENDIX A Survey of Supply Vessel

Summary of supply vessel survey is given in table below.

Vessel Name	Length (m)	Breadth (m)	Draft (m)	Year	Deadweight (tons)
Blue Power	82	18	5.4	2013	4240
Blue Protector	82	18	5.4	2013	4200
Bourbon Mistral	89	20	5.6	2006	4779
Bourbon Monsoon	88	20	5.5	2007	4779
Bourbon Rainbow	88	19	5.6	2013	4400
Bourbon Sapphire	91	19	5.4	2008	4678
Caledonian Vanguard	93	22	6.2	2005	4312
Caledonian Victory	93	22	6.4	2006	4380
Caledonian Vigilance	81	18	6.3	2006	5300
Caledonian Vision	93	22	6.3	2006	4312
E.R Kristiansand	73	16	5.1	2005	3544
E.R. Georgina	93	20	6.2	2010	4831
Edda Frigg	84	19	4.5	1997	3974
Energy Swan	93	19	5.5	2005	5304
F.D. Incomparable	75	16	5.3	2012	3161
F.D. Indomitable	75	16	4.8	2011	3105
Far Serenade	94	21	6	2009	4000
Far Solitaire	92	22	5.6	2012	5800
Far Spica	81	18	5.3	2013	4000
Far Symphony	86	19	6	2003	4929
Grampian Sceptre	83	18	4.6	2013	2515
Grampian Talisker	82	17	5.2	2009	3890
Grampian Talisman	73	17	5	2007	3614
Grimshader	80.9	17.5	3.5	1983	3324
Havila Aurora	74.87	16.4	6.22	2009	3205
Havila Borg	78.6	17.6	7.7	2009	3787
Havila Charisma	95	20	5.5	2012	4976
Havila Clipper	80.4	17.6	6.5	2011	3683
Havila Commander	85	20	6.8	2010	5486

Vessel Name	Length (m)	Breadth (m)	Draft (m)	Year	Deadweight (tons)
Havila Crusader	85	20	6.8	2010	5433
Havila Faith	82.85	19	6.31	1998	4679
Havila Fanø	80.4	17.6	6.48	2010	3879
Havila Favour	82.85	19	6.31	1999	4679
Havila Foresight	93.6	19.7	6.3	2007	4785
Havila Fortress	82.85	19	6.32	1996	4679
Havila Fortune	74.87	16.4	6.22	2009	3205
Havila Herøy	80.4	17.6	6.5	2009	3683
Havila Princess	73.4	16.6	6.4	2005	3719
Highland Duke	75	16	4.9	2012	3105
Highland Laird	72	16	4.3	2006	3105
Highland Prestige	86	18	5.4	2007	4993
Highland Prince	87	19	6	2009	4826
Highland Star	81.9	18	3.8	1991	3075
Island Challenger	93	20	6	2007	4100
Island Champion	93	20	5.8	2007	4100
Island Chieftain	94	20	5.6	2009	4100
Island Contender	96	20	6.5	2012	4750
Island Duchess	85	17	4.8	2013	3750
Island Empress	77	16	5	2007	3180
Malayiva Seven	82.5	18.8	5.2	1994	4568
Malayiva Twenty	72	16	4.5	2004	3316
Normand Aurora	86	19	5.5	2005	4813
Normand Flipper	80	20	4.4	2003	4276
North Mariner	84	18	5.4	2002	4545
North Purpose	86	19	5.5	2010	4826
North Stream	84	19	5	1998	4320
Northern Supporter	67	16	4.6	1996	3100
Ocean Scout	77	16	4.8	2013	3200
Ocean Viking	70	16	5	1986	2629
Olimpic Energy	94	20	5.2	2012	5066

Vessel Name	Length (m)	Breadth (m)	Draft (m)	Year	Deadweight (tons)
Olympic Commander	94	20	6	2012	4857
Olympic Electra	80	17	5.2	2011	3000
Olympic Princess	84	20	5.6	1999	4159
Rem Commander	85	20	6.1	2011	4500
Rem Fortress	85	20	5.7	2011	4500
Rem Fortune	86	20	5.8	2013	4000
Rem Leader	90	24	6.2	2013	4800
Rem Mermaid	80	16	5.3	2008	3336
Rem mist	89	19	6	2011	4400
Rem Ocean	107	22	6.5	2014	5520
Rem Server	94	20	5	2011	5300
Rem Supporter	94	20	6.2	2012	5300
Saeborg	86	18	6	2011	4300
Sayan Princess	78	16	5.8	2013	3800
SBS Tempest	74	14	5.4	2006	3677
Sea Tantalus	82	17	5.6	2013	4000
Sea Trout	73	16	5.8	2008	3678
Siddis Supplier	73	17	5	2010	3350
Skandi Caledonia	84	20	5.3	2003	4100
Skandi Feistein	88	19	5.8	2011	4700
Skandi Flora	95	20	5	2009	5005
Skandi Foula	83	20	5.1	2002	4200
Skandi gamma	95	20	6	2011	5054
Skandi Kvitsoy	88	19	6	2012	4700
Skandi Maroy	82	17	5.2	2012	3594
Skandi Marstein	83.7	19.7	5.4	1996	4170
Skandi Mongstad	97	22	6	2008	4423
Skandi Nova	82	17	5.9	2012	3100
Skandi Seven	121	22	7	2008	6000
Skandi Sotra	83	20	5	2003	3933
Skandi Texel	69	16	4.8	2006	3500

Vessel Name	Length (m)	Breadth (m)	Draft (m)	Year	Deadweight (tons)
Stril Explorer	76.4	16.2	4.6	2010	1400
Stril Mermaid	79	18	5.8	2010	3755
Stril Myster	90	19	6	2003	4500
Stril Orion	93	19	6	2011	4900
Stril Polar	93	19	5.5	2012	4900
Strill Mariner	79	18	5	2009	3755
Strilmoy	86	20	4.2	2005	4248
Troms Arcturus	95	21	6.5	2014	5580
Troms Artemis	85	20	6.1	2011	4900
Troms Castor	85	20	5.6	2009	4900
Troms Lyra	82	18	5.5	2013	3650
Vestland Mira	86	18	5.5	2012	4000
Viking Athene	74	17	4.7	2006	3546
Viking Dynamic	90	19	5.4	2002	4505

APPENDIX B Example of Input File

Structural Model

```
HEAD
'
'        Node ID        X          Y          Z    Boundary code
 NODE       10001     -24.892      1.718    -109.000  1 1 1 1 1
 NODE       10002     -24.579      0.379    -109.000
 NODE       10003     -24.265     -0.961    -109.000
 NODE       10004     -23.952     -2.300    -109.000
 NODE       10005     -23.639     -3.639    -109.000  1 1 1 1 1
 NODE       10006     -23.669      1.288    -109.000
 NODE       10007     -22.446      0.859    -109.000
 NODE       10008     -21.223      0.430    -109.000
 NODE       10009     -20.000      0.000    -109.000
 NODE       10010     -19.569     -1.212    -109.000
 NODE       10011     -19.137     -2.424    -109.000
 NODE       10012     -18.705     -3.636    -109.000
 NODE        10013     -18.274     -4.848      -109.000   1 1 1 1 1
'            Elem ID    np1    np2   material  geom   lcoor   ecc1   ecc2
BEAM       10129   10201   10202   10001   10001   10001
BEAM       10130   10202   10203   10001   10001   10001
BEAM       10131   10203   10204   10001   10001   10001
BEAM       10132   10201   10205   10001   10002   10002
BEAM       10349   10325   10335   10003   10022   10035   10006   10007
'        Elem ID   np1    np2    np3    np4   mater  geom    ec1   ec2   ec3   ec4
QUADSHEL    10001   10005   10004   10017   10014   10003   10023
QUADSHEL    10002   10004   10003   10018   10017   10003   10023
QUADSHEL    10003   10003   10002   10019   10018   10003   10023
QUADSHEL    10004   10002   10001   10006   10019   10003   10023
'        Geom ID     Do       Thick   (Shear_y  Shear_z    Diam2 )
 PIPE       10016     0.500     0.016
 PIPE       10022     1.200     0.080
 PIPE       10024     2.736     0.090
 PIPE       10025     0.457     0.016
 PIPE       10027     1.200     0.030
 PIPE       10028     1.220     0.040
'        Geom ID    H    T-web   W-top  T-top   W-bot   T-bot Sh_y Sh_z
 IHPROFIL    10018   0.390  0.011   0.300  0.019   0.300  0.019
 IHPROFIL    10164   0.890  0.016   0.300  0.030   0.300  0.030
 IHPROFIL    10169   0.490  0.012   0.300  0.023   0.300  0.023
 IHPROFIL    10170   0.600  0.015   0.300  0.030   0.300  0.030
'        Geom ID    H    T-sid  T-bot  T-top   Width   Sh_y Sh_z
```

```
BOX       10001   0.800   0.016   0.020   0.020   0.700
BOX       10002   1.500   0.016   0.020   0.020   0.700
BOX       10003   1.500   0.016   0.025   0.025   0.800
BOX       10004   0.900   0.012   0.020   0.020   0.700
BOX       10005   0.900   0.012   0.025   0.025   0.800
BOX       10006   1.300   0.016   0.020   0.020   0.700

'         Loc-Coo        dx          dy          dz
UNITVEC      10001       -1.000       0.000       0.000
UNITVEC      10002        0.000       0.000       1.000
UNITVEC      10003        0.000       1.000       0.000
UNITVEC      10004       -0.028       0.011       1.000

'         Ecc-ID         Ex          Ey          Ez
ECCENT       10001        1.291      -0.453       1.583
ECCENT       10002        0.430      -0.151       0.528
ECCENT       10003        0.430      -0.151       0.528
ECCENT       10004        1.291      -0.453       3.166
ECCENT       10005        0.645      -0.227       1.583

'         Mat  ID    E-mod      Poiss     Yield      Density     ThermX
MISOIEP     10001   2.100E+11   3.000E-01   4.200E+08   7.850E-09   1.200E-05
MISOIEP     10002   2.100E+11   3.000E-01   3.550E+08   7.850E+03   1.200E-05
MISOIEP     10003   2.100E+11   3.000E-01   4.200E+08   7.850E+03   1.200E-05
MISOIEP     10004   2.100E+11   3.000E-01   3.550E+08   7.850E+03   1.200E-05
MISOIEP     10005   2.100E+11   3.000E-01   4.200E+08   7.850E+03   1.200E-05
MISOIEP     10006   2.100E+11   3.000E-01   4.770E+08   7.850E+03   1.200E-05
MISOIEP     10007   2.100E+11   3.000E-01   3.450E+08   7.850E+03   1.200E-05
'         Node ID                    M A S S
NODEMASS     10456           4.75000E+06  ! node mass added to account for topside weight
NODEMASS     10371           4.75000E+06  ! node mass added to account for topside weight
NODEMASS     13106           4.75000E+06  ! node mass added to account for topside weight
NODEMASS     13188           4.75000E+06  ! node mass added to account for topside weight

'           End 1          End 2       Elem ID
BEAMHING    1 1 0 0 0 0     1 1 1 1 1 1      10599
BEAMHING    1 1 0 0 0 0     1 1 1 1 1 1      10600
BEAMHING    1 1 1 1 1 1     1 1 0 0 0 0      10602
BEAMHING    1 1 1 1 1 1     1 1 0 0 0 0      10603

'         Load Case   Acc_X      Acc_Y      Acc_Z
GRAVITY          1  0.0000E+00  0.0000E+00 -9.3719E+00

'         GroupID       ListType       { List }
```

```
'       Type=Group  GroupID Label
NAME Group 100 Conductor
GROUPDEF 100 Element    12594    11980    11419    11287    12619    12005
    11444    11312    12638    12024    11463    11331    12663    12049
    11488    11356    12591    11977    11416    11284    11283    11415
    11976    12590    12616    12002    11441    11309    11308    11440
    12001    12615    12635    12021    11460    11328    11327    11459
```

Control File

```
12001    12615    12635    12021    11460    11328    11327    11459
HEAD     Units in [kg, N, m]

        Platform A - Boat Impact Analysis
' GENERAL ANALYSIS PARAMETERS
' Refine 2  15002 ' 15001
CMAXSTEP   100000
CUNFAL    6
'       INPRINT OUTRINT TERMPRINT
CPRINT     1       1       1
'
'      RESTART   RESULTS   PRINT
CSAVE      0       -1      -1
'
'=====================================================================================
'Control Nodes
'=====================================================================================
'        ncnods
CNODES     1
'        nodex     idof    dfact
'         14001      2       1.0  ! For load comb  01, Impact point
'         11232      2       1.0  ! For load comb  02 , Impact point
         14002      2       1.0  ! For load comb  03, 05,& 07 Impact point
'=======================================================================================
' LOAD CONTROL << ACTIVATE/ DEACTIVATE LOAD COMBINATION AS NEEDED
'=======================================================================================
'        nloads    npostp  mxpst   mxpis
CUSFOS      2       1000   0.5    1.0
'        lcomb     lfact   mxld    nstep     minstp
          1       0.1    1.0      1000       0.01
'=======================================================================================
'                                                                    IMPACT LOADS
'=======================================================================================
```

```
'      LDCS    Elem.    Pos.      Energy      Ext.   X-dir    Y-dir  Z-dir   Ship
BIMPACT    40     15002    1       90.0E6      1.6      0.0      1.0   0.0      0  'B
BIMPACT    41     11557    1       90.0E6      1.4      0.0      1.0   0.0      0  'B
BIMPACT    42     11554    2       90.0E6      1.0      0.0      1.0   0.0      0  'B
BIMPACT    43     13768    1       90.0E6      1.0     -1.0      0.0   0.0      0  'B
BIMPACT   411     11556    2        0.0        0.0      0.0      1.0   0.0      0
BIMPACT    44     11149    2       00.0E6      1.0      0.0      1.0   0.0      0  'B
'==========================================================================================
'                                          JOINT CAPACITY CHECK
'==========================================================================================
'          Node       Chord1     Chord2   geono   MSL       CapLevel        Qf
''CHJOINT     11232      11557    11556     0     NOR_R3      'mean         1.0
CHJOINT     10367      10400    10399     0     NOR_R3      'mean         1.0
CHJOINT     13017      13704    13705     0     NOR_R3      'mean         1.0
CHJOINT     10364      10396    10397     0     NOR_R3      'mean         1.0
CHJOINT     12992      13698    13699     0     NOR_R3      'mean         1.0
'CHJOINT     11234      11551    11550     0     NOR_R3      'mean         1.0
'==========================================================================================
'        List_type       Type      {Crit.}  ID_List
'           ElmID   Type    {Crit.}
'USERFRAC    Material      strain    0.12    10005
'USERFRAC    Material      strain    0.12    10008
'======================================================================
'Non structural members: Risers, Conductors, J tubes, Caissons
'======================================================================
NONSTRU Element        11287     11312     11331     11356     11419     11444 'Conductors
    11463    11488    11980    12005    12024    12049    12594    12619
    12638    12663    11284    11309    11328    11353    11416    11441
    11460    11485    11977    12002    12021    12046    12591    12616
    12635    12660    12659    12634    12615    12590    12045    12020
    12001    11976    11484    11459    11440    11415    11352    11327
    11308    11283    11280    11305    11324    11349    11412    11437
    11456    11481    11973    11998    12017    12042    12587    12612
```

APPENDIX C Example of Output File

Load step 50 / 35

======== I N C R E M E N T A L S O L U T I O N ========

USFOS load combination no = 50

Load step no. = 35

Load increment = 0.300

New load level = 9.386

Current stiffness parameter = 0.334

Solution accuracy parameter = 1.359*E-00007

Determinant of tangential matrix = 1.048*E 78329

Number of Negative Pivot Element = 0

Total energy absorbtion = 4.924*E 00007

Denting of the tube wall = 2.716E-01

Ship indentation = 0.000E+00

Dent deformation energy = 3.073E+06

Ship deformation energy = 0.000E+00

Structure deformation energy = 1.027E+07

Total Absorbed Ship Impact Energy = 1.334E+07

-------- I N T E R A C T I O N F U N C T I O N V A L U E S Fb(Fy) ---

ELEM	ES	Node1	Midspan	Node2	
100557	0	-0.39(-0.22)	-0.94(-0.93)	-0.27(-0.08)	
100631	0	-0.30(-0.12)	-0.92(-0.89)	-0.46(-0.32)	
101276	0	-0.10(-0.02)	-0.92(-0.89)	-0.02(-0.03)	
101280	0	-0.32(-0.13)	-0.92(-0.89)	-0.22(-0.01)	
101325	0	-0.24(-0.02)	-0.81(-0.75)	-0.55(-0.42)	
101327	0	-0.15(0.08)	-0.87(-0.82)	-0.34(-0.15)	
101331	0	-0.03(-0.03)	-0.90(-0.87)	-0.13(0.06)	
101491	2	-0.84(-0.78)	-0.49(-0.35)	-0.13(0.09)	+---+---O
101492	2	-0.80(-0.73)	-0.46(-0.30)	-0.10(0.03)	+---+---O
101493	0	-0.90(-0.85)	-0.66(-0.56)	-0.32(-0.12)	
101495	0	-0.92(-0.89)	-0.62(-0.51)	-0.29(-0.09)	
101496	2	-0.86(-0.81)	-0.59(-0.47)	-0.14(0.10)	+---+---O
101782	0	-0.35(-0.06)	-0.79(-0.73)	-0.88(-0.84)	
101792	0	-0.66(-0.56)	-0.67(-0.57)	-0.65(-0.04)	
101804				Fracture at end 2	

-------- G L O B A L T O T A L D I S P L A C E M E N T S --------

NODE	X-dis	Y-dis	Z-dis	X-rot	Y-rot	Z-rot
101440	-7.746E-01	7.070E-04	-1.400E-01	7.268E-05	5.443E-02	5.481E-04

-------- G L O B A L   R E A C T I O N   F O R C E S --------

NODE	X-for	Y-for	Z-for	X-mom	Y-mom	Z-mom
100001	5.582E+06	1.097E+06	1.746E+07	6.658E+06	-3.415E+07	1.551E+05
100007	-2.935E+06	2.214E+06	1.122E+07	-1.523E+07	-2.125E+07	2.223E+05
100009	-2.748E+06	-2.070E+06	1.119E+07	1.517E+07	-2.118E+07	-2.158E+05
100015	5.645E+06	-1.101E+06	1.738E+07	-6.633E+06	-3.401E+07	-1.450E+05
100025	2.224E+06	6.235E+06	2.181E+07	3.800E+07	-1.264E+07	-2.773E+05
100027	2.167E+06	-6.026E+06	2.170E+07	-3.782E+07	-1.260E+07	2.841E+05
100061	3.138E+06	-4.045E+06	1.525E+07	2.621E+07	1.855E+07	-4.052E+05
100063	3.255E+06	4.209E+06	1.518E+07	-2.612E+07	1.846E+07	4.058E+05

ForceDir	ShearForce	M_Center	Overturn_Mom
180	1.877E+07	-1.435E+02	2.812E+09

APPENDIX D Evaluation of Axial Capacity of Tubular

The following page is taken directly from NORSOK N004. This is the procedure to evaluate axial capacity of tubular steel.

6.3.3 Axial compression

Tubular members subjected to axial compressive loads should be designed to satisfy the following condition:

$$N_{Sd} \le N_{c,Rd} = \frac{Af_c}{\gamma_M} \qquad (6.2)$$

where

N_{Sd} = design axial force (compression positive)
f_c = characteristic axial compressive strength
γ_M = see 6.3.7

In the absence of hydrostatic pressure the characteristic axial compressive strength for tubular members shall be the smaller of the in-plane or out-of-plane buckling strength determined from the following equations:

$$f_c = [1.0 - 0.28\bar{\lambda}^2]f_{cl} \quad \text{for } \bar{\lambda} \le 1.34 \qquad (6.3)$$

$$f_c = \frac{0.9}{\bar{\lambda}^2}f_{cl} \quad \text{for } \bar{\lambda} > 1.34 \qquad (6.4)$$

$$\bar{\lambda} = \sqrt{\frac{f_{cl}}{f_E}} = \frac{kl}{\pi i}\sqrt{\frac{f_{cl}}{E}} \qquad (6.5)$$

where

f_{cl} = characteristic local buckling strength
$\bar{\lambda}$ = column slenderness parameter
f_E = smaller Euler buckling strength in y or z direction
E = Young's modulus of elasticity, $2.1 \cdot 10^5$ MPa
k = effective length factor, see 6.3.8.2
l = longer unbraced length in y or z direction
i = radius of gyration

The characteristic local buckling strength should be determined from:

$$f_{cl} = f_y \quad \text{for } \frac{f_y}{f_{cle}} \le 0.170 \qquad (6.6)$$

$$f_{cl} = \left(1.047 - 0.274\frac{f_y}{f_{cle}}\right)f_y \quad \text{for } 0.170 < \frac{f_y}{f_{cle}} \le 1.911 \qquad (6.7)$$

$$f_{cl} = f_{cle} \quad \text{for } \frac{f_y}{f_{cle}} > 1.911 \qquad (6.8)$$

and

$$f_{cle} = 2C_eE\frac{t}{D}$$

NORSOK standard Page 15 of 264

Impacted leg section of Platform A

Element profile			
D	=	1600 mm	Outer diameter
t	=	70 mm	Wall thickness
ID	=	1460 mm	Inner diameter
L	=	23 m	Member length
Fy	=	420 MPa	Yield stress
E	=	210000 MPa	Elastic modulus

Cross section properties			
A	=	0.34 m2	Cross section area
W	=	0.1233 m3	Elastic section modulus
Z	=	0.1640 m3	Plastic section modulus
I	=	0.0987 m4	Moment Inertia of cross section
i	=	0.542 m	Radius of gyration

Calculation of characteristic local buckling strength			
f-cle	=	5513 MPa	Characteristic elastic local buckling strength
C-e	=	0.3	Critical buckling coefficient
fy/f-cle	=	0.08	
f-cl	=	420 MPa	Charasteristic local buckling strength

Calculation of charasteristic axial compressive strength			
λ-bar	=	0.605	Column slenderness parameter
k	=	1	Effective length factor
fc	=	377 MPa	Characteristic axial compressive strength
γ-m	=	1.15	Material factor, assumed

N-rd	**=**	**110 MN**	**Capacity of axial compression of tubular steel**

Impacted leg section of Platform B

Element profile			
D	=	2000 mm	Outer diameter
t	=	85 mm	Wall thickness
ID	=	1830 mm	Inner diameter
L	=	23 m	Member length
Fy	=	420 MPa	Yield stress
E	=	210000 MPa	Elastic modulus

Cross section properties			
A	=	0.51 m2	Cross section area
W	=	0.2349 m3	Elastic section modulus
Z	=	0.3119 m3	Plastic section modulus
I	=	0.2349 m4	Moment Inertia of cross section
i	=	0.678 m	Radius of gyration

Calculation of characteristic local buckling strength			
f-cle	=	5355 MPa	Characteristic elastic local buckling strength
C-e	=	0.3	Critical buckling coefficient
fy/f-cle	=	0.08	
f-cl	=	420 MPa	Charasteristic local buckling strength

Calculation of charasteristic axial compressive strength			
λ-bar	=	0.485	Column slenderness parameter
k	=	1	Effective length factor
fc	=	392 MPa	Characteristic axial compressive strength
ɣ-m	=	1.15	Material factor, assumed

N-rd	**=**	**174 MN**	**Capacity of axial compression of tubular steel**

Impacted leg section of Platform C

Element profile			
D	=	1308 mm	Outer diameter
t	=	74 mm	Wall thickness
ID	=	1160 mm	Inner diameter
L	=	16.6 m	Member length
Fy	=	420 MPa	Yield stress
E	=	210000 MPa	Elastic modulus

Cross section properties			
A	=	0.29 m2	Cross section area
W	=	0.0838 m3	Elastic section modulus
Z	=	0.1128 m3	Plastic section modulus
I	=	0.0548 m4	Moment Inertia of cross section
i	=	0.437 m	Radius of gyration

Calculation of characteristic local buckling strength			
f-cle	=	7128 MPa	Characteristic elastic local buckling strength
C-e	=	0.3	Critical buckling coefficient
fy/f-cle	=	0.06	
f-cl	=	420 MPa	Charasteristic local buckling strength

Calculation of charasteristic axial compressive strength			
λ-bar	=	0.541	Column slenderness parameter
k	=	1	Effective length factor
fc	=	386 MPa	Characteristic axial compressive strength
ɣ-m	=	1.15	Material factor, assumed

N-rd	**=**	**96 MN**	**Capacity of axial compression of tubular steel**

Impacted leg section of Platform D

Element profile			
D	=	1984 mm	Outer diameter
t	=	52 mm	Wall thickness
ID	=	1880 mm	Inner diameter
L	=	21 m	Member length
Fy	=	480 MPa	Yield stress
E	=	210000 MPa	Elastic modulus

Cross section properties			
A	=	0.32 m2	Cross section area
W	=	0.1486 m3	Elastic section modulus
Z	=	0.1941 m3	Plastic section modulus
I	=	0.1474 m4	Moment Inertia of cross section
i	=	0.683 m	Radius of gyration

Calculation of characteristic local buckling strength			
f-cle	=	3302 MPa	Characteristic elastic local buckling strength
C-e	=	0.3	Critical buckling coefficient
fy/f-cle	=	0.15	
f-cl	=	480 MPa	Charasteristic local buckling strength

Calculation of charasteristic axial compressive strength			
λ-bar	=	0.463	Column slenderness parameter
k	=	1	Effective length factor
fc	=	451 MPa	Characteristic axial compressive strength
ɣ-m	=	1.15	Material factor, assumed

N-rd	**=**	**124 MN**	**Capacity of axial compression of tubular steel**